Unobserved Grouped Patterns in Panel Data and Prior Wisdom[†]

Boyuan Zhang[‡]
University of Pennsylvania

First Version: June 14, 2022
This Version: October 13, 2022

Abstract

Group heterogeneity has recently been proven to be useful in panel data models. We develop a constrained Bayesian grouped estimator that effectively exploits researchers' prior beliefs on groups in a flexible form of pairwise constraints. To utilize the pairwise constraints, we propose an intuitive and coherent prior building upon a standard nonparametric Bayesian prior. The resulting Gibbs sampler is closely related both to the constrained clustering algorithm and to grouped fixed-effects estimators. Monte Carlo experiments reveal that adding prior knowledge yields more accurate estimates and scores predictive gains over alternative estimators. We apply our method to two empirical applications. In a first application to U.S. CPI inflation, we illustrate that prior knowledge of group structure improves density forecasts when the data is not entirely informative. A second application revisits the relationship between a country's income and its democratic transition; we identify heterogeneous income effects on democracy with a reasonable group pattern.

JEL CLASSIFICATION: C11, C14, C23, E31

KEY WORDS: Grouped Heterogeneity; Bayesian Nonparametrics; Dirichlet Process Prior; Density Forecast; Inflation Rate Forecasting; Democracy and Development.

[†]Please check here for the latest version.

[‡]Department of Economics, Perelman Center for Political Science and Economics, University of Pennsylvania, 133 S. 36th St., Philadelphia, PA 19104-6297. Email: boyuanz@sas.upenn.edu. I am extremely grateful to my advisors Francis X. Diebold and Frank Schorfheide, and my dissertation committee, Xu Cheng and Minchul Shin, for their invaluable guidance and support. I would also like to thank Karun Adusumilli, Siddhartha Chib, Wayne Yuan Gao, Philippe Goulet Coulombe, and Daniel Lewis for helpful comments and suggestions. I further benefited from many helpful discussions with Econometrics Lunch seminar participants at the University of Pennsylvania, as well as participants at the 2022 North American Summer Meeting of the Econometric Society, the 2022 IAAE Annual Conference, the 42nd International Symposium on Forecasting, the 16th International Symposium on Econometric Theory and Applications, the 2022 Asian Meeting of the Econometric Society, the 2022 Australasia Meeting of the Econometric Society, the NBER-NSF Seminar on Bayesian Inference in Econometrics and Statistics. All remaining errors are my own.

1 Introduction

Numerous studies have examined and demonstrated the important role of panel data models in empirical research throughout the social and business sciences, as the availability of panel data has increased. Using fixed-effects, panel data permits researchers to model unobserved heterogeneity across individuals, firms, regions, and countries as well as possible structural changes over time. As individual heterogeneity is often empirically relevant, fixed-effects are a parameter of interest in numerous empirical studies. For example, teachers' fixed-effects are viewed as a measure of teacher quality in the literature on teacher valued-added (Rockoff, 2004; Chetty et al., 2014); the heterogeneous coefficients are crucial for panel data forecasting (Liu et al., 2020; Pesaran et al., 2022). In practice, however, researchers may face a short panel where N is large and T is short and fixed. When applying the least squares estimator for the fixed-effects, a significant number of noisy estimates are produced. To alleviate this issue, a popular and parsimonious assumption that has recently been used is to introduce a grouped pattern into the individual coefficients, so that units within each group have identical coefficients (Bonhomme and Manresa (2015, BM hereafter), Su et al. (2016), Bonhomme et al. (2022)).

To recover the grouped pattern, we essentially face a clustering problem, e.g., dividing N units into several unknown groups. Existing methods assume that units are exchangeable and treat every unit equally *a priori*. This indicates that, before observing the real data, all units are assumed to be identical and have an equal chance of being grouped with any other. As a result, the prior probability of any group structure of N units is the same, even if we swap pairs of units from different groups. The assumption of exchangeablility might not be reasonable since correlations are common between observations at proximal times and locations and researchers may have knowledge of the underlying group structure coming from expertise, theories or empirical findings. For instance, in a cross-country application of evaluating the impact of climate change on economic growth, it is reasonable to believe that countries in the same region are more likely to belong to the same group. In such a scenario, it is preferable to use prior knowledge to break the exchangeability between countries to facilitate grouping, as opposed to clustering based solely on data. Other examples relate to temporal relationships, such as firms in similar development stages, countries witnessed linked historical events, etc. The availability of this information drives us to formalize such prior knowledge, which we wish to leverage to improve model performance.

In this paper, we focus on the group heterogeneity in the linear panel data model and improve the associated clustering procedure by leveraging available prior knowledge of the group structure in a nonparametric Bayesian framework. Specifically, we suggest an intuitive and coherent prior to incorporate prior knowledge, which is based on a typical nonparametric Bayesian prior. Prior knowledge is considered as an additional source of information that not only aids in clustering units into groups but also sharpens the inference of group structure and parameters, particularly when units are not well-separated.

The derivation of the proposed prior starts from the pairwise constraints, which is the key structure that represents our prior knowledge. Pairwise constraints describe the bilateral relationship between any two units. We consider two types of constraints: *must-link* and *cannot-link* constraints (Wagstaff and Cardie, 2000). These constraints describe whether two units must be members of the same group or distinct groups. In general, supervision in the form of pairwise constraints is relatively practical and flexible since it eliminates the need to predetermine the number of groups and focuses on the bilateral relationships within any *subset* of units. Instead of imposing constraints, each constraint is given a level of accuracy that shows how confident the researchers are in their choice.

We modify the standard nonparametric Bayesian prior to incorporate pairwise constraints. The baseline model is a linear panel data model with an unknown grouped pattern in fixed-effects, slope coefficients, and cross-sectional variances. We estimate the model using a nonparametric Bayesian prior, specifically the Dirichlet process (DP) (Ferguson, 1973, 1974) prior with stick-breaking representation (Sethuraman, 1994). In this framework, the number of groups is considered as a random variable and is subject to posterior inference. As a result, we do not impose a restriction on the number of groups, and model selection is not required. The pairwise constraints are combined with the prior distribution of the group partitioning, shrinking the distribution toward our prior knowledge. There is a hyperparameter that controls the overall strength of the prior knowledge: a small value partially recovers the exchangeablity assumption on units, whereas a large value confines the prior distribution of group partitioning around group structure based on prior knowledge. We refer to the estimator using the proposed prior as the Bayesian fixed-effects (BGFE) estimator.

We derive a posterior sampling algorithm for nonparametric estimation under pairwise constraints. In the current framework, adopting conjugate priors enables us to draw directly from posteriors using a computationally efficient Gibbs sampler. With the newly proposed prior, it can be shown that, relative to the framework using a standard Dirichlet process prior, a simple modification to the posterior of the group indices is sufficient to account for the implementation of pairwise constraints. According to the results of the simulation, this modification has little effect on computation expenses.

Our pairwise constraint-based framework is closely related and applicable to other models where group structure plays a role. Although we concentrate primarily on the panel data model, the DP prior with pairwise constraints also applies to the clustering problem utilizing mixture models, the estimate of heterogeneous treatment effects, and the development of Granger networks based on panel VARs (Holland et al., 1983). Moreover, the proposed Gibbs sampler with pairwise constraints is connected to the *KMeans*-type algorithm, motivating a frequentist's counterpart of our estimator with a fixed K. Essentially, the assignment step in the *PC-KMeans* algorithm (Basu et al., 2004a), a constrained version of the *KMeans* algorithm (MacQueen et al., 1967), is remarkably similar to the step of drawing a group membership indicator from its posterior. The same exact equivalence can be achieved by applying small-variance asymptotics to the posterior densities under certain conditions.

To obtain the frequentist's analog of our pairwise constrained Bayesian estimators, one can utilize the same approach in BM with the *PC-KMeans* algorithm.

We compare the performance of the BGFE estimator to that of other well-known estimators using simulated data. The Monte Carlo simulation demonstrates that the BGFE estimator gives a more accurate estimate. The improved performance is mostly attributable to the precise group structure estimation. Unsurprisingly, the accurate estimates translate into the predictive power of the underlying model; the BGFE estimator excels at point, set, and density forecasting. We combine different versions of the BGFE estimators and show that incorporating prior information further enhances the performance. Even if the constraints are wrong, the BGFE estimator can still improve the accuracy of forecasts by using correct and relevant prior knowledge.

We conclude by applying our methods to two empirical applications. An application to the inflation of the U.S. CPI sub-indices demonstrates that the suggested predictor yields more accurate density predictions. The better forecasting performance is mostly attributable to three key characteristics: the nonparametric Bayesian prior, prior belief on group structure, and grouped cross-sectional heteroskedasticity. The method proposed in this paper is applicable beyond forecasting. In a second application, we revisit the relationship between a country's income and its democratic transition, where estimation of heterogeneous parameters is the object of interest. We recover a reasonable cluster pattern with a moderate number of groups. Each group has a clear and distinct path to democracy. We also identify heterogeneous income effects on democracy and find that there is a positive income effect in some groups of countries, though quantitatively small.

LITERATURE. Our paper relates to the econometric literature on clustering in panel data models. Early contributions include Sun (2005) and Buchinsky et al. (2005). Hahn and Moon (2010) provide economic and theoretical foundations for fixed effects with a finite support. Most recent work focus on linear[1] panel data models with discrete unobserved group heterogeneity. Lin and Ng (2012) and Sarafidis and Weber (2015) apply the *KMeans* algorithm to identify the unobserved group structure of slope coefficients. Bonhomme and Manresa (2015) also use the *KMeans* algorithm to recover the group pattern, but they assume group structure in the additive fixed effects. Bonhomme et al. (2022) modify this method and split the procedure into two steps. They first classify individuals into groups using *KMeans* algorithm and then estimate the coefficients. Ando and Bai (2016) improved on BM's approach by allowing for group structure among the interactive fixed effects. The underlying factor structure in the interactive fixed effects is the key to forming groups. Su et al. (2016) develop a new variant of Lasso to shrink individual slope coefficients to the unknown group-specific coefficients. This method is then extended by Su and Ju (2018) and Su et al. (2019). Freeman and Weidner (2022) consider two-way grouped fixed effects that allow for different group patterns in time and cross-sectional dimensions. Okui and Wang (2021) and Lumsdaine

[1]See Wang and Su (2021); Bonhomme et al. (2022), among others, for procedures to identify latent group structures in nonlinear panel data models.

et al. (2022) identify structure breaks in parameters along with grouped patterns. From the Bayesian perspective, Kim and Wang (2019), Zhang (2020), and Liu (2022) adopt the Dirichlet process prior to estimate grouped heterogeneous intercepts in linear panel data models in the semiparametric Bayesian framework. Others methods such as binary segmentation (Wang et al., 2018) and other assumptions such as multiple latent groups structure (Cytrynbaum, 2021) have also been explored to flourish group heterogeneity literature.

None but Aguilar and Boot (2022) explores heterogeneous error variance, and they extend BM's grouped fixed-effects (GFE) estimator to allow for group-specific error variances. They modify the objective function to avoid the singularity issue in pseudo-likelihood. Despite the fact that their work paves the way for identifying groups in the error variance, their framework is not ready to incorporate prior knowledge satisfactorily because they face the same issue as BM. Building on these works, we investigate the value of prior knowledge on group structure.

Bonhomme and Manresa (2015)'s grouped fixed-effects (GFE) estimator is able to include prior knowledge, but it is plagued by practical issues to some extent. They add a collection of individual group probabilities as a penalty term in the objective function, which is a N by K matrix describing the probability of assigning each unit to all potential groups. This additional penalty term balances the respective weights attached to prior and data information in estimation. The main challenge is providing the set of individual group probabilities for each potential value of K. It is rather cumbersome to assess these probabilities for each possible K and to adjust for modest changes in reallocating probabilities across possible K. In addition, model selection is required, the finite-sample results of which might be unreliable, especially when facing a short panel with noisy groups.

This paper also relates to the literature of constraint-based semi-supervised clustering in statistics and computer science. Pairwise constraints have been widely implemented in numerous models and have been shown to improve clustering performance. In the past two decades, various pairwise constrained *KMeans* algorithms using prior information have been suggested (Wagstaff et al., 2001; Basu et al., 2002, 2004a; Bilenko et al., 2004; Davidson and Ravi, 2005; Pelleg and Baras, 2007; Yoder and Priebe, 2017). Prior information is also introduced in the model-based method. Shental et al. (2003) develop a framework to incorporate prior information for the density estimation with Gaussian Mixture Models. The Dirichlet process mixture model with pairwise constraints has been discussed in Vlachos et al. (2008), Vlachos et al. (2009), Orbanz and Buhmann (2008), Vlachos et al. (2010), Ross and Dy (2013). Lu and Leen (2004), Lu (2007) and Lu and Leen (2007) assume the knowledge on constraints is incomplete and penalize the constraints in accordance to their weights. Law et al. (2004) extents Shental et al. (2003) to allow for soft constraints in mixture model by adding another layer of latent variables for the group label. Nelson and Cohen (2007) propose a new framework that samples pairwise constraints given a set of probabilities related to the weights of constraints.

Our paper is closely related to Paganin et al. (2021), who address a similar problem using a novel Bayesian framework. Their proposed method shrinks the prior distribution of group partitioning toward a *full* target group structure, which is an initial clustering of *all* units provided by experts. This is demanding since not every application can have a full target group structure, as their birth defects epidemiology study did. Our framework circumvents this problem by eliciting prior information of pairwise constraints. In addition, the induced shrinkage of their framework is produced by the distance function defined by Variation of Information. It can be demonstrated that a partition can readily become caught in local modes, preventing it from ever shrinking toward the prior partition. The use of pairwise relationships in this paper circumvents this issue. By fixing the group indices of other pairs, our framework makes sure that the partition with a specific pair that fits our prior belief has a strict higher prior probability than the partition with a pair that goes against our prior belief.

OUTLINE. In section 2, we present the specification of the dynamic panel data model with grouped pattern in slope coefficients and error variances, and provide details on nonparametric Bayesian prior without prior knowledge which is then extended to accommodate soft pairwise constraints. Section 3 focus on the posterior analysis, where the posterior sampling algorithm is provided. We also highlight the posterior estimate of group structure and discuss the connection to constrained *KMeans* models. We briefly discussion the extensions of the baseline model in section 4. In section 5, we present empirical analysis in which we forecast the inflation rate of the U.S. CPI sub-indices and estimate the country's income effect on its democracy. Finally, we conclude in section 6. Monte Carlo simulations, additional empirical results, and proofs are relegated to the appendix.

2 Model and Prior Specification

We begin our analysis by setting up a linear panel data model with group heterogeneity in fixed-effects, slope coefficients, and cross-sectional heteroskedasticity. We then discuss a nonparametric Bayesian prior for the unknown parameters without considering any prior beliefs about the group pattern, which is modified in the next section to integrate prior beliefs.

2.1 A Basic Linear Panel Data Model

We consider a panel with observations for cross-sectional units $i = 1, \ldots, N$ in periods $t = 1, \ldots, T$. Given the panel data set (y_{it}, x'_{it}), a simple linear panel data model with grouped heterogeneous slope coefficients and grouped heteroskedasticity takes the following form:

$$y_{it} = \alpha'_{g_i} x_{it} + \varepsilon_{it}, \quad \varepsilon_{it} \sim N\left(0, \sigma^2_{g_i}\right), \tag{2.1}$$

where x_{it} are a $p \times 1$ vector of covariates, which may contain intercept, lagged y_{it}, covariates and lagged covariates. α_{g_i} denote the group-specific slope coefficients (including fixed effects). $\sigma^2_{g_i}$ are the group-specific variance. $g_i \in \{1, ..., K\}$ is the latent group index with an unknown number of groups K. ε_{it} are the idiosyncratic errors that are independent across i and t conditional on g_i. They feature by zero mean and grouped heteroskedasticity $\sigma^2_{g_i}$, with cross-sectional homoskedasticity being a special case where $\sigma^2_{g_i} = \sigma^2$. This setting leads to a heterogeneous panel with group pattern modeled through both α_{g_i} and $\sigma^2_{g_i}$.

It is convenient to reformulate the model in (2.1) is the matrix form by stacking all observations for unit i:

$$\boldsymbol{y_i} = \boldsymbol{x_i}\alpha_{g_i} + \boldsymbol{\varepsilon_i}, \quad \boldsymbol{\varepsilon_i} \sim N\left(\mathbf{0}, \sigma^2_{g_i} I_T\right), \tag{2.2}$$

where $\boldsymbol{y_i} = [y_{i1}, y_{i2}, \ldots, y_{iT}]'$, $\boldsymbol{x_i} = [x_{i1}, x_{i2}, \ldots, x_{iT}]'$, $\boldsymbol{\varepsilon_i} = [\varepsilon_{i1}, \varepsilon_{i2}, \ldots, \varepsilon_{iT}]'$, and $G = [g_1, \ldots, g_N]$ is a vector of group indices.

Group structure is the key element in our approach. It can be either represented as a vector of group indices G describing to which group each unit belongs or as a collection of disjoint blocks $\mathcal{B} = \{B_1, B_2, \ldots, B_K\}$ induced by G, where B_k contains all the units in the k-th group and K is the number of group in the sample of size N. $|B_k|$ denotes the cardinality of the set B_k with $\sum_{k=1}^{K} |B_k| = N$.

Remark 2.1. *Identification issues may arise in certain specifications. If the grouped fixed-effects in α_{g_i} are allowed to vary over time, for example, $\sigma^2_{g_i}$ cannot be identified when the group $g = g_i$ contains only one unit. This problem is beyond the scope of this work, but Aguilar and Boot (2022) suggest revising the likelihood function to solve it. Additionally, the effects of fixed-effects and the categorical variable cannot be distinguished when all units in one group have the same level for one or more categorical variables in x_i. By controlling for categorical variables but not assuming they have group effects, one may effectively avoid this issue.*

Following Sun (2005), Lin and Ng (2012) and BM, we assume that the composition of groups does not change over time. In addition, for any group $k \neq k'$, we assume that they have different slope coefficients, e.g., $\alpha_k \neq \alpha_{k'}$, and no single unit can simultaneously belong to these two groups: $B_k \bigcap B_{k'} = \varnothing$. It is possible to generate overlapping groups using the Indian Buffet Process, but this is beyond the scope of this study.

The primary objective of this paper is to estimate the grouped heterogeneity α_{g_i}, grouped heteroskedasticity $\sigma^2_{g_i}$ and group membership G using full sample and prior knowledge on the group structure. We also offer the point, set, and density forecasts of y_{it+h} for each unit i. Throughout this paper, we will concentrate on the one-step ahead forecast where $h = 1$. For multiple-step forecasting, the procedure can be extended by iterating y_{iT+h} in accordance with (2.1) given the estimates of parameters or estimating the model in the style of direct forecasting.

2.2 Nonparametric Bayesian Prior

The baseline model contains the parameters listed below: $(\alpha, \sigma^2, \pi, \xi, a, \phi)$. We rely mostly on nonparametric Bayesian models.[2] Bayesian nonparametric models have emerged as rigorous and principled paradigms to bypass the model selection problem in parametric models by introducing a nonparametric prior distribution on the unknown parameters. The prior assumes that a collection of α and σ^2 is drawn from the Dirichlet process, $\left(\alpha_i, \sigma_i^2\right) \sim DP\left(a, B_0(\phi)\right)$. π is a vector of mixture probabilities in Dirichlet process that is produced by the stick-breaking approach with stick length ξ. a is the concentration parameter in the Dirichlet process, whereas ϕ is a collection of hyperparameters in the base measure B_0. We consider prior distributions in the partially separable form,[3]

$$p(\alpha, \sigma^2|a, \phi, \xi)p(\xi|a)p(a).$$

We tentatively focus on the random coefficients model where, conditional on G, α_{g_i} and $\sigma_{g_i}^2$ are independent to the conditional set that includes initial value of each unit y_{i0}, the initial values of predetermined variables, and the whole history of exogenous variables. The assumption guarantees that α_{g_i} and σ_{g_i} can be sampled separately and simplifies the inference of the underlying distribution of α_{g_i} and σ_{g_i} to an unconditional density estimation problem, therefore lowering computational complexity. The joint distribution of heterogeneous parameters as a function of the conditioning variables can then be modeled to extend the model to the correlated random coefficient model. A full explanation and derivation for the correlated random coefficient model are provided in the online appendix.

2.2.1 Prior on Group-Specific Parameters

In the nonparametric Bayesian literature, the Dirichlet Process (DP) prior (Ferguson, 1973, 1974; Sethuraman, 1994) is a canonical choice, notable for its capacity to construct group structure and accommodate an infinite number of possible group components. The DP mixture is also known as a "infinite" mixture model due to the fact that the data indicate a finite number of components, but fresh data can uncover previously undetected components (Neal, 2000). When the model is estimated, it chooses automatically an appropriate subset of groups to characterize any finite data set. Therefore, there is no need to determine the "proper" number of groups.

The Dirichlet process defines a distribution over distributions, which is denoted as

$$B \sim \mathrm{DP}\left(a, B_0\right), \tag{2.3}$$

[2]For a more comprehensive review of the nonparametric Bayesian literature, see Ghosal and Van der Vaart (2017) and Müeller et al. (2018)

[3]The joint prior includes ξ but not π. Because the stick-breaking formulation of ξ is a deterministic transformation of ξ, knowing ξ is identical to knowing π.

where B is a random distribution. There are two parameters. The base distribution B_0 is a distribution over the same space as B. For example, if B_0 is a distribution on reals then B must be a distribution on reals too. The concentration parameter a is a positive scalar. One property of the DP is that random distributions B are discrete, and each places its mass on a countably infinite collection of atoms drawn from B_0.

We next define a typical DP prior for (α, σ^2):

$$\begin{aligned}(\alpha_i, \sigma_i^2) &\sim B, \\ B &\sim \text{DP}\,(a, B_0)\,,\end{aligned} \tag{2.4}$$

where we adopt an Independent Normal Inverse-Gamma (INIG) distribution for the base distribution B_0:

$$B_0(\phi) := INIG\left(\mu_\alpha, \Sigma_\alpha, \frac{\nu_\sigma}{2}, \frac{\delta_\sigma}{2}\right), \tag{2.5}$$

with a set of hyperparameters $\phi = \left(\mu_\alpha, \Sigma_\alpha, \frac{\nu_\sigma}{2}, \frac{\delta_\sigma}{2}\right)$.

In fact, the DP prior in (2.4) exhibits an important *clustering property*, such that the draws (α_i, σ_i^2) are generally *not* distinct. Upon marginalizing out the random mixing measure B, one obtains the DP prediction rule (Blackwell and MacQueen, 1973) or the conditional distribution of (α_i, σ_i^2) given $(\alpha_{1:i-1}, \sigma_{1:i-1}^2)$, which follows a Polya urn distribution,

$$\alpha_i, \sigma_i^2 | \alpha_{1:i-1}, \sigma_{1:i-1}^2, a, B_0 \sim \frac{1}{a+i-1} \sum_{j=1}^{i-1} \delta_{(\alpha_j, \sigma_j^2)} + \frac{a}{a+i-1} B_0. \tag{2.6}$$

Equation (2.6) reveals the clustering nature of the DP prior: there is a positive probability that each (α_i, σ_i^2) will take on the value of another (α_j, σ_j^2), leading some of the variables to share values. This equation also reveals the roles of scaling parameter a and base distribution B_0. The unique values contained in $(\alpha_{1:N}, \sigma_{1:N}^2)$ are drawn independently from B_0, and the parameter a determines how likely α_i, σ_i^2 is to be a newly drawn value from B_0 rather than take on one of the values from $\alpha_{1:i-1}, \sigma_{1:i-1}^2$.

To facilitate posterior sampling, the DP prior is rewritten as an infinite mixture of point mass with the probability mass function

$$\left(\alpha_i, \sigma_i^2\right) \sim \sum_{k=1}^{\infty} \pi_k \delta_{\left(\alpha_k, \sigma_k^2\right)} \text{ with } \left(\alpha_k, \sigma_k^2\right) \sim B_0(\phi), \tag{2.7}$$

where δ_x denotes the Dirac-delta function concentrated at x. The group probabilities π_k are constructed by an infinite-dimensional stick-breaking process (Sethuraman, 1994) governed by the concentration parameter a,

$$\pi_k \equiv \xi_k \prod_{j<k} (1 - \xi_j) \text{ for } k > 1, \text{ and } \pi_1 = \xi_1, \tag{2.8}$$

where stick lengths ξ_k are independent random variables drawn from the beta distribution $Beta(1, a)$. The group probability will be random, but will satisfy $\sum_{k=1}^{\infty} \pi_k = 1$ almost surely.

Equation (2.8) is essential to understanding how the DP prior controls the number of groups. The building of group probabilities is compared to the breaking of a stick of unit length, in which the length of each break is assigned to the current value of π_k. As the number of groups increases, the probability created by the stochastic process decreases because the remaining stick becomes shorter with each break. In practice, the number of groups does not increase as fast as N due to the characteristic of the stick-breaking process that leads the group probability to soon approach zero.

Although in principle we do not restrict the maximum number of groups and allow the number to rise as N increases, a finite number of instances will only occupy a finite number of K components. The concentration parameter a in the prior of ξ_k determines the degree of discretization – the complexity of the mixture and, consequently, K, as also revealed in (2.6). As $a \to 0$, the realizations are all concentrated at a single value, however as $a \to \infty$, the realizations become continuous-valued as its based distribution. Specifically, Antoniak (1974) derives the relationship between a and the number of unique groups,

$$E\left(K|a\right) \approx a \log\left(\frac{a+N}{a}\right) \quad \text{and} \quad \text{Var}\left(K|a\right) \approx \alpha\left[\log\left(\frac{\alpha+N}{\alpha}\right) - 1\right],$$

that is, the expected number of unique groups is increasing in both a and the number of units N.

Escobar and West (1995) highlights the importance of specifying a when imposing prior smoothness on an unknown density and demonstrates that the number of estimated groups under a DP prior is sensitive to a. This suggests that a data-driven estimate of a is more reasonable. Moreover, Ascolani et al. (2022) emphasizes the importance of introducing a prior for a as it is crucial for learning the true number of groups as N increases and hence establishing the posterior consistency. We define a gamma hyperprior for a and update it based on the observed data in order to alter the smoothness level. This step generates a posterior estimate of a, which indirectly determines the number of groups K without reestimating the models with different group sizes. Essentially, this represents "automated" model selection.

Collectively, we specify a DP prior for $\left(\alpha_i, \sigma_i^2\right)$. The DP prior is a mixture of an infinite number of possible point masses, which can be constructed through the stick-breaking process. The discretization of the underlying distribution is governed by the concentration parameter a. With a hyerprior on a, we permit the data to determine the number of groups K present in the data, which can expand unboundedly along with the data.

2.2.2 Prior on Group Partitions

In a formal Bayesian formulation, a prior distribution is specified to partition $\mathcal{B}$ with associated indices G. Despite the fact that DP prior does not specify this prior distribution ex-

plicitly, we can characterize it using the exchangeable partition probability function (EPPF) (Pitman, 1995).

The EPPF characterizes the distribution of a partition $\mathcal{B} = \{B_1, B_2, \ldots, B_K\}$ induced by G. As the Dirichlet process assumes units are exchangeable, any permutation has no effect on the joint probability distribution of G; hence, the EPPF is determined entirely by the number of groups and the size of each group. Pitman (1995) demonstrates that the EPPF of the Dirichlet process has the closed form,

$$p(G) = \frac{\Gamma(a)}{\Gamma(a+N)} a^K \prod_{k=1}^{K} \Gamma\left(|B_k|\right), \tag{2.9}$$

where a is the concentration parameter and $\Gamma(x) = (x-1)!$ denotes the Gamma function. Noting that the partition $\mathcal{B}$ is conceived as a random object and hence the group number K is not predetermined, but rather is a function of G, $K = K(G)$.

A predominant feature of the EPPF in (2.9) is that it defines a prior distribution over G. To obtain the prior from EPPF, we must first identify all possible group partitions of N units. This problem can be recast as a prototypical "balls and urns" problem: what are the ways of putting N distinguishable balls into N indistinguishable urns if empty urns are allowed?

Example 2.1. Consider a simple case in which $N = 3$ and $a = 1$. It is easy to show that there are five ways to group three units. Then the prior distribution over G under Dirichlet process is given by,

$$\begin{aligned}
\Pr(g_1 = g_2 = g_3 = 1) &= \frac{\Gamma(1)}{\Gamma(4)}\Gamma(3) = \frac{1}{3}, \\
\Pr(g_1 = g_2 = 1, g_3 = 2) &= \frac{\Gamma(1)}{\Gamma(4)}\Gamma(2)\Gamma(1) = \frac{1}{6}, \\
\Pr(g_1 = g_3 = 1, g_2 = 2) &= \frac{\Gamma(1)}{\Gamma(4)}\Gamma(2)\Gamma(1) = \frac{1}{6}, \\
\Pr(g_2 = g_3 = 1, g_1 = 2) &= \frac{\Gamma(1)}{\Gamma(4)}\Gamma(2)\Gamma(1) = \frac{1}{6}, \\
\Pr(g_1 = 1, g_2 = 2, g_3 = 3) &= \frac{\Gamma(1)}{\Gamma(4)}\Gamma(1)\Gamma(1)\Gamma(1) = \frac{1}{6}.
\end{aligned}$$

Finding all solutions to the "balls and urns" problem with big N is computationally impossible in general. For a certain number of groups K, the number of ways to assign N unit to K groups is described by the *Stirling number of the second kind*,

$$\mathcal{S}_{N,K} = \frac{1}{K!} \sum_{j=0}^{K} (-1)^j C_K^j (K-j)^N. \tag{2.10}$$

The sum of $\mathcal{S}_{N,K}$ over all possible K, also known as the N-th Bell number, $\mathcal{B}_N = \sum_{K=1}^{N} \mathcal{S}_{N,K}$ describes the number of all possible partitions of N balls. Owing to the rapid growth of

the space, listing all feasible partitions becomes computationally impossible. For example from a moderate $N = 12$ to 15, the number of partitions increases from $\mathcal{B}_{12} = 4,213,597$ to $\mathcal{B}_{15} = 1,382,958,545$. Sethuraman (1994) and Pitman (1996) constructively show that group indices/partitions can be drawn from the EPPF for DP using the stick-breaking process defined in (2.8). As a result, the EPPF does not explicitly appear in the posterior analysis in the current setting so long as the priors for the stick lengths are included.

Furthermore, as we shall demonstrate in the following section, the EPPF plays a significant role in connecting the prior belief on group structure to the DP prior when prior information on the grouping is provided and included in the prior.

2.3 Nonparametric Bayesian Prior with Knowledge on G

We briefly discuss the drawbacks of existing models that incorporate prior knowledge of G. Then, to address all those issues, we introduce the concept of pairwise constraint and propose a novel constrained Bayesian grouped estimator with soft constraints. Finally, we demonstrate the effect of soft constraints and hyperparameters on the group structure.

2.3.1 Drawbacks of Existing Methods

Bonhomme and Manresa (2015) incorporates prior knowledge of group membership by adding a penalty term to the objective function. They assume that prior information is in the form of probabilities which describe the prior probability of unit i belonging to group k with at most K groups as $\omega_{ik}^{(K)}$. Consequently, the estimated group index is given by:

$$\widehat{g}_i(\beta, \alpha) = \underset{k \in \{1,\dots,K\}}{\operatorname{argmin}} \sum_{t=1}^{T} \left(y_{it} - \beta^{(K)\prime} x_{it} - \alpha_{kt}^{(K)} \right)^2 - C \ln \omega_{ik}^{(K)}, \tag{2.11}$$

where $C > 0$ is a hyperparameter need to be tuned further and K is the predetermined number of groups.

The penalty determines the weights assigned to prior and data information in estimation. Due to the fact that K is frequently unknown in advance, this method requires model selection to determine the ideal number of groups. Assume we have n_K alternative options for K. We have a $N \times K$ matrix $\omega^{(K)} = \left\{ \omega_{ik}^{(K)} \right\}$ for prior information for a given K. As a result, in order to pick a model, we must therefore provide n_K sets of prior probability matrix $\omega^{(K)}$, which is cumbersome and inconvenient. For instance, if K has values ranging from $3, 5, 10$ and $N = 200$, there are 3,600 entries for ω, none of which can be missing or undefined. In addition, the information criteria may be unreliable in the finite-sample results, necessitating further care when selecting an appropriate variant for empirical application.

Paganin et al. (2021) offer a statistical framework for including concrete prior knowledge on the partition. Their proposed method aims to shrink the prior distribution towards a

complete prior clustering structure, which is an initial clustering involving *all* units provided by experts. Specifically, they suggest a prior on group partition that is proportional to a baseline EPPF of the DP prior multiplied by a penalization term,

$$p\left(G|G_0,\psi\right) \propto p(G)e^{-Cd(G,G_0)} \tag{2.12}$$

with $C > 0$ a penalization parameter, $d\left(G, G_0\right)$ a suitable distance measuring how far G is from G_0 and $p(G)$ indicates a baseline EPPF define in (2.9). Because of the penalization term, the resulting group indices G shrink toward the initial target G_0.

This framework is parsimonious and easy to implement, but it comes with a price. The method is incapable of coping with an initial clustering in a subset of the units under study or multiple plausible prior partitions; otherwise, the distance measure is not well-defined. In addition, the authors suggest utilizing Variation of Information (Meilă, 2007) as the distance measure. It can be shown that the resulting partition can easily become trapped in local modes, leading the partition to never shrink toward G_0. They also argue that other available distance methods have flaws. As a result, the penalty term does not function as anticipated.

2.3.2 Soft Pairwise Constraints

Having the aforementioned practical issues in mind, we offer a new Bayesian framework based on pairwise constraints. Pairwise constraints are bilateral relationships that reflect and summarize the prior knowledge on group pattern, which has been wildly used in the computer science literature for constrained clustering.

According to the literature on semi-supervised learning (Wagstaff and Cardie, 2000), we consider two types of pairwise constraints that represent econometricians' prior knowledge on the group structure: (1) must-link (ML) constraints $\mathcal{M}$, and (2) cannot-link (CL) constraints $\mathcal{C}$. A must-link constraint specifies that two units should be assigned to the same group, whereas a cannot-link constraint indicates that the units should be assigned to separate groups.

Summarizing prior knowledge through such a bilateral connection is often more practical than the aforementioned framework and is by far the most common constraint utilized in clustering algorithms. It is more preferable than providing individual group probabilities since researchers do not need to know the number of groups or group membership *a priori*. Pairwise relationships can be derived intuitively from researchers' input without requiring in-depth knowledge of the underlying groups - one only needs to specify pairs of units belonging to the same or different groups. Moreover, pairwise relationships are more flexible than adopting a target partition. Essentially, the target partition in Paganin et al. (2021) can be viewed as a special case of the pairwise constants, in which every unit must be involved in at least one ML constraint. Our framework could manage partitions involving arbitrary subsets of the units by tactically specifying pairwise constraints. Most importantly, when

the group indices of other pairs are fixed, this framework ensures that the partition containing a specific pair that is consistent with our prior belief would receive a strictly greater prior probability than the partition that is inconsistent with our prior belief. This ensure the generated G shrinks in the direction of our prior belief.

The structure of pairwise constraints alone is insufficient to fulfill all practical requirements, given that we may have different degrees of confidence in constraints. To explicitly define our confidence and provide a flexible framework, we specify two characteristics for pairwise constraints : accuracy and type. Accuracy $\psi_{ij} \in [0.5, 1)$ describes the user-specified probability of assigning a constraint for unit i and j being correct given our prior preference. Specifically, $\psi_{ij} = 1$ implies the constraint between i and j must be imposed since we confident that it is accurate, while specifying $\psi_{ij} = 0.5$ is equivalent to a random guess or no information is provided. ψ_{ij} is bounded below by 0.5, following the assumption that leaving the pair unrestricted is more rational than setting a less likely constraint. The type of constraints is denoted by T_{ij}. $T_{ij} = 1$ if unit i and j are specified to be must-linked, and $T_{ij} = -1$ for a CL constraints. If the pair (i, j) doesn't involve any constraint, we assume $T_{ij} = 0$. With (ψ, T), we are able to describe the relationship between any pair of units with any degree of confidence, and hence we refer to these constraints as *soft* pairwise constraints.

2.3.3 A New Prior with Soft Pairwise Constraints

We now formally characterize our prior belief in the form of soft pairwise constraints. To incorporate these constraints into the prior, we propose modifying the exchangeable partition probability function, $p(\boldsymbol{G})$, of the baseline Dirichlet process so that the induced group partition has a strictly higher (lower) probability if it is (in)consistent with pairwise constraints. Thus, the induced prior on the group indices G should directly depend on the characteristics of user-specific pairwise constraints and be able to increase or decrease the likelihood of a certain G.

In the presence of soft constraints, we modify the EPPF defined in (2.9) by multiplying a function of characteristics of constraints,

$$p(G|\psi, T) \propto p(G)p(\psi, T|G) = p(G) \prod_{i,j} \left(\frac{\psi_{ij}}{1 - \psi_{ij}} \right)^{cT_{ij}\delta_{ij}}, \tag{2.13}$$

where $\psi_{ij}/(1 - \psi_{ij})$ is the prior odds for the constraint between unit i and j, δ_{ij} is a transformed Kronecker delta function such that

$$\delta_{ij} = \begin{cases} 1 & \text{if } g_i = g_j \\ -1 & \text{if } g_i \neq g_j \end{cases}, \tag{2.14}$$

and c is a positive number that controls the overall strength of prior belief. For $c \to 0$, $p(G|\psi, T)$ corresponds to the baseline EPPF $p(G)$, while for $c \to \infty$, $p\left(G = G^*|\psi, T\right) \to 1$, where G^* satisfies all pairwise constraints.

Remark 2.2. *Due to the presence of pairwise constraints, the partition probability function presented in (2.13) no longer satisfies the exchangeable assumption as we now distinguish units within each group.*

Remark 2.3. *The current framework enables us to impose some constraints. It is an extreme case of soft constraint and thus handy to implement, requiring only setting $\psi_{ij} \to 1$ for the pair (i, j). Intuitively, any group partition violating the pairwise constraint between i and j (i.e., $T_{ij}\delta_{ij} = -1$) will have zero probability, since for such partition,*

$$\left(\frac{\psi_{ij}}{1-\psi_{ij}}\right)^{cT_{ij}\delta_{ij}} \to \left(\frac{1}{\infty}\right)^{c} = 0, \text{ this imples } p(G|\psi, T) = 0,$$

and hence the constraint on (i, j) is imposed and referred to as a hard constraint as opposed to soft constraint. By assigning proper ψ_{ij} for the pairs (i, j), we can flexibly combine soft and hard constraints inside a single specification.

Remark 2.4. *Soft pairwise constraints solve the transitivity issue that might be a problem for hard pairwise constraints. For instance, if we have $(1, 2) \in \mathcal{M}$ and $(2, 3) \in \mathcal{M}$, we can still have $(1, 3) \in \mathcal{C}$ in the framework of soft pairwise constraints since it preserves the possibility of violating any of these constraints. This is not the case in hard pairwise constraints, as $(1, 2) \in \mathcal{M}$ and $(2, 3) \in \mathcal{M}$ implies $(1, 3) \in \mathcal{M}$ by transitivity.*

Intriguingly, the partition probability function suggested is strongly related to the penalized probabilistic clustering proposed by Lu and Leen (2004) and Lu and Leen (2007). They introduce a weighting factor to penalize the objective function to incorporate the clustering preferences. In fact, motivated by their work, we combine the accuracy ψ_{ij} and the type T_{ij} into a single characteristic W_{ij}, termed weights, which takes the following form,

$$W_{ij} = \log\left(\frac{\psi_{ij}}{1-\psi_{ij}}\right)^{T_{ij}}. \tag{2.15}$$

As depicted in Figure 1, W_{ij} is continuously valued on the real line, representing hard CL, soft CL, no prior information, soft ML, and hard ML as W_{ij} goes from $-\infty$ to ∞. Consequently, W_{ij} is sufficient to summarize all the information for a constraint: the absolute value of W_{ij} reflects the certainty of the prior knowledge and the sign of W_{ij} specifies the type of the constraint. Detailed discussion and derivation are documented in Appendix D.2.

Figure 1: The Relationship Between W_{ij} and Pairwise Constraints

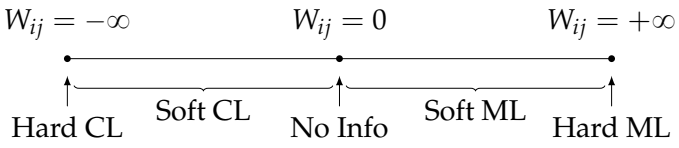

With the definition of W_{ij}, we rewrite the partition probability function defined in (2.13) in terms of W_{ij} to ease notation,

$$p(G|\psi, T) = p(G|W) \propto p(G) \exp\left(c \sum_{i,j} W_{ij}\delta_{ij}\right), \tag{2.16}$$

and we will use the this specification hereinafter. In practice, we will first specify $(T_{ij}, \psi_{ij}) =$ (type, accuracy) for the constraint between unit i and j and then construct the corresponding weight W_{ij} via the equation (2.15).

Remark 2.5. *In the particular case where we don't have any constraint information,* $\exp\left(c \sum_{i,j} W_{ij}\delta_{ij}\right)$ *reduces to 1 as* $W_{ij} = 0$ *for all* i *and* j*, and recovers the original DP prior. Hence, our method can cater to all levels of supervision, ranging from hard constraints to a complete lack of constraints.*

Our proposed partition probability function in (2.13) defines a prior on group indices in a similar fashion as the baseline DP prior in Section 2.2.2.

Example 2.2. Consider again the three-unit case in Example 2.1 with $a = 1$. Assume there is a must-link constraint between units 1 and 2 and that is the only constraint in this example. Then the prior probabilities of the five partitions are adjusted to account for the effect of W_{12}:

$$\begin{aligned}
\Pr(g_1 = g_2 = g_3 = 1) &= \frac{1}{3} \cdot \frac{2\exp(4cW_{12})}{\exp(4cW_{12}) + 1} > \frac{1}{3}, \\
\Pr(g_1 = g_2 = 1, g_3 = 2) &= \frac{1}{3} \cdot \frac{\exp(4cW_{12})}{\exp(4cW_{12}) + 1} > \frac{1}{6}, \\
\Pr(g_1 = g_3 = 1, g_2 = 2) &= \frac{1}{3} \cdot \frac{1}{\exp(4cW_{12}) + 1} < \frac{1}{6}, \\
\Pr(g_2 = g_3 = 1, g_1 = 2) &= \frac{1}{3} \cdot \frac{1}{\exp(4cW_{12}) + 1} < \frac{1}{6}, \\
\Pr(g_1 = 1, g_2 = 2, g_3 = 3) &= \frac{1}{3} \cdot \frac{1}{\exp(4cW_{12}) + 1} < \frac{1}{6},
\end{aligned}$$

Note that $c > 0$ and $W_{12} > 0$. Comparing to the results in Example 2.1, the probabilities of the first two partitions become higher since they all meet the ML constraint between units 1 and 2, while the rest of the partitions violate the constraint and hence the probabilities drop.

Figure 2 depicts the procedure for incorporating soft constraints within a Bayesian framework. Both the ML and CL constraints are associated with accuracy - how confidence we are when assigning a particular constraint. The information about constraints is then summarized in weights W. The weights are immediately included in the original prior of G as an additional factor and form a new prior.

Figure 2: Graphical Representation of Group Assignment with Soft Constraints

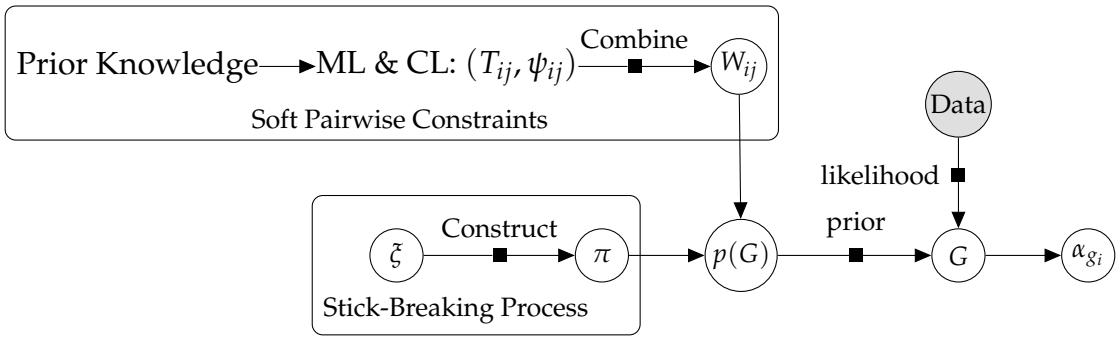

2.3.4 The Effect of Constraints and Scaling Constant

The function $p(\psi, T|G)$ is crucial in shifting the prior probability of G. It is straightforward to show that $T_{ij}\delta_{ij} = 1$ when the constraint between i and j is met in a group partitioning defined by G. The prior probability for G is therefore increased since $\left[\psi_{ij}/(1-\psi_{ij})\right]^c \geqslant 1$. Similarly, if a group partitioning G violates the constraint between i and j, then $T_{ij}\delta_{ij} = -1$ and the prior probability for G drops due to $\left[\psi_{ij}/(1-\psi_{ij})\right]^{-c} \leqslant 1$. Therefore, with $p(\psi, T|G)$, the resulting group partition is shrunk toward our prior knowledge without imposing any constraint.

We then examine the effect of constraints on the prior distribution with fixed c. Let's consider a simplified scenario with $N = 2$ units where there are at most two groups. We repeatedly draw samples from the DP prior utilizing the stick-breaking procedure and record the group indices and number of groups. For illustrative purpose, we fix the concentration parameter $a = 1$ so that $\Pr(g_1 = g_2) = \Pr(g_1 \neq g_2) = 0.5$[4] when there is no constraints. We specify ML and CL constraints with two different levels of accuracy each. The units are then randomly assigned to each group according to (2.13).

Figure 3 illustrates the effect of soft constraints on group assignment when $c = 0.5$. We consider five distinct scenarios where (T_{12}, ψ_{12}) are different. We record the number of groups and then calculate the fraction of one group or two groups. In the baseline scenario *"No Cstr"*, there is no prior belief, therefore the probability of $K = 1$ and $K = 2$ are equal. Next, we employ two distinct level of accuracy for each type of soft constraint. For each soft constraint, we have $\psi_{12} = 0.75$ in the first case (#1) while $\psi_{12} = 0.55$ in the second case (#2), indicating that we are confident and relatively less confident in our prior knowledge, respectively. The bars in the figures depict the fraction of group partitions containing one or two groups. As demonstrated by the black dashed lines, the theoretical value for the probability of having one or two groups in the absence of constraints is 0.5.

In this example, we demonstrate how a soft ML constraint between units 1 and 2 considerably decreases the number of groups by assigning both units to the same group. A higher

[4] Antoniak (1974) provides analytical formulas for probabilities of more general events with larger N. In this example, $\Pr(g_1 = g_2) = \frac{1}{a+1}$.

ψ_{12}, in particular, results in a greater proportion of the single group. In contrast, the soft CL constraint separates and assigns these two units to different groups. A more precise CL constraint increases the likelihood of forming two groups. Notably, even with a large ψ_{12}, the soft constraint framework maintains the possibility of breaching the constraint, which is another important feature that preserves the chance of correctly assigning group indices even if the constraint is erroneous. Lastly, ML and CL constraints affect group partitioning symmetrically.

Figure 3: Impacts of Soft *Must-Link* and *Cannot-Link* Constraints on the Group Partitioning

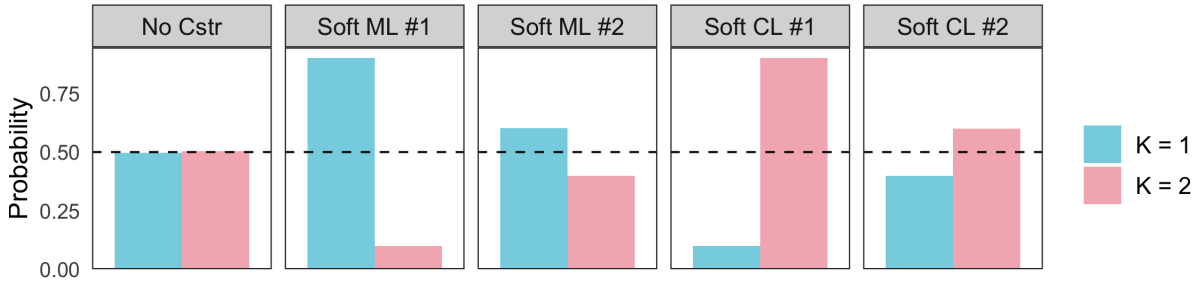

Notes: The results are based on 50,000 draws. In the cases with soft constraints, we draw samples using rejection sampling in which the target distribution is $p(G|W)$ and proposal distribution is $p(G)$.

Next, we explore the role of the scaling constant c given (ψ, T). We are able to derive the analytical formulae for $\Pr(K = 1)$ and $\Pr(K = 2)$ in this example. When $N = 2$, listing all partitions G is possible and we can calculate the probabilities for each G using (2.16). It is straightforward to express $\Pr(K = 1)$ as a function of c and (ψ_{12}, T_{12}):

$$\Pr(K = 1) = \frac{1}{1 + \exp(-4cW_{12})} = \frac{1}{1 + \left(\frac{\psi_{12}}{1-\psi_{12}}\right)^{-4cT_{ij}}} \tag{2.17}$$

Figure 4 traces out the equation (2.17) for a range of c values. The left panel (a) displays the curve for an ML constraint. Firstly, observe that when $c = 0$, $\Pr(K = 1)$ remains unchanged at 0.5 regardless of the value of ψ. This is the situation in which c eliminates the constraint's effect on the prior. Next, given a particular c, $Pr(K = 1)$ increases in ψ, which agrees with the example in 3. When ψ is fixed, increasing c can easily result in a higher $\Pr(K = 1)$, indicating that a larger c value magnifies the effect of the ML constraint. In contrast, panel (b) depicts the curve for a CL constraint. It is evident that c has a similar effect to that of ML constraint, but in the other direction. $\Pr(K = 1)$ reduces significantly as c increases. Overall, a large c augments the influence of constraints on G, whereas a small c diminishes it.

In the general case where numerous ML and CL constraints are enforced, c concurrently affects all constraints. In other words, the value of c determines the "strength" of the prior belief regarding G. If the prior belief is coherent with the real group partition, it would be preferable to have a large c to intensify the effect on constraints, allowing prior information to take precedence over data information, and vice versa.

Figure 4: $\Pr(K = 1)$ as a Function of Accuracy ψ_{ij} and c

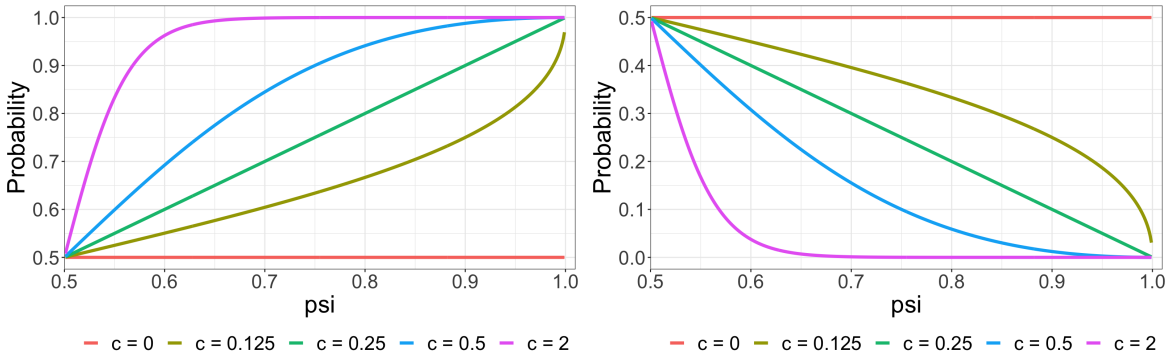

(a) Must-Link (b) Cannot-Link

Remark 2.6. *We propose to find the optimal c that maximizes marginal data density using grid search, see details in Appendix B.1.2. Alternatively, the scaling constant c can be pair-specific and data-driven. Basu et al. (2004b), for instance, assume that c_{ij} is a function of observables, i.e., $c_{ij} = \psi(x_i, x_j; T_{ij})$. $\psi(x_i, x_j; T_{ij})$ is monotonically increasing (decreasing) in the distance between units i and j if they are involved in must-link (cannot-link) constraints. This reflects the belief that if two more distant units are assumed to be must-linked (cannot-linked), their constraint should be given more (less) weight.*

2.3.5 Specification of Soft Pairwise Constraints

In reality, it is practical to establish soft pairwise constraints based on existing information on group, even if it is not the genuine group partitioning. In the empirical analysis, for instance, we use the official expenditure categories of CPI sub-indices to construct soft pairwise constraints. When information on group partitioning is insufficient, especially when the number of units is large, these official spending categories may serve as a trustworthy starting point. Before formalizing the idea, we first introduce the prior similarity matrix $\mathcal{C}$ which is a $N \times N$ symmetric matrix describing the prior probability of any two units belonging to the same group, i.e., $\mathcal{C}_{ij} = \Pr(g_i = g_j)$ conditional on all hyperparameters in the prior.

The general idea to derive soft pairwise constraints using the existing information on a preliminary group partitioning $\bar{G}$. We start with the type of constraints T_{ij} between any two units. Given the preliminary group structure, such as geographic classifications, we specify ML constraints for all pairs of units within the same group and CL constraints for all pairs of units from different groups. This means that we believe the preliminary group structure is correct *apriori*. Despite the fact that more elaborate and subtle constraints might be implemented, this rough specification is usually a great starting point.

The accuracy psi_ij for constraints is then specified. When our prior knowledge is limited or the number of units is large, we cannot specify ψ_{ij} for all pairs with solid knowledge of

them. Instead, one desirable yet simple choice is to assume ψ_{ij} again based on preliminary group partitioning $\bar{G}$. More specifically, all units in the same group are must-linked with identical ψ_{ij}^{ML}, i.e., for units i and j from the group $\bar{g}_i = \bar{g}_j = \bar{g}$, we have $\psi_{ij}^{ML} = c_{\bar{g}}$. Units from different groups are assumed to be cannot-linked with identical ψ_{ij}^{CL}, i.e., for units i and j from distinct groups, we assume $\psi_{ij}^{CL} = c_{\bar{g}_i\bar{g}_j}$ and $c_{\bar{g}_i\bar{g}_j} = c_{\bar{g}_j\bar{g}_i}$. Following this strategy, ψ_{ij} depends solely on $\bar{G}$ and hence two units from the same group would have identical soft pairwise constraints with other units. Notice that the number of possible distinct ψ_{ij} reduces from $N(N-1)/2$ to $\bar{K}(\bar{K}+1)/2$, where $\bar{K}$ is the number of groups in $\bar{G}$ and $\bar{K} \ll N$.

The aforementioned specification strategy induces a block prior similarity matrix, i.e., for an unit i, $\mathcal{C}_{ij} = \mathcal{C}_{ik}$ if $\bar{g}_j = \bar{g}_k$. Intuitively, if two units have identical soft pairwise constraints and hence posit an identical relationship with all other units, they are equivalent and exchangeable. As a result, these units should have an equal prior probability of sharing the same group index with any other units. More formally,

Theorem 1 (Stochastic Equivalence)**.** *Given two units j, k from the same prior group, if $\psi_{jm} = \psi_{km}$ for all $m = 1, 2, .., N$, then $\Pr(g_i = g_j) = \Pr(g_i = g_k)$ for all unit i.*

Theorem 1 echos the concept of *stochastic equivalence* (Nowicki and Snijders, 2001) in stochastic block model[5] (SBM) (Holland et al., 1983). In less technical terms, for nodes p and q in the same group, p has the same (and independent) probability of connecting with node r, as q does. Interestingly, this relationship is not coincidental. The prior draw of group membership with the aforementioned specification of T_{ij} and ψ_{ij} can be viewed as a simulation of a simple SBM. In a simple SBM, there are two essential components: a vector of group memberships and a block matrix, each element of which represents the edge probability of two nodes, given their group memberships. In our case, the preliminary group structure serves as the group membership in SBM. The DP prior and the weight (or T_{ij} and ψ_{ij}) of each constraint induce a prior similarity probability comparable to the block matrix.

Figure 5 shows the prior similarity matrix of an example of 90 units. The preliminary group structure divides units into 3 groups, with groups 1, 2 and 3 containing 25, 30 and 35 units, respectively. This prior similarity matrix is based on the aforementioned specification strategy, so it becomes a block matrix with equal entries in each of nine blocks. Units within the same group are stochastically equivalent, as their prior probabilities of being grouped not only with each other but also with units from other groups are the same. As a result, the similarity probability of each pair depends solely on their preliminary membership (and ψ).

3 Posterior Analysis

This section describes the procedure for analyzing posterior distributions for the baseline model described in (2.1) with the priors specified in Section 2.3.3. The joint posterior distri-

[5]For a more comprehensive review of the stochastic block model, see Lee and Wilkinson (2019).

Figure 5: Prior Similarity Matrix under Stochastic Equivalence

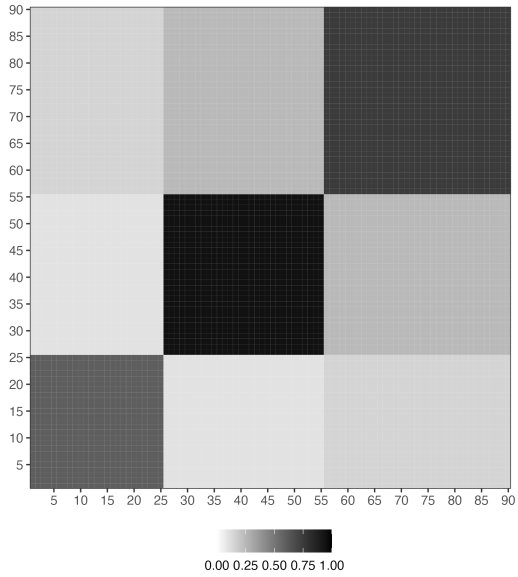

bution of model parameters is

$$\begin{aligned} & p(\alpha, \sigma^2, \Xi, a, G|Y, X, W, \phi) \\ \propto\ & p(Y|X, \alpha, \sigma^2, G)p(\alpha, \sigma^2|\phi)p(G|\Xi)p(W|G)p(\Xi|a)p(a), \end{aligned} \tag{3.1}$$

where $p(Y|X, \alpha, \sigma^2, G)$ is the likelihood function given by equation (2.1) for an i.i.d. model conditional on group indices G, and $p(W|G)$ is the additional term of pairwise constraints with the form $p(W|G) = \prod_{i=1}^{N} \prod_{j=1}^{N} \exp\left(cW_{ij}\delta_{ij}\right)$.

3.1 Posterior Sampling

Draws from the joint posterior distribution can be obtained by using blocked Gibbs sampling. The algorithm is derived from Ishwaran and James (2001) and Walker (2007). Due to the use of a finite-dimensional prior and truncation, the method described in Ishwaran and James (2001) cannot truly address our demand for estimating the number of groups without a predetermined value or upper bound. We employ the slice sampler (Walker, 2007), which is the exact block Gibbs sampler for the posterior computation in infinite-dimensional Dirichlet process models, modifying the block Gibbs sampler of Ishwaran and James (2001) to avoid truncation approximations. Walker (2007) augments the posterior distribution with a set of auxiliary variables consisting of i.i.d. standard uniform random variables, i.e., $u_i \overset{iid}{\sim} U(0,1)$ for $i = 1, 2, .., N$. The augmented posterior is then represented as

$$\begin{aligned} & p(\alpha, \sigma^2, \Xi, a, G, u|Y, X, W, \phi) \\ \propto\ & p(Y|X, \alpha, \sigma^2, G)p(\alpha, \sigma^2|\phi)p(W|G)p(\Xi|a)p(a) \prod_i \mathbf{1}(u_i \leqslant \pi_{g_i}). \end{aligned} \tag{3.2}$$

where $\prod_i \mathbf{1}(u_i \leqslant \pi_{g_i})$ is substituted for $p(G|\Xi)$ in the equation (3.1).

There are two advantages to incorporating the auxiliary variable u into the model. First and foremost, u directly determines the largest possible number of groups in each sampling iteration. This reduces the support of G and Ξ to a finite space, enabling us to solve a problem of finite dimensions without truncation. Furthermore, u have no effect on the joint posterior of other parameters because the original posterior can be restored by integrating out u_i for $i = 1, 2, ..., N$.

The Gibbs sampler in Algorithm 1 below simulates the joint posterior distribution of $\left(\alpha, \sigma^2, \Xi, a, G, u\right)$, by breaking this vector into blocks and sequentially sampling for each block conditional on the current draws for the other parameters and the data. The full conditional distributions for each block are easily derived using the conjugate priors specified in Section 2.

Algorithm 1. *(Gibbs Sampler for Random Coefficients Model with Soft Pairwise Constraints)*
For each iteration $s = 1, 2, .., N_{sim}$,

(i) Calculate number of active groups: $K^a = \max_{1 \leqslant i \leqslant N} g_i^{(s-1)}$.

(ii) Group heterogeneity: draw $\alpha_k^{(s)}$ *from* $p\left(\alpha_k | \sigma^{2(s-1)}, G^{(s-1)}, Y, X\right)$ *for* $k = 1, 2, ..., K^a$.

(iii) Group heteroscedasticity: draw $\sigma_k^{2(s)}$ *from* $p\left(\sigma_k^2 | \alpha^{(s)}, G^{(s-1)}, Y, X\right)$ *for* $k = 1, 2, ..., K^a$.

(iv) Group "stick length": draw $\xi_k^{(s)}$ *from* $p\left(\xi_k | a^{(s-1)}, G^{(s-1)}\right)$ *for* $k = 1, 2, ..., K^a$ *and update group probability in accordance to the stick-breaking procedure.*

(v) Auxiliary variable: draw $u_i^{(s)}$ *from* $p\left(u_i | \Xi^{(s)}, G^{(s-1)}\right)$ *for* $i = 1, 2, ..., N$ *and calculate* $u^* = \min_{1 \leqslant i \leqslant N} u_i$.

(vi) DP concentration parameter: draw a latent variable η *from Beta*$(a + 1, N)$ *and draw* $a^{(s)}$ *from* $p\left(a | \eta, K^a\right)$.

(vii) Generate potential groups based on u^* *and find the maximal number of group* K^*.

(xi) Group indices: draw g_i *from* $p\left(g_i = k | \alpha^{(s)}, \sigma^{2(s)}, G^{(i)}, u, Y, X, W\right)$ *for* $i = 1, 2, ..., N$ *and* $k = 1, 2, ..., K^*$.

For illustrative purposes, we focus primarily on the posterior densities of major parameters and omit details on step (vii). In short, step (vii) creates potential groups if the current iteration permits more groups. Detailed derivations and explanation of each step are provided in Appendix C.2.

It is worth noting that the steps for implementing the DP prior with or without soft pairwise constraints are the same, except for the last step for group indices. This is due to

the fact that soft pairwise constraints only affect other parameters through the group indices. Without soft pairwise constraints, the conditional posterior of G is given by,

$$p\left(g_i = k|\alpha, \sigma^2, G^{(i)}, u, Y, X\right) \propto p\left(y_i|\alpha_k, \sigma_k^2, Y, X\right) \mathbf{1}\left(u_i < \pi_k\right). \tag{3.3}$$

In this framework, adding soft pairwise constraints merely requires including additional term $p(W_i|G) = \prod_{j \neq i, g_j = k} \exp\left(2cW_{ij}\delta_{ij}\right)$ to rewards (penalizes) the abidance (violation) of constraints,

$$p\left(g_i = k|\alpha, \sigma^2, G^{(i)}, u, Y, X, W\right) \propto p\left(y_i|\alpha_k, \sigma_k^2, Y, X\right) \mathbf{1}\left(u_i < \pi_k\right) p(W_i|G). \tag{3.4}$$

which is fairly handy to implement.

Remark 3.1. *Notice that the algorithm 1 is a conditional Gibbs sampling algorithm, which might be quite computationally expensive when analyzing large datasets. In a typical application of forecasting monthly individual US firm-level stock returns, for example, a balanced panel might easily include more than 3,000 firms, so that one may devote several hours (or days) to computation. In this case, we may implement the sequential updating and greedy search (SUGS) algorithm by Wang and Dunson (2011) which essentially simplifies the algorithm 1 with approximation. The SUGS algorithm allows fast yet accurate approximate Bayes inferences under DP priors with just a single cycle of simple calculations for each unit, while also producing marginal likelihood estimates to be used in selecting the constant c.*

3.2 Determining Partition

In contrast to popular algorithms such as agglomerative hierarchical clustering or the *KMeans* algorithm, which return a single clustering solution, Bayesian nonparametric models provide a posterior over the entire space of partitions, enabling the assessment of statistical properties, such as the uncertainty on the number of groups.

However, when the group structure is part of the major conclusion of an empirical analysis, the point estimate of group structure becomes crucial. Wade and Ghahramani (2018) discuss in detail an appropriate point estimate of the group partitioning based on the posterior draws. From the decision theory, the point estimate G^* minimizes the posterior expected loss,

$$G^* = \underset{\widehat{G}}{\operatorname{argmin}}\, \mathbb{E}\left[L(G, \widehat{G})|Y\right] = \underset{\widehat{G}}{\operatorname{argmin}} \sum_{G} L(G, \widehat{G}) p\left(G|Y\right)$$

where the loss function $L(G, \widehat{G})$ is the variation of information by Meilă (2007), which measures the amount of information lost and gained in changing from partition G to $\widehat{G}$. Specifically, they show that the optimal group partitioning can be identified based on the posterior

similarity matrix,

$$g^* = \underset{\hat{g}}{\operatorname{argmin}} \sum_{i=1}^{N} \log \left(\sum_{j=1}^{N} \mathbf{1}\left(\hat{g}_j = \hat{g}_i\right) \right) - 2 \sum_{i=1}^{N} \log \left(\sum_{j=1}^{N} P\left(g_j = g_i | Y, X, W\right) \mathbf{1}\left(\hat{g}_j = \hat{g}_i\right) \right) \tag{3.5}$$

where $P\left(g_j = g_i | Y, X, W\right)$ is the (i, j) entry of the posterior similarity matrix. We refer to Wade and Ghahramani (2018) for additional properties and empirical evaluations.

Remark 3.2. *Another way to find group memberships is to assign units to the groups with the highest posterior probability. This is equivalent to using the 0-1 loss function* $L(G, \widehat{G}) = \mathbf{1}(G = \widehat{G})$ *and the resulting point estimate is the posterior mode. Though it looks natural, this is in fact flawed. A partition that deviates from the truth in the allocation of only one observation is penalized the same as a partition that deviates from the truth in the allocation of numerous observations, making this loss function undesirable since it ignores similarity between two partitions. Furthermore, it is generally recognized that the mode may not accurately reflect the distribution's center. As a result, we don't go in that direction.*

3.3 Connection to Constrained *KMeans* Algorithm

The procedure of Gibbs sampling with soft constraints in Algorithm 1 is closely related to constrained clustering in the computer science literature. In this parallel literature, constrained clustering refers to the process of introducing prior knowledge to guide a clustering algorithm. For a subset of the data, the prior knowledge takes the form of constraints that supplement the information derived from the data via a distance metric.

We start with a brief review of the Pairwise Constrained KMeans (*PC-KMeans*) clustering algorithm by Basu et al. (2004a), which is a well-known clustering algorithm in the field of semi-supervised machine learning. It's a pairwise constrained variant of the standard *KMeans* algorithm in which an augmented objective function is used in the assignment step. Given a collection of observations $(y_1, y_2, \ldots, y_N)$, a set of must-link constraints $\mathcal{M}$, a set of cannot-link constraints $\mathcal{C}$, the cost of violating constraints $w = \{w_{ij}^m, w_{ij}^c\}$ and the number of groups K, the *PC-KMeans* algorithm divides N observations into K groups (the *assignment* step) so as to minimize the following objective function,

$$\underbrace{\frac{1}{2} \sum_{k=1}^{K} \sum_{i \in B_k} \|y_i - \mu_k\|^2}_{\text{within-cluster sum of squares}} + \underbrace{\sum_{(i,j) \in \mathcal{M}} \omega_{ij}^m \mathbf{1}\left(g_i \neq g_j\right) + \sum_{(i,j) \in \mathcal{C}} \omega_{ij}^c \mathbf{1}\left(g_i = g_j\right)}_{\text{cost of violation}}, \tag{3.6}$$

where μ_k is the centroid of group k, i.e., $\mu_k = \frac{1}{|B_k|} \sum_{i \in B_k} y_i$, B_k is the set of units assigned to group k, and $|B_k|$ is the size of group k. The first part is the objective function for the conventional *KMeans* algorithm, while the second part accounts for the incurred cost of violating either ML constraints (w_{ij}^m) or CL constraints (w_{ij}^c).

Similar to *KMeans*, *PC-KMeans* alternates between reassigning units to groups and recomputing the means. In the assignment step, it determines a disjoint K partitioning that minimizes (3.6). Then the update step of the algorithm recalculates centroids of observations assigned to each cluster and updates μ_k for all k.

By applying asymptotics to the variance of distributions within the model, we demonstrate linkages between the posterior sampler of our constrained BGFE estimator and *KMeans*-type algorithms in Theorem 2. We investigate small-variance asymptotics for posterior densities, motivated by the asymptotic connection between the Gibbs sampling algorithm for the Dirichlet process mixture model and *KMeans* (Kulis and Jordan, 2011), and demonstrate that the Gibbs sampling algorithm for the CBG estimator with soft constraints encompasses the constrained clustering algorithm *PC-KMean* in the limit.

Theorem 2. (Equivalency between BGFE with Soft Constraints and *PC-KMeans*)
If the following conditions hold,

(i) Grouped pattern is in fixed-effects but not in slope coefficients, i.e., $x_{it} = 1$. Other covariates might be introduced, but they cannot have grouped effects on y_{it};

(ii) The number of group is fixed at K;

(iii) Homoscedasticity: $\sigma_k^2 = \sigma^2$ for all $k = 1, 2, ..., K$;

(iv) Constraint weights is scaled by the variance of errors: $W_{ij} \to W_{ij}/\sigma^2$;

then the proposed Gibbs sampling algorithm for the BGFE estimator with soft constraint embodies the PC-KMeans clustering algorithm in the limit as $\sigma^2 \to 0$. In particular, the posterior draw of group indices G is the solution to the PC-KMeans algorithm.

We return to the world of grouped fixed-effects models. In fact, the clustering algorithm is essential for BM and Bonhomme et al. (2022), who use the *KMeans* algorithm to reveal the group pattern in the fixed-effects. With the theorem described above, it motivates a *constrained* version of BM's GFE estimator. We show that it is straightforward to incorporate prior knowledge in the form of soft paired restrictions into the GFE estimator. The *soft pairwise constrained* grouped fixed-effects (SPC-GFE) estimator is defined as the solution to the following minimization problem given the number of groups K:

$$\left(\widehat{\theta}, \widehat{\alpha}, \widehat{G}\right) = \underset{\theta,\alpha,G}{\operatorname{argmin}} \sum_{i=1}^{N}\sum_{t=1}^{T} \left(y_{it} - x_{it}'\theta - \alpha_{g_i t}\right)^2 + c\left[\sum_{(i,j)\in\mathcal{M}} w_{ij}^m \mathbf{1}\left(g_i \neq g_j\right) + \sum_{(i,j)\in\mathcal{C}} w_{ij}^c \mathbf{1}\left(g_i = g_j\right)\right], \quad (3.7)$$

where the minimum is taken over all possible partitions G of the N units into K groups, common parameters θ, and group-specific time effects α. w_{ij}^m and w_{ij}^c are the user-specified costs on ML and CL constraints.

For given values of θ and α, the optimal group assignment for each individual unit is

$$\widehat{g}_i(\theta,\alpha) = \underset{g\in\{1,\dots,K\}}{\operatorname{argmin}} \sum_{i=1}^{N}\sum_{t=1}^{T}\left(y_{it} - x_{it}'\theta - \alpha_{g_i t}\right)^2 + c\left[\sum_{(i,j)\in\mathcal{M}} w_{ij}^{m}\mathbf{1}\left(g_i \neq g_j\right) + \sum_{(i,j)\in\mathcal{C}} w_{ij}^{c}\mathbf{1}\left(g_i = g_j\right)\right], \quad (3.8)$$

where we essentially apply the *PC-KMeans* algorithm to get the group partition. The SPC-GFE estimator of (θ,α) in (3.7) can then be written as

$$(\widehat{\theta},\widehat{\alpha}) = \underset{\theta,\alpha}{\operatorname{argmin}} \sum_{i=1}^{N}\sum_{t=1}^{T}\left(y_{it} - x_{it}'\theta - \alpha_{\widehat{g}_i t}\right)^2, \quad (3.9)$$

where $\widehat{g}_i = \widehat{g}_i(\theta,\alpha)$ is given by (3.8). θ and α are computed using an OLS regression that controls for interactions of group indices and time dummies. The SPC-GFE estimate of g_i is then simply $\widehat{g}_i(\widehat{\theta},\widehat{\alpha})$.

Remark 3.3. *While the SPC-GFE estimator takes use of soft constraints, it still requires a predetermined number of group K and model selection.*

4 Extensions

Within the domain of panel data models, the proposed constrained-based BGFE framework can be extended in multiple directions to allow for more subtle group structures or more covariates. In addition, the DP prior with soft pairwise constraints also applies to other related topics and models, such as clustering problems, heterogeneous treatment effects, and panel VARs.

4.1 Subtle Group Structure

Through the Dirichlet process defines a prior that possesses the clustering property and is flexible enough to incorporate pairwise constraints, the group structure itself is elementary. Aside from our prior belief on the group, the group structure, which is introduced in all α_i and σ_i^2, is entirely governed by the stick-breaking process defined in Equation (2.8). The stick length ξ_k, on which we have a prior, is independent of any regressors or time. Consequently, each unit is associated with a single group, and the membership remains constant across time.

To create an even more flexible and richer group structure, we provide insight into three possible extensions, each of which requires a set of more distinctive nonparametric priors. (1) overlapping group and (2) time-varying group and (3) dependent group.

Overlapping group structures allow for multi-dimensional grouping. This is a natural extension without having to greatly modify the proposed DP prior. Following Cheng et al.

(2019), each of α_i's and σ_i^2 may have its own group structure and a separate Dirichlet process is specified to each of them. As a result, units simultaneously belong to multiple groups based on the heterogeneous effects among regressors or cross-sectional heteroskedasticity.

Time-varying group structures allow the membership of the group to change over time. We could replace the DP by variants of the hierarchical Dirichlet process (Teh et al., 2006) to achieve this feature. In short, the hierarchical Dirichlet process (HDP), a nonparametric Bayesian approach to clustering grouped data, is now the foundation of the prior. The time dimension naturally divides the panel data into T groups, and a Dirichlet process is assumed for each group, with all Dirichlet processes having the same base distribution, which is distributed according to a global base distribution. The HDP allows each group to have its own cluster, but most importantly, these clusters are shared across groups. This lays the groundwork for time-varying group structures, as it assumes that the number of clusters remains constant over time, while cluster memberships are subject to change. Variants of the HPD are then proposed to capture the time-persistence in group structures, including dynamic HDP (Ren et al., 2008) and sticky HDP (Fox et al., 2008, 2011). A closely related area in the frequentists' methods is to identify structure breaks in parameters with grouped patterns, see Okui and Wang (2021); Lumsdaine et al. (2022).

Dependent group structures allow the prior group probability to rely directly on a collection of characteristics. The dependence is introduced through a modification of the stick-breaking representation for DPs, where the group probabilities vary with the characteristics. Rodriguez and Dunson (2011) introduced the probit-stick breaking (PSB) process where the Beta random variables are replaced by normally distributed random variables transformed using the standard normal CDF. The PSB is defined by,

$$\pi_k(w_i) = \Phi(\zeta_k(w_i)) \prod_{j<k} \left[1 - \Phi(\zeta_j(w_i))\right], \tag{4.1}$$

where stochastic function ζ_k is drawn from Gaussian process $\zeta_k \sim GP(0, V_k)$ for $k = 1, 2, \cdots$ and w_i is the set of characteristics that are informative to the latent group. Other forms of dependence are also available, see Quintana et al. (2022) for a comprehensive review. A caveat of this approach is that analysis of group structure is confined to w_i observed by the researcher. The approach requires researchers to know possible key characteristics, be able to observe them and ensure they are informative. In many cases, however, these characteristics might be hard to justify by researchers.

4.2 More Covariates

The model in (2.1) can be combined with additive terms that capture individual and common effects of covariates,

$$y_{it} = \alpha_{g_i t}' x_{it} + \beta_i' w_{it} + \gamma' z_{it} + \varepsilon_{it}, \quad \varepsilon_{it} \sim N\left(0, \sigma_{g_i}^2\right), \tag{4.2}$$

where w_{it} has individual-specific effect on y_{it} and z_{it} has common effect on y_{it}. The Dirichlet process prior shown in this section is straightforward to extend to the model in (4.2) by specifying additional normal priors for both β_i and γ. The framework nests several popular approaches:

Example 4.1 (Grouped fixed-effects model)**.** Bonhomme and Manresa (2015), Kim and Wang (2019)

$$y_{it} = \alpha_{g_i t} + \beta' x_{it} + \varepsilon_{it}, \quad \varepsilon_{it} \sim N\left(0, \sigma^2\right). \tag{4.3}$$

Example 4.2 (Linear panel with grouped slope coefficients)**.** Lin and Ng (2012), Sarafidis and Weber (2015) and Su et al. (2016)

$$y_{it} = \alpha'_{g_i} w_{it} + \beta_i + \varepsilon_{it}. \tag{4.4}$$

Example 4.3 (Interactive fixed-effects model with grouped slope coefficients)**.** Su and Ju (2018)

$$y_{it} = \alpha'_{g_i} x_{it} + \beta'_i w_t + \varepsilon_{it}. \tag{4.5}$$

Example 4.4 (Dynamic panel data model)**.**

$$y_{it} = \alpha_{g_i t} + \rho_i y_{it-1} + \gamma' z_{it} + \varepsilon_{it}. \tag{4.6}$$

Example 4.5 (Standard fixed-effects model)**.**

$$y_{it} = \alpha_t + \beta_i + \gamma' z_{it} + \varepsilon_{it}. \tag{4.7}$$

4.3 Beyond Panel Data Models

Although we concentrate on panel data model, our framework of the DP prior with soft pairwise constraints applies to other models where the group structure are crucial.

Gaussian Mixture Model

If we ignore covariates and focus exclusively on group membership, we essentially face a classical clustering problem with an infinite-dimensional mixture model. A typical probabilistic model is the infinite Gaussian mixture model (Rasmussen, 1999), where the data itself is assumed to be drawn from a mixture of Gaussian components

$$y_i \sim \sum_{k=1}^{\infty} \pi_k N(\mu_k, \Sigma_k), \tag{4.8}$$

where π_k are the mixture weights. With soft pairwise constraints, observations are clustered in accordance with prior belief.

Heterogeneous Treatment Effects

Following the potential outcomes framework of Rubin (1974), we posit the existence of potential outcomes $y_i(1)$ and $y_i(0)$ corresponding respectively to the response the i th subject would have experienced with and without the treatment, and define the treatment effect at x as

$$\tau(x) = \mathbb{E}\left[y_i(1) - y_i(0) \mid x_i = x\right]. \tag{4.9}$$

Existing methods estimate (4.9) by using several machine learning algorithms (Hill, 2011; Athey and Imbens, 2016; Wager and Athey, 2018). These methods are built on the idea that researchers find the subsamples across which the effect of a treatment differs out of all possible subsamples on the basis of the values of x_i. Instead of trying to discover valid subsets of the data, Shiraito (2016) directly models the outcome as a function of the treatment and pre-treatment covariates x_i and estimate of the distribution of conditional average treatment effects (CATE) across units by employing the Dirichlet process.

$$y_i = \tau_{g_i} T_i + \gamma'_{g_i} x_i + \varepsilon_i, \quad \varepsilon_i \overset{\text{iid}}{\sim} \mathcal{N}\left(0, \sigma^2_{g_i}\right), \tag{4.10}$$

where T is the binary treatment variable. *** what can we do with constraints?

Panel VARs

Panel VARs (Holtz-Eakin et al., 1988; Canova and Ciccarelli, 2013, and references therein.) has been widely used in macroeconomic analysis and policy evaluations to capture the interdependency across sectors, markets, and countries. Nevertheless, the large dimension of panel VARs typically makes the curse of dimensionality a severe problem. Billio et al. (2019) propose nonparametric Bayesian priors that cluster the VAR coefficients and induce group-level shrinkage. Our paradigm with the DP prior with soft pairwise constraints is applicable to their method and injects prior information on groups into the underlying Granger causal networks.

Panel VARs have the same structure as VAR models, in the sense that all variables are assumed to be endogenous and interdependent, but a cross-sectional dimension is added to the representation. Thus, let Y_t be the stacked version of y_{it}, the vector of J variables for each unit $i = 1, \ldots, N$, i.e., $Y_t = (y'_{1t}, y'_{2t}, \ldots y'_{Nt})'$. Then a panel VAR is

$$Y_t = A_0 + A_1 Y_{t-1} + A_2 Y_{t-2} + ... + A_p Y_{t-p} + u_t, \quad i = 1, \ldots, N, \tag{4.11}$$

where u_t is a $J \times 1$ vector of idiosyncratic errors and A_0 and A_j are $NJ \times NJ$ matrices of coefficients.

The main feature of Billio et al. (2019) is to specify a prior that blends the DP prior with Lasso prior for each of A_0 and A_j, such that the VAR coefficients are either shrunk toward 0 or clustered at multiple non-zero locations. Our proposed DP prior with soft pairwise constraints, in the meantime, fit into their framework by replacing the original DP prior and permitting richer structure within each coefficient matrix. As the values for nonzero

coefficients form Granger causal networks, equipping with soft pairwise constraints may result in a more plausible network by taking researchers' expertise into account.

5 Empirical Applications

We apply our panel forecasting methods to the following two empirical applications: inflation of the U.S. CPI sub-indices and the income effect on democracy. The first application focuses mostly on predictive performance, whereas the second application focuses primarily on parameter estimation and group structure.

5.1 Posterior Predictive Densities and Performance Evaluation

5.1.1 Posterior Predictive Densities

We generate one-step ahead forecasts of $y_{i,T+1}$ for $i = 1, ..., N$ conditional on the history of observations

$$Y = [y_1, y_2, ..., y_N], y_i = [y_{i1}, y_{i2}, ..., y_{iT}]',$$
$$X = [x_1, x_2, ..., x_N], x_i = [x_{i1}, x_{i2}, ..., x_{iT}]',$$

and newly available variables x_{iT+1} at $T + 1$.

The posterior predictive distribution for unit i is given by

$$p(y_{iT+1}|Y, X) = \int p(y_{iT+1}|Y, X, \Theta)p(\Theta|Y, X)d\Theta, \tag{5.1}$$

where Θ is a vector of parameters $\Theta = \left(\alpha_{g_i}, \sigma^2_{g_i}, g_i\right)$. This density is the posterior expectation of the following function:

$$p(y_{iT+1}|Y, X, \Theta) = \sum_{k=1}^{K(G)} \mathbf{1}(g_i = k)p\left(y_{iT+1}|Y, X, \Theta\right), \tag{5.2}$$

which is invariant to relabeling the components of the mixture and $K(G)$ is the number of groups in G. Given S posterior draws, the posterior predictive distribution estimated from the MCMC draws is

$$\hat{p}(y_{iT+1}|Y, X) = \frac{1}{S}\sum_{j=1}^{S}\left[\sum_{k=1}^{K^{(j)}(G)} \mathbf{1}(g_i = k)p\left(y_{iT+1}|Y, X, \Theta^{(j)}\right)\right]. \tag{5.3}$$

We can therefore draw samples from $\hat{p}(y_{iT+1}|Y, X)$ by simulating (2.1) forward conditional on the posterior draws of Θ and observations. Note that MCMC exhibits the true Bayesian predictive distribution, implicitly integrating over the entire underlying parameter space.

5.1.2 Point Forecasts

We evaluate the point forecasts via the Root Mean Squared Forecast Error (RMSFE) under the quadratic compound loss function averaged across units. Let $\hat{y}_{iT+1|T}$ represent the predicted value conditional on the observed data up to period T, the loss function is written as

$$L\left(\widehat{y}_{1:N,T+1|T}, y_{1:N,T+1}\right) = \frac{1}{N}\sum_{i=1}^{N}\left(\hat{y}_{iT+1|T} - y_{iT+1}\right)^2 = \frac{1}{N}\sum_{i=1}^{N}\hat{\varepsilon}^2_{iT+1|T}, \tag{5.4}$$

where $y_{i,T+1}$ is the realization at $T+1$ and $\hat{\varepsilon}_{iT+1|T}$ denote the forecast error.

The optimal posterior forecast under quadratic loss function is obtain by minimizing the posterior risk,

$$\begin{aligned}\hat{y}_{1:N,T+1|T} &= \underset{\hat{y}\in\mathbb{R}^N}{\operatorname{argmin}} \int_{-\infty}^{\infty} L\left(\hat{y}, y_{1:N,T+1}\right) p(y_{1:N,T+1}|Y) dy_{1:N,T+1} \\ &= \underset{\hat{y}\in\mathbb{R}^N}{\operatorname{argmin}} \frac{1}{N}\sum_{i=1}^{N} E\left[\left(\hat{y} - y_{iT+1}\right)^2 |Y\right]. \end{aligned} \tag{5.5}$$

This implies optimal posterior forecast is the posterior mean,

$$\hat{y}_{i,T+1|T} = E\left(y_{iT+1}|Y\right), \text{ for } i = 1, \ldots, N. \tag{5.6}$$

Conditional on posterior draws of parameters, the mean forecast can be approximated by the Monte Carlo averaging,

$$\hat{y}_{i,T+1|T} \approx \frac{1}{S}\sum_{j=1}^{S}\hat{y}^{(j)}_{iT+1|T} = \frac{1}{S}\sum_{j=1}^{S}\hat{\alpha}^{(j)'}_{g_i} x_{iT+1}. \tag{5.7}$$

Finally, the RMSFE across units is given by

$$RMSFE_{T+1} = \sqrt{\frac{1}{N}\sum_{i=1}^{N}\left(y_{i,T+1} - \hat{y}_{i,T+1}\right)^2}. \tag{5.8}$$

5.1.3 Density Forecasts

To compare the performance of density forecasts for various estimators, we report the average log predictive scores (LPS) to assess the performance of the density forecast from the view of the probability distribution function. As suggested in Geweke and Amisano (2010), the LPS for a panel reads as,

$$LPS_{T+1} = -\frac{1}{N}\sum_{i=1}^{N}\ln\int p\left(y_{iT+1}|Y, X, \Theta\right) p(\Theta|Y, X) d\Theta, \tag{5.9}$$

where the expectation can be approximated using posterior draws:

$$\int p\left(y_{iT+1}|Y,X,\Theta\right)p(\Theta|Y,X)d\Theta \approx \frac{1}{S}\sum_{j=1}^{S} p\left(y_{iT+1}|Y,X,\Theta^{(j)}\right). \tag{5.10}$$

The following results are also robust to other metrics such as the continuous ranked probability score (Matheson and Winkler, 1976; Hersbach, 2000).

5.2 Inflation of the U.S. CPI Sub-Indices

Policymakers and market participants are very interested in the abilities to reliably predict the future disaggregated inflation rate. Central banks predict future inflation trends to justify interest rate decisions, control and maintain inflation around their targets. The Federal Reserve Board forecasts disaggregated price categories for short-term inflation forecasting (Bernanke, 2007). They rely primarily on the bottom-up approach that focuses on estimating and forecasting price behavior for the various categories of goods and services that make up the aggregate price index. On the other hand, Investors in fixed-income markets in the private sector wish to forecast future sectoral inflation in order to anticipate future trends in discounted real returns. Also, some private firms need to predict specific inflation components in order to forecast price dynamics and reduce risks accordingly.

In this section, we illustrate the use of constrained BGFE estimators with prior knowledge on the group pattern to forecast inflation rates for sub-indices of the U.S. Consumer Expenditure Index (CPI). We focus primarily on the one-step ahead point and density forecast. Due to space constraints, we only report the group partitioning for the most recent month in the main text.

5.2.1 Model Specification and Data

Model: We start by investigating the out-of-sample forecast performance of a simple, generic Phillips curve model. It is an autoregressive distributed lag (ADL) model with a group pattern in the intercept, coefficients, as well as error variance. The model is given by

$$y_{it+1} = \alpha_{g_i} + \sum_{j=0}^{p-1} \rho_{g_{i,j}} y_{it-j} + \beta_{g_i} u_t + \varepsilon_{it+1}, \quad \varepsilon_{it+1} \sim N(0, \sigma^2_{g_i}). \tag{5.11}$$

where y_{it} is year-over-year inflation rate, i.e., $y_{it} = \log(\text{price}_{it}/\text{price}_{it-12})$. u_t is the slack measure for the labor market, the unemployment gap. We fix p at 3 as the benchmark model would have the best predictive performance.

Data: We use the sub-indices of CPI for all urban consumer (CPI-U) that include food and energy. The raw data is obtained from the U.S. Bureau of Labor Statistics (BLS), which is

recorded on a monthly basis from January 1947 to August 2022. The CPI-U is a hierarchical composite index system that partitions all consumer goods and services into a hierarchy of increasingly detailed categories. It consists of eight major expenditure categories (1) Apparel; (2) Education and Communication; (3) Food and beverages; (4) Housing; (5) Medical Care; (6) Recreation; (7) Transportation; (8) Other goods and services. Each sector is composed of finer and finer sub-indexes until the entry levels or "leaves" are reached. This hierarchical structure can be represented as a tree structure, as shown in Figure 6. It is important to note that the parent series and its child series may be highly correlated and readily form a group due to the fact that parent series are generated from child series. For instance, the *Energy Services* is expected to correlated with its child series *Utility gas service* and *Electricity*. Due to our focus on group structure, it is vital to eliminate all parent series in order to prevent not just double-counting but also dubious grouping results. More details regarding the data are provided in Appendix F.1.

We focus on the CPI sub-indices after January 1990 for two reasons: (1) the number of sub-indices before 1990 was relatively small, diminishing the importance of the group structure; and (2) the consumption has been changed and more expenditure series were introduced in the 1990s as a result of the popularity of electronic products, food care, etc. After the elimination of all parent nodes, the unbalanced panel consists of 156 sub-indices in eight major expenditure categories. We employ rolling estimation windows of 48 months[6] and require each estimation sample to be balanced, removing individual series lacking a complete set of observations in a given window. Finally, we generate 324 samples with the first forecast computed for April 1995.

Figure 6: Hierarchical Structure of CPI

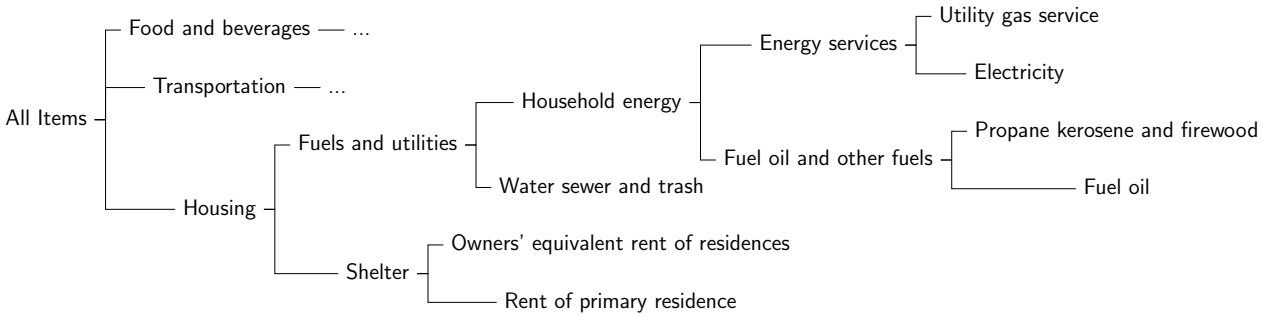

Estimators: We consider six estimators:

(i) *BGFE-he*: The baseline Bayesian grouped fixed-effects (BGFE) estimator. It assumes true model exhibits time-invariant grouped heterogeneity and grouped heteroskedasticity.

[6]The benchmark AR-he model has the best overall performance with a window size of 48.

(ii) *BGFE-ho*: homoskedastic version of *BGFE-he*.

(iii) *BGFE-he-cstr*: *BGFE-he* + constraints. The official expenditure categories are used to build ML and CL constraints: all units within the same categories are presumed to be must-linked, while units from different categories are believed to be cannot-linked. We specify equal accuracy for all ML and CL constraints, i.e., $\psi_{ij}^{ML} = 0.65$ and $\psi_{ij}^{CL} = 0.6$, following the method described in Section 2.3.5.

(iv) *Pooled OLS*: Bayesian pooled estimator that views α_i as a common parameter and ignore heteroskedasticity.

(v) *AR-he*: flat-prior estimator that assumes $p(\alpha_i) \propto 1$ corresponds to standard AR model with additional regressor u_t in this environment.

(vi) *AR-he-PC*: *AR-he* + the lagged value of the first principal component.

5.2.2 Results

We begin the empirical analysis by comparing the performance of point and density forecasts across 324 samples.Throughout the analysis, the Flat-he estimator serves as the benchmark as it essentially assumes individual effects.

In Figure 7, we present the frequency of each estimator with the lowest RMSFE in the panel (a) and the boxplot[7] of the ratio of RMSFE relative to the *AR-he* estimator in the panel (b). First, the AR-he and AR-he-PC estimators, which rely only on an individual's own past data, are not competitive in point forecasts and perform considerably worse than the others. This implies that it is highly advantageous to explore cross-sectional information to improve point forecasts. Moreover, there is no apparent victor in this setting despite the fact that BGFE-he-cstr, BGFE-he, BGFE-ho, and pooled OLS estimators all utilize cross-sectional information. Examining the box plot, we find that the BGFE-ho and pooled OLS estimators, which overlook heteroskedasticity, can achieve greater performance in some samples, but make poorer forecasts more often than the other estimators. BGFE-he-cstr and BGFE-h, on the other hand, typically outperform the benchmark and provide less variable forecasts, although they do not generally have the lowest RMSFE.

The revealing patterns of the density forecast are significantly distinct from those of the point forecast. Figure 8 depicts the log predictive score (LPS) for density forecast. The most notable pattern from the panel (a) is that our BGFE estimators are dominating and outperform the rest in over 90% of the samples. They emerge as the apparent winners in this case. Furthermore, the superiority of BGFE-ho and pooled OLS in point forecast vanishes when generating density forecast, as they never get the lowest LPS across samples. This also conforms that the heteroscedasticity is a well-known feature of the inflation time series (Clark

[7]The boundaries of the whiskers is based on the 1.5 IQR value. All other points outside the boundary of the whiskers are plotted as outliers in red crosses.

and Ravazzolo, 2015). We provide more results in Section 5.2.4 to explore the importance of heteroskedasticity in density forecast for the inflation. In the boxplot, we ignore BGFE-ho and pooled OLS and show the difference in LPS between the respective estimator and the AR-he estimator. As LPS differences represent percentage point differences, BGFE-he-cstr can provide density forecasts that are up to 30% more accurate comparing to the benchmark model. Finally, despite the fact that BGFE-he-cstr and BGFE-he estimators are mainly based on the same algorithm, the use of prior knowledge on group pattern further enhances the performance, resulting in the BGFE-he-cstr estimator having lower LPS and scoring the best model with the highest frequency.

With pairwise constraints across sub-indices, we provide a prior on G that shrinks the group structure toward the eight official expenditure categories with equal accuracy for all pairs inside each category. As Theorem 1 suggested, our prior specification essentially assumes that the probability of any two units in the same expenditure category being in the same group is equal and the prior group pattern is actually official expenditure category. We now examine the posterior of group structure to demonstrate how the distribution of G gets updated by data. In order to accomplish this, we construct a posterior similarity matrix (PSM) that contains the marginal posterior probabilities of any two units being in the same group. For illustrative purposes, we present the results for the last sample, in which we forecast CPI in August 2022. Figure 9 depicts the PSM generated by BGFE-he-crst for the series in the category of *Food and Beverages* and *Transportation*. A darker block indicates a higher posterior probability of being in one group. A common pattern emerges: even though some sub-indices join together more frequently, it is extremely unlikely that all series within the category belong to the same group, indicating that the official expenditure categories do not have the optimal group structure that would result in accurate forecasting. Instead, our suggested framework uses information from both prior beliefs and data to reinvent the group pattern, leading to improved forecasting performance.

Finally, we restrict our analysis to the point estimate of group partition, i.e., the single grouping solution, rather than the posterior over the whole universe of partitions. Figure 10 depicts the posterior point estimate of G for the last sample ended in August 2022, derived using the approach described in Section 3.2. Eight expenditure categories are divided into twelve groups of varied sizes. Two different forms of groups are generated based on the arrangement of their components. Groups 2, 3, 4, and 5 contain sub-indices from a variety of categories, with no clear dominance. In contrast, the majority of the series in groups 1 and 8, for example, belong to a certain category. Group 1 may refer to a *Food* group, whereas group 8 is a *Transportation* group. The detailed group 8 components are depicted in Figure 11. There are seven sub-indices from *Transportation*, including car and truck rentals, gasoline (regular, midgrade, and premium), other motor fuels, airline fares, and ship fares, and one series from *Housing* - fuel oil (for residential heating). Clearly, all sub-indices share a common trend and have a close relationship with energy and oil prices, which have increased since the Pandemic. This is an example demonstrating that our proposed algorithm exploits cross-

Figure 7: RMSFE - All Samples

(a) Freq. lowest RMSFE

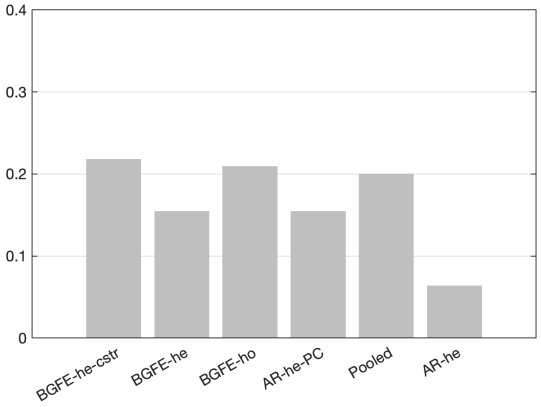

(b) Boxplot: RMSE_m / RMSE_{AR-he}

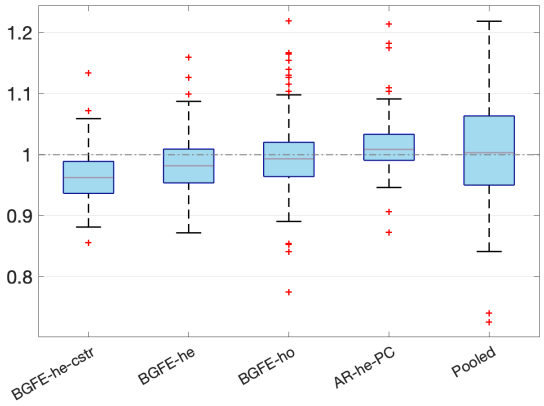

Figure 8: Log Predictive Scores - All Samples

(a) Freq. lowest LPS

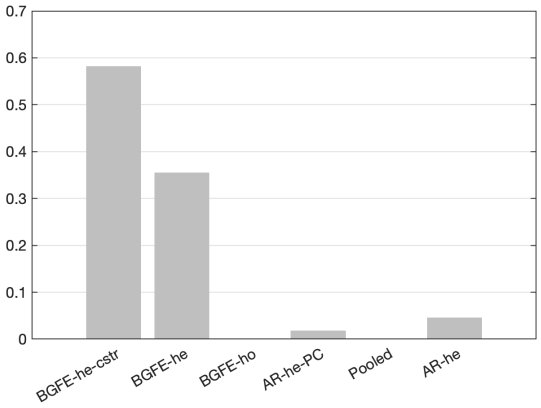

(b) Boxplot: LPS_m - LPS_{AR}

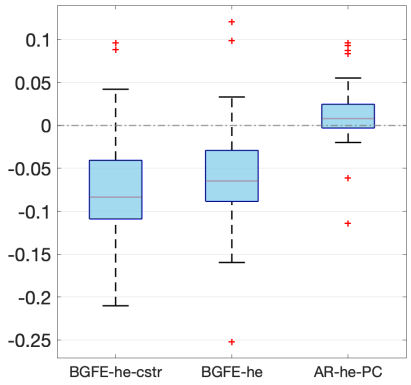

Figure 9: Posterior Similarity Matrices for Selected Categories

(a) Food and beverages (Category 3)

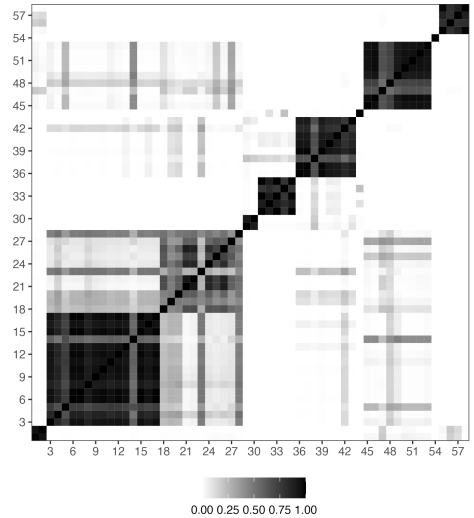

(b) Transportation (Category 7)

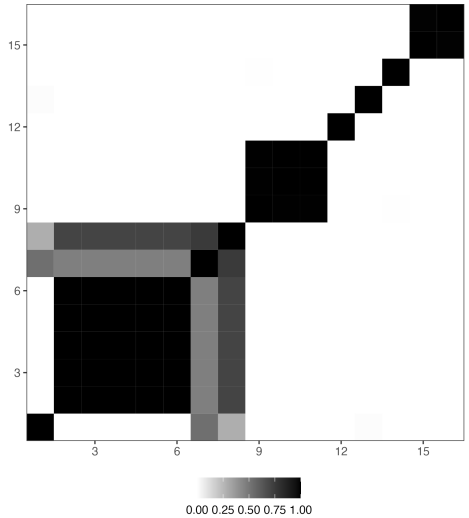

sectional information, not limited to our prior knowledge, and forms meaningful groups for forecasting.

Figure 10: Posterior Point Estimate of the Group Partition, August 2022

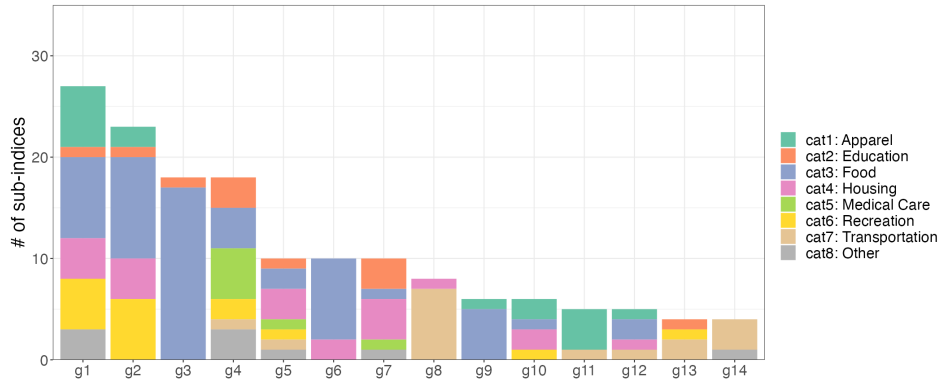

Figure 11: Components in the Group #9, August 2022

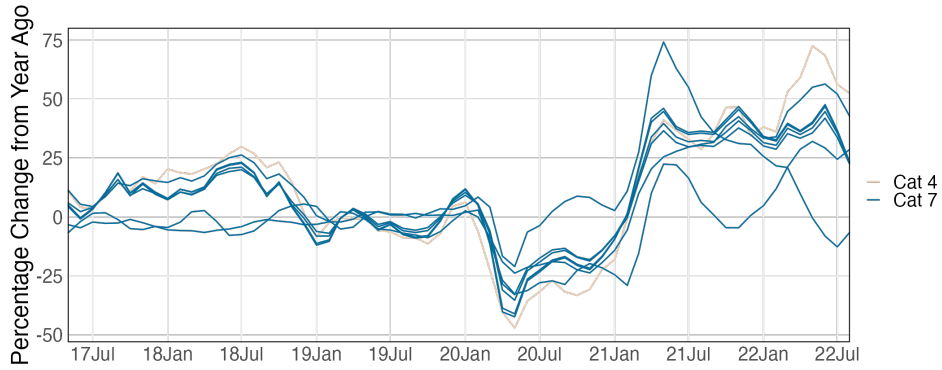

5.2.3 Impact of the Accuracy of Constraints

We examine how the accuracy of pairwise constraints influences the point estimate of group partitioning. For demonstration purposes, we restrict our analysis to ML constraints solely by setting $\psi_{ij}^{CL} = 0.5$ and changing ψ_{ij}^{ML}. We do not select the constant c in the setup since it would balance the impact of the ML restrictions with a different level of accuracy. We set c to 0.5. Again, ML constraints are derived from the official expenditure categories, with the assumption that all units within the same category are must-linked with equal probability of being in the same group.

Figure 12 presents the point estimates of the group structure with two different levels of accuracy. The "weaker" ML constraints with $\psi_{ij}^{ML} = 0.55$, as shown in panel (a), demonstrate a limited influence of prior knowledge on the group structure. The eleven groups are composites of CPI sub-indices from the various categories, which is diverse from the official spending categories. Panel (b), on the other hand, illustrates the group structure with

"stronger" ML constraints. By setting a high level of accuracy for ML constraints, such as $\psi_{ij}^{ML} = 0.95$, the prior knowledge dominates and pushes the group structure towards the official expenditure categories. As anticipated, panel (b) shows fewer groups, and the majority of CPI sub-indices within each group belong to the same category, bringing the group structure closer to that of the prior.

Figure 12: Impact of the Strength of Constraints

(a) Weaker ML $\left(\psi_{ij}^{ML} = 0.55\right)$ (b) Stronger ML $\left(\psi_{ij}^{ML} = 0.95\right)$

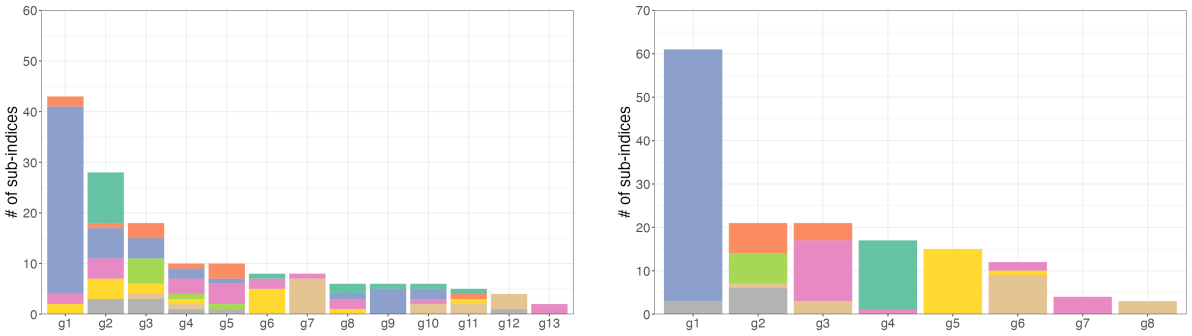

5.2.4 Heteroskedasticity vs. Homoskedasticity

We conclude by examining how grouped heteroskedasticity impacts forecast accuracy and why this is important. For illustrative purposes, we focus on the two BGFE estimators, BGFE-he and BGFE-ho, that do not involve pairwise constraints.

A distinguishing characteristic between BGFE-he and BGFE-ho is the estimated number of groups. Figure 13 depicts the number of groups over samples. BGFE-he estimator forms 9 groups for the beginning of the sample, and increase it during the Great Recession and the Pandemic. However, the estimated number of groups for BGFE-ho is rather low in the 1990s, and progressively increases to around seven by the end of the sample. It is noticeable that when heteroskedasticity is allowed, there are more groups than when it is not. This is intuitive. Two groups can be expected to have comparable estimates of grouped fixed-effects and slope coefficients, but vastly different error variances. As a result, allowing for heteroskedasticity would result in a more refined group structure and increase the overall number of groups.

As seen in Figure 7 and 8, the grouped heteroskedasticity doesn't improve the point forecast but the density forecast. Figure 14 depicts a clear perspective of it and demonstrates the performance of point and density forecasts through time. In panel (a), we observe that the ratio of RMSE is generally around one over the whole sample, meaning that heteroskedasticity cannot improve the point forecast in general. In panel (b), the difference in LPS is consistently negative. This demonstrates that the improved density prediction performance

Figure 13: Number of Groups

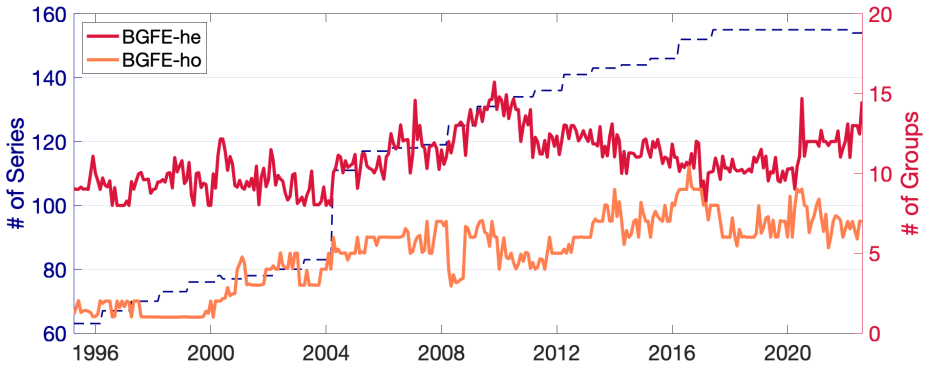

is not a fluke and that enabling heteroskedasticity improves the density forecast regardless of sample. This is actually in line with the simulation results presented in Table E.4.

Figure 14: Results of BGFE-he vs. BGFE-ho

(a) RMSE_{he} / RMSE_{ho}

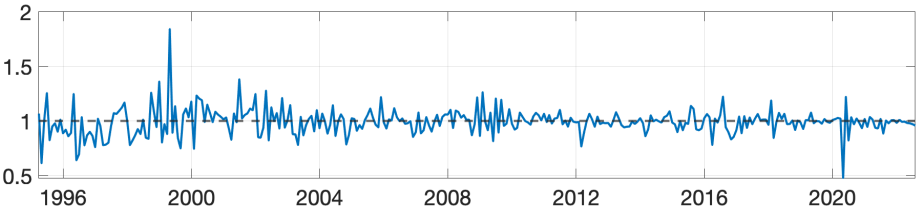

(b) LPS_{he} - LPS_{ho}

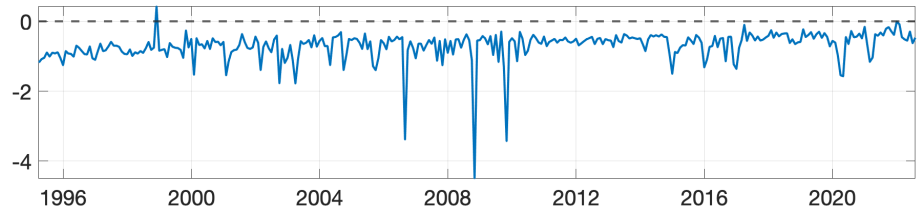

Density forecasts vary substantially across categories. We pick three typical sub-categories and plot their posterior predictive densities of August 2022 in Figure 15. The vertical dashed black lines represent the actual values. Several insights emerge while comparing these three subcategories. First, BGFE-he and BGFE-ho provide comparable posterior means for all three subcategories - the posterior predictive densities concentrate around the similar price levels. This explains why BGFE-he and BGFE-ho have comparable results in point forecasting. Second, BGFE-he reveals different predictive variance. As the rolling sample size is set to 4 years, all observations throughout the Pandemic are included, and it is anticipated that the price levels of elementary and high school (basic education) tuition and fees, major appliances, and airline prices would respond differently to the shock. Intuitively, education tuition and fees should not fluctuate as much as other prices, while airline fares have been strongly influenced by the fluctuating oil prices since the beginning of the Pandemic. Conse-

quently, accounting for heteroskedasticity successfully captures this characteristic, such that college tuition and fees have a smaller predictive variance than that of BGFE-ho, but airline fares have a greater predictive variance.

Combing these two observations together reveals why BGFE-he has a better density forecast: the capacity to optimally cluster units according to the error variance and accommodate heteroskedasticity. For elementary and high tuition and fees, providing that both BGFE-he and BGFE-ho yields accurate posterior mean, BGFE-he yields much lower predictive variance, decreasing the LPS dramatically. Both BGFE-he and BGFE-ho underestimate the inflation rate for airline fares, but BGFE-he subtly creates a greater predicted variance to account for the wild probable shift in this sub-category and hence reduces the LPS significantly. Major appliances is an example to show that BGFE-he and BGFE-ho generate comparable density forecasts for some sub-categories.

Figure 15: Predictive Posteriors for Selected Series: BGFE-he vs. BGFE-ho

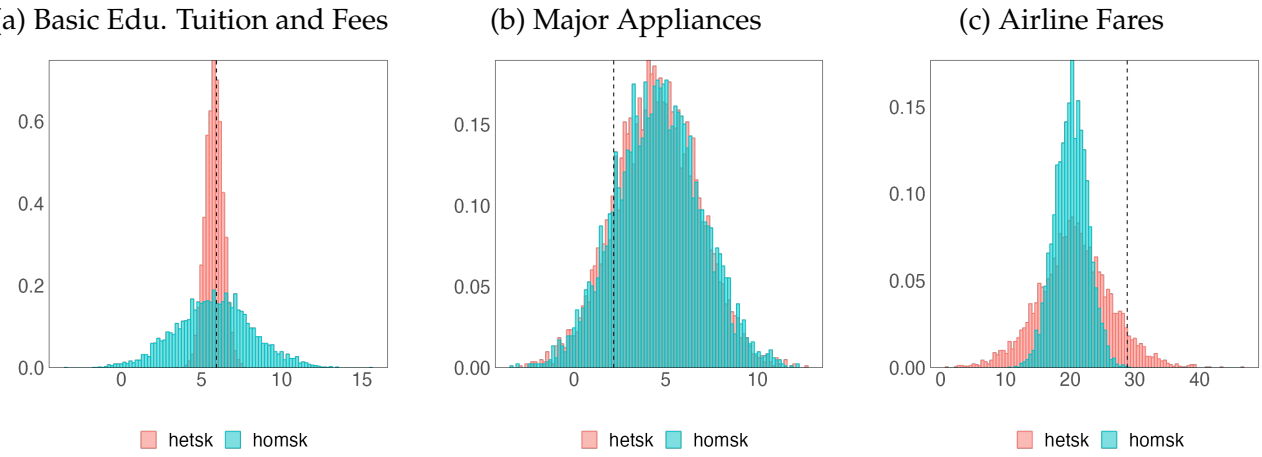

5.3 Income and Democracy

An important stylized fact in political science and economics is the casual relationship between countries' income and the level of democracy (Lipset, 1959; Sirowy and Inkeles, 1990; Przeworski et al., 1995; Barro, 1999). When controlling for additive country- and time-effects, Acemoglu et al. (2008) discover that the positive correlation between income and democracy disappears. Bonhomme and Manresa (2015) introduce the grouped time-varying fixed-effects into the panel data model and reach the same conclusions. In particular, their analysis highlights the presence of diverse group-specific paths of democratization in the data. The group pattern is consistent with the empirical finding that regime types and transitions tend to cluster in time and space (Gleditsch and Ward, 2006; Ahlquist and Wibbels, 2012).

This section revisits the relationship between countries' income and the level of democracy, focusing primarily on the group pattern in the evolution of democratization. We examine several model specifications and, in particular, introduce group structure in time fixed-

effects, slope coefficients and the variance of errors. We find richer group patterns when prior knowledge on group is introduced in the model and heterogeneous income effects on democracy.

5.3.1 Model Specification and Data

Model: Time effects are essential to this analysis as they capture highly persistent historical shocks. Following Bonhomme and Manresa (2015), we introduce group-specific time patterns of heterogeneity $\alpha_{g_i t}$ and consider the following two specifications:

SP1 *Time-varying GFE*

$$y_{it} = \alpha_{g_i t} + \rho y_{it-1} + \beta x_{it-1} + \varepsilon_{it},\ \varepsilon_{it} \sim N(0, \sigma^2_{g_i}) \tag{5.12}$$

SP2 *Time-varying GFE + grouped slope coefficients*

$$y_{it} = \alpha_{g_i t} + \rho_{g_i} y_{it-1} + \beta_{g_i} x_{it-1} + \varepsilon_{it},\ \varepsilon_{it} \sim N(0, \sigma^2_{g_i}) \tag{5.13}$$

where y_{it} is the democracy score (measured by the Freedom House indicator) of country i in period t. The lagged value of this variable on the right-hand side is included to capture persistence in democracy and also potentially mean-reverting dynamics (i.e., the tendency of the democracy score to return to some equilibrium value for the country). x_{it-1} is the lagged value of log income (GDP) per capita. In addition, $\alpha_{g_i t}$ denote a set of group-specific time fixed-effects; ε_{it} is an error term with grouped variance $\sigma^2_{g_i}$, capturing all other omitted factors.

Specification 1 in (5.12) nests the linear dynamic panel data model in BM as a special case. If we assume homoskedasticity, it is the equation (22) in BM. This specification enables us to reproduce BM's results and provide fresh insight into their framework. Specification 2 in (5.13), on the other hand, generalizes specification 1 by introducing group-dependent slope coefficients. As we shall demonstrate in the following section, specification 2 yields a more refined group structure and provides a clearer view of the income effects.

Data: All data in this section are taken from the replication files of BM[8] . The data set contains a balanced panel of 89 countries[9] and 7 periods at a five-year interval over 1970-2000. The summary statistics are reported in Table F.1. The main measure of democracy is the Freedom House Political Rights Index. A country receives the highest score if its political rights come closest to the ideals suggested by a checklist of questions. The countries' income is measured by the logarithm of GDP per capita.

Estimator: We consider three estimators:

[8] https://www.dropbox.com/s/ssjabvc2hxa5791/Bonhomme_Manresa_codes.zip?dl=0

[9] We remove a few regions that are not considered as countries in a general sense.

(i) *BGFE-he*: The baseline BGFE estimator. It assumes true model exhibits time-varying grouped heterogeneity and grouped heteroskedasticity.

(ii) *BGFE-ho*: homoskedastic version of *BGFE-he*.

(iii) *BGFE-he-cstr*: BGFE-he + constraints. We propose two prior grouping strategies as specified below and assume all units within the same prior group are presumed to be must-linked, while units from different prior groups are believed to be cannot-linked. We specify equal accuracy for all ML and CL constraints, i.e., $\psi_{ij}^{ML} = 0.70$ and $\psi_{ij}^{CL} = 0.55$, following the method described in Section 2.3.5.

Prior group structure: We propose two pre-grouping strategies

(i) Given the countries available in the dataset, we form six groups according to their geographic locations:[10] (1) North America; (2) Europe; (3) Latin America and the Caribbean; (4) Asia and Australasia; (5) Sub-Saharan Africa; (6) Middle East and North Africa. We refer this prior to *geo-prior*.

(ii) Alternately, countries could be categorized according to their initial level of democracy in year 1970. As the Freedom House Index has six possible values, we cluster countries into three primary groups with a reasonable number of countries in each: (1) low democracy, $y_{i,1970} = 0$ or 0.166; (2) medium democracy, $y_{i,1970} = 0.333$, 0.5, or 0.667; (3) high democracy, $y_{i,1970} = 0.833$ or 1. We refer this prior to *demo-prior*.

Figure 16 presents the world maps with countries colored differently according to their respective groups. The panel on the left illustrates the geographic groups, while the panel on the right depicts the democratic groups. All gray nations/regions are excluded from the dataset. We concentrate primarily on the first pre-grouping strategy, as it needs no country-specific knowledge beyond geographic information. We then compare the results using different pre-grouping strategies in Section 5.3.3.

5.3.2 Results

Specification 1: The results for specification 1 are reported in Appendix G.2. In short, the results are comparable to the key findings in BM. BGFE-ho in specification 1 is identical to the main model in BM; it produces eight groups, which is consistent with the upper bound on the number of groups in BM based on BIC. BGFE-he-cstr, on the other hand, is more preferable and has the highest marginal data density. The point estimate of group partitioning based on BGFE-he-cstr consists of four groups that all have the similar pattern as BM's

[10] The regions are assigned by the Economist Intelligence Unit, and may slightly differ from conventional classifications.

Figure 16: Specifications of Prior Grouping

(a) Geographic Location

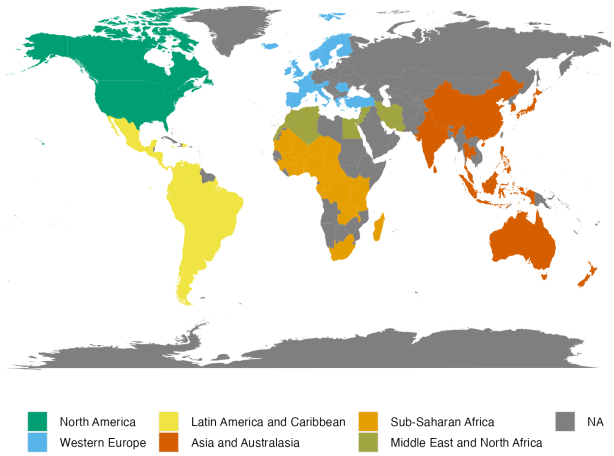

(b) Initial Level of Democracy

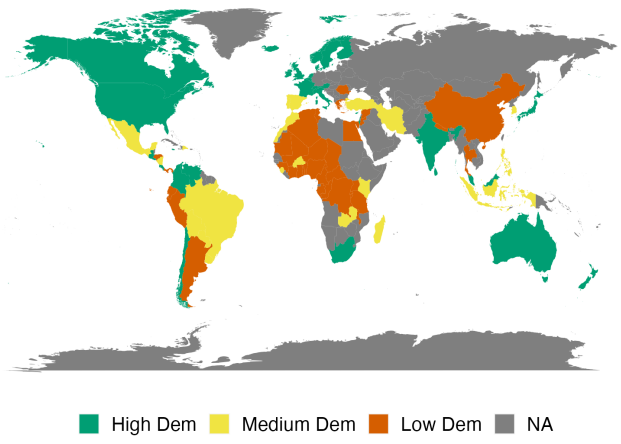

group structure. This justifies BM's choice of four groups. Regarding the estimated coefficients, there is moderate persistence and a positive effect of income on democracy, but the cumulative effect of income is quantitatively small: $\beta/(1-\rho) = 0.08$.

Specification 2: We now turn to specification 2 where group-specific slope coefficients are allowed and new findings emerge. Table 1 presents the posterior probability of the number of groups utilizing various estimators. BGFE-ho creates more than 5 groups in all posterior draws. Intriguingly, accounting for heteroskedasticity drastically reduces the number of groups, with BGFE-he identifying four groups. Adding pairwise constraints based on geographic information increases the number of groups to five, whereas six groups are expected in the prior.

Table 1: Probability for Number of Groups

	BGFE-he-cstr	BGFE-he	BGFE-ho
$Pr(K < 4)$	0.000	0.000	0.000
$Pr(K = 4)$	0.000	**1.000**	0.000
$Pr(K = 5)$	**1.000**	0.000	0.000
$Pr(K > 5)$	0.000	0.000	**1.000**

The marginal data density (MDD) of each estimator in Table 2 provides some insight on different models. Among all the estimators, the BGFE-ho estimator has the lowest MDD; it is even lower than that of specification 1. BGFE-he-cstr and BGFE-he, on the other hand, benefit from the introduction of group-specific slope coefficients, since both achieve substantially greater MDD than in specification 1. BGFE-he-cstr has the highest MDD since

the pairwise constraints give direction on grouping and identify the ideal group structure, which BGFE-he cannot uncover without our prior knowledge.

Table 2: Marginal Data Density

	BGFE-he-cstr	BGFE-he	BGFE-ho
SP2	544.324	501.904	327.077
SP1	425.690	381.218	368.918

We concentrate on the BGFE-he-cstr estimator and use the approach outlined in Section 3.2 to identify the unique group partitioning $\widehat{G}$. The left panel of Figure 17 presents the world map colored by $\widehat{G}$, while the right panel present the group-specific averages of democracy index over time. The estimated group structure $\widehat{G}$ features five distinct groups which we refer to as the "high-democracy", "low-democracy", "flawed-democracy", "late-transition" and "progressive-transition" group, respectively. With the exception of the "flawed-democracy" and "progressive-transition" group, the group-specific averages of the democracy index are comparable to those in BM for all other groups. BGFE-he-cstr does not identify the "early transition" group in comparison to BM but instead produces two new groups. Group 3 ("flawed-democracy") comprises primarily of relatively democratic but not the most democratic nations, including India, Sri Lanka, and Venezuela, among others. Group 5 ("progressive transition") contains 30 countries that have had a steady expansion of democracy, including Argentina, Greece, and Panama. Consequently, by incorporating group-specific slope coefficients, we recover a more refined group structure than that of BM.

Figure 17: Posterior Point Estimate of Group Partitioning and Average Democracy

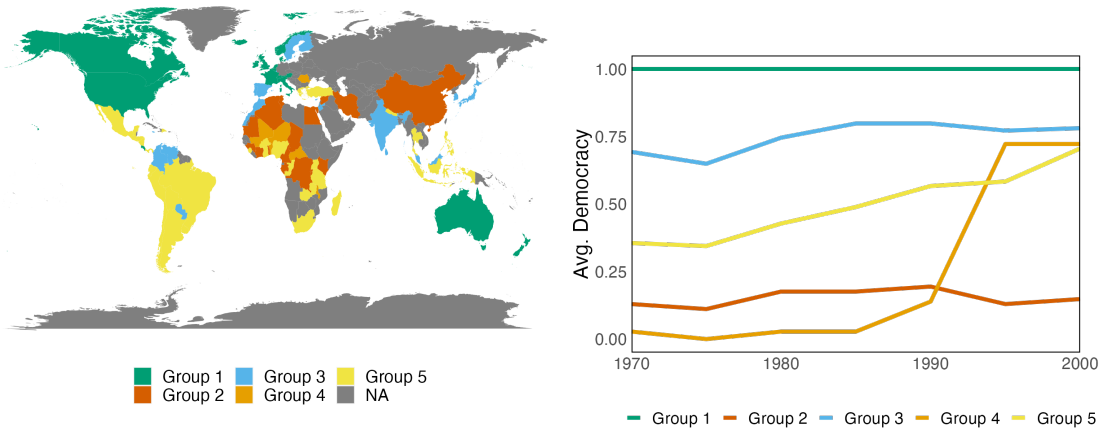

Table 3 presents the posterior mean and 90% credible set for each coefficient across all groups, with G fixed at the point estimate $\widehat{G}$. The key feature of using the specification 2 is that we are able to see distinct (cumulative) income effects across groups as group-specific

coefficients are allowed. The effect of income on democracy is negligible for group 1 ("full-democracy") and group 4 ("late-transition") as the posterior means of β are close to 0 and the associated credible intervals for $\hat{\beta}$ contain 0. Countries in group 1 kept their democracy index at the highest level throughout the time, demonstrating that income has no effect on democracy. Moreover, the transition to democracy for countries in group 4 was primarily driven by historical events[11] captured by time fixed-effects, as the credible intervals for $\hat{\beta}$ and $\hat{\rho}$ cover zero. As the coefficient on income is positive and well above zero, the effect of income on democracy is comparable small for group 2 ("low-democracy") and group 3 ("flawed-democracy"). However, the cumulative income effects are different - it is negligible for group 2 (0.079) and modest for group 3 (0.244). Group 5 ("progressive-transition"), on the other hand, has the largest positive income coefficient, although the cumulative income effect is quantitatively small (0.156).

Table 3: Coefficient estimates across groups

	Lagged democracy (ρ)		Lagged Income (β)		Error variance (σ^2)	
	Coef.	Cred. Set	Coef.	Cred. Set	Coef.	Cred. Set
Group 1 (16)	0.058	[-0.263, 0.360]	0.000	[-0.012, 0.012]	0.001	[0.001, 0.001]
Group 2 (18)	0.484	[0.354, 0.606]	0.041	[0.019, 0.062]	0.010	[0.008, 0.011]
Group 3 (19)	0.775	[0.703, 0.850]	0.055	[0.031, 0.078]	0.013	[0.011, 0.016]
Group 4 (6)	-0.178	[-0.468, 0.115]	-0.025	[-0.066, 0.017]	0.008	[0.005, 0.011]
Group 5 (30)	0.206	[0.091, 0.310]	0.125	[0.090, 0.163]	0.057	[0.048, 0.066]
Pooled OLS	0.665	[0.616, 0.718]	0.082	[0.065, 0.100]	0.039	[0.035, 0.043]

5.3.3 Different Pre-Grouping Strategies

All results presented thus far are based on pairwise constraints derived from geospatial information. In this section, we implement the alternative pre-grouping strategy based on the initial level of democracy. We stick with the BGFE-he-cstr estimator in exercise specification 2.

Figure 18 displays the point estimates of group partitioning under different pre-grouping strategies. Countries that receive different group assignments are mostly encircled in the black dashed rectangle, including Portugal, Spain, Romania, Mali, Niger, Central African Republic, Benin, Malawi, and Jordan. Another country is South Korea.

Using the initial level of democracy as prior knowledge results in four groups, as indicated in the right panel. The demo-prior has two major impacts comparing with the geo-prior. It combines the "late-transition" group (group 4 in geo-prior) with the "progressive-

[11] Group 4 consists of Benin, Central African Republic, Mali, Malawi, Niger, and Romania. Romania began a transition towards democracy after the 1989 Revolution. All other countries involved in the third wave of democratization in sub-Saharan Africa beginning in 1989.

Figure 18: Posterior Point estimate of Group Structure

(a) Geographic Location

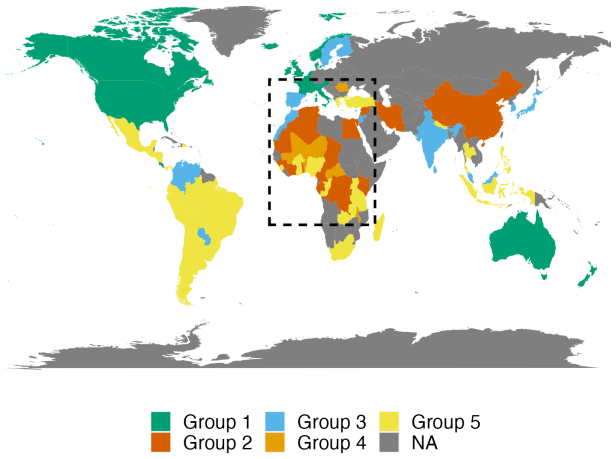

(b) Initial Level of Democracy

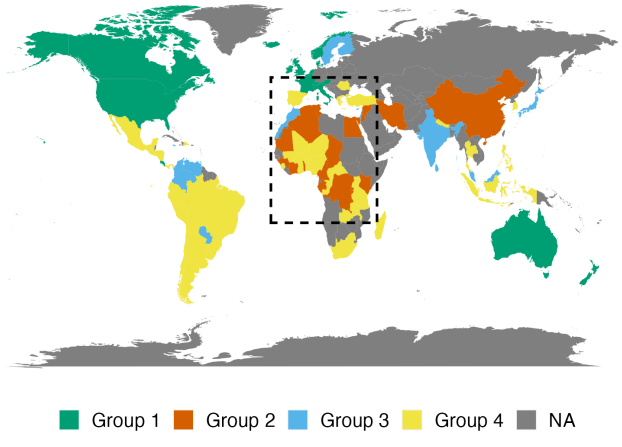

transition" group (group 5 in geo-prior) to form a bigger and boarder "progressive-transition" group. Furthermore, Portugal and Spain are no longer categorized as "flawed-democracy" countries, but rather as "progressive-transition" group in a boarder sense.

6 Concluding Remarks

This paper proposes a Bayesian framework for estimating and forecasting in panel data models when prior group knowledge is available and informative for the group pattern. We include prior knowledge in the form of soft pairwise constraints into the Dirichlet process prior. Then, an intuitive and coherent prior is presented. The constrained grouped estimator proposed examines both heteroskedasticity and heterogeneous slope coefficients to endogenously reveal group structure. Our framework immediately estimates the number of groups as opposed to relying on ex-post model selection, and the structure of pairwise restrictions circumvents the computational difficulties and limitations that afflict conventional approaches. In addition, when utilizing small-variance asymptotics, the suggested Gibbs sampler with pairwise constraint contains a clustering procedure comparable to that of the constrained *KMeans* algorithm. In Monte Carlo simulations, we demonstrate that constrained Bayesian grouped estimators outperform conventional estimators even in the presence of incorrect prior knowledge. Our empirical application to forecasting sub-indices of CPI inflation rates demonstrates that incorporating prior knowledge on the latent group structure yields more accurate density predictions. The better forecasting performance is mostly attributable to three key characteristics: nonparametric Bayesian prior, prior belief on group structure, and grouped cross-sectional heteroskedasticity. The method proposed in this paper is applicable beyond forecasting. In a second application, we revisit the re-

lationship between a country's income and its democratic transition, where estimation of heterogeneous parameters is the object of interest. We recover a reasonable cluster pattern with a moderate number of groups and identify heterogeneous income effects on democracy.

The current work raises exciting questions for future research. It is desirable to investigate overlapping group structures, in which a unit might belong to many groups. This would allow us to increase the flexibility of a panel data model, potentially enhancing its predictive performance. Second, the assumption that an individual cannot change its group identity for the entire sample time can be amended, resulting in a specification that is even more flexible. Thirdly, our method is applicable to other econometric models, such as panel VARs with latent group structures in macro series.

References

ACEMOGLU, D., S. JOHNSON, J. A. ROBINSON, AND P. YARED (2008): "Income and Democracy," *American Economic Review*, 98, 808–42.

AGUILAR, J. AND T. BOOT (2022): "Grouped Heterogeneity in Linear Panel Data Models with Heterogeneous Error Variances," *Available at SSRN 4031841*.

AHLQUIST, J. S. AND E. WIBBELS (2012): "Riding the Wave: World Trade and Factor-Based Models of Democratization," *American Journal of Political Science*, 56, 447–464.

ALDOUS, D. J. (1985): "Exchangeability and Related Topics," in *École d'Été de Probabilités de Saint-Flour XIII—1983*, Springer, 1–198.

ANDERSON, T. W. AND C. HSIAO (1982): "Formulation and Estimation of Dynamic Models using Panel Data," *Journal of Econometrics*, 18, 47–82.

ANDO, T. AND J. BAI (2016): "Panel Data Models with Grouped Factor Structure under Unknown Group Membership," *Journal of Applied Econometrics*, 31, 163–191.

ANTONIAK, C. E. (1974): "Mixtures of Dirichlet Processes with Applications to Bayesian Nonparametric Problems," *The Annals of Statistics*, 2, 1152–1174.

ASCOLANI, F., A. LIJOI, G. REBAUDO, AND G. ZANELLA (2022): "Clustering Consistency with Dirichlet Process Mixtures," *arXiv preprint arXiv:2205.12924*.

ATHEY, S. AND G. IMBENS (2016): "Recursive Partitioning for Heterogeneous Causal Effects," *Proceedings of the National Academy of Sciences*, 113, 7353–7360.

BARRO, R. J. (1999): "Determinants of Democracy," *Journal of Political economy*, 107, S158–S183.

BASU, S., A. BANERJEE, AND R. MOONEY (2002): "Semi-Supervised Clustering by Seeding," in *Proceedings of 19th International Conference on Machine Learning*, Citeseer.

BASU, S., A. BANERJEE, AND R. J. MOONEY (2004a): "Active Semi-Supervision for Pairwise Constrained Clustering," in *Proceedings of the 2004 SIAM international conference on data mining*, SIAM, 333–344.

BASU, S., M. BILENKO, AND R. J. MOONEY (2004b): "A Probabilistic Framework for Semi-Supervised Clustering," in *Proceedings of the Tenth ACM SIGKDD International Conference on Knowledge Discovery and Data Mining*, 59–68.

BERNANKE, B. S. (2007): "Inflation Expectations and Inflation Forecasting," in *Speech at the Monetary Economics Workshop of the National Bureau of Economic Research Summer Institute, Cambridge, Massachusetts*, vol. 10.

BILENKO, M., S. BASU, AND R. J. MOONEY (2004): "Integrating Constraints and Metric Learning in Semi-Supervised Clustering," in *Proceedings of the 21st International Conference on Machine Learning*, 81–88.

BILLIO, M., R. CASARIN, AND L. ROSSINI (2019): "Bayesian Nonparametric Sparse VAR Models," *Journal of Econometrics*, 212, 97–115.

BLACKWELL, D. AND J. B. MACQUEEN (1973): "Ferguson Distributions via Pólya Urn Schemes," *The Annals of Statistics*, 1, 353–355.

BONHOMME, S., T. LAMADON, AND E. MANRESA (2022): "Discretizing Unobserved Heterogeneity," *Econometrica*, 90, 625–643.

BONHOMME, S. AND E. MANRESA (2015): "Grouped Patterns of Heterogeneity in Panel Data," *Econometrica*, 83, 1147–1184.

BUCHINSKY, M., J. HAHN, AND V. HOTZ (2005): "Cluster Analysis: A Tool for Preliminary Structural Analysis," *Unpublished manuscript*.

CANOVA, F. AND M. CICCARELLI (2013): "Panel Vector Autoregressive Models: A Survey," in *VAR Models in Macroeconomics–New Developments and Applications: Essays in Honor of Christopher A. Sims*, Emerald Group Publishing Limited.

CHENG, X., F. SCHORFHEIDE, AND P. SHAO (2019): "Clustering for Multi-Dimensional Heterogeneity," *Manuscript*.

CHETTY, R., J. N. FRIEDMAN, AND J. E. ROCKOFF (2014): "Measuring the Impacts of Teachers I: Evaluating Bias in Teacher Value-Added Estimates," *American Economic Review*, 104, 2593–2632.

CLARK, T. E. AND F. RAVAZZOLO (2015): "Macroeconomic Forecasting Performance under Alternative Specifications of Time-Varying Volatility," *Journal of Applied Econometrics*, 30, 551–575.

CYTRYNBAUM, M. (2021): "Blocked Clusterwise Regression," *arXiv preprint arXiv:2001.11130*.

DAVIDSON, I. AND S. RAVI (2005): "Clustering with Constraints: Feasibility Issues and the K-Means Algorithm," in *Proceedings of the 2005 SIAM International Conference on Data Mining*, SIAM, 138–149.

ESCOBAR, M. D. AND M. WEST (1995): "Bayesian Density Estimation and Inference using Mixtures," *Journal of the American Statistical Association*, 90, 577–588.

FERGUSON, T. S. (1973): "A Bayesian Analysis of Some Nonparametric Problems," *The Annals of Statistics*, 1, 209–230.

——— (1974): "Prior Distributions on Spaces of Probability Measures," *The Annals of Statistics*, 2, 615–629.

FOX, E. B., E. B. SUDDERTH, M. I. JORDAN, AND A. S. WILLSKY (2008): "An HDP-HMM for Systems with State Persistence," in *Proceedings of the 25th International Conference on Machine Learning*, 312–319.

——— (2011): "A Sticky HDP-HMM with Application to Speaker Diarization," *The Annals of Applied Statistics*, 5, 1020–1056.

FREEMAN, H. AND M. WEIDNER (2022): "Linear Panel Regressions with Two-Way Unobserved Heterogeneity," *arXiv preprint arXiv:2109.11911*.

FRUCHTERMAN, T. M. AND E. M. REINGOLD (1991): "Graph Drawing by Force-Directed Placement," *Software: Practice and Experience*, 21, 1129–1164.

GEWEKE, J. AND G. AMISANO (2010): "Comparing and Evaluating Bayesian Predictive Distributions of Asset Returns," *International Journal of Forecasting*, 26, 216–230.

GHOSAL, S. AND A. VAN DER VAART (2017): *Fundamentals of Nonparametric Bayesian Inference*, vol. 44, Cambridge University Press.

GLEDITSCH, K. S. AND M. D. WARD (2006): "Diffusion and the International Context of Democratization," *International Organization*, 60, 911–933.

HAHN, J. AND H. R. MOON (2010): "Panel Data Models with Finite Number of Multiple Equilibria," *Econometric Theory*, 26, 863–881.

HAMILTON, J. D. (2018): "Why You Should Never Use the Hodrick-Prescott Filter," *Review of Economics and Statistics*, 100, 831–843.

HERSBACH, H. (2000): "Decomposition of the Continuous Ranked Probability Score for Ensemble Prediction Systems," *Weather and Forecasting*, 15, 559–570.

HILL, J. L. (2011): "Bayesian Nonparametric Modeling for Causal Inference," *Journal of Computational and Graphical Statistics*, 20, 217–240.

HOLLAND, P. W., K. B. LASKEY, AND S. LEINHARDT (1983): "Stochastic Blockmodels: First Steps," *Social Networks*, 5, 109–137.

HOLTZ-EAKIN, D., W. NEWEY, AND H. S. ROSEN (1988): "Estimating Vector Autoregressions with Panel Data," *Econometrica*, 56, 1371–1395.

ISHWARAN, H. AND L. F. JAMES (2001): "Gibbs Sampling Methods for Stick-Breaking Priors," *Journal of the American Statistical Association*, 96, 161–173.

KIM, J. AND L. WANG (2019): "Hidden Group Patterns in Democracy Developments: Bayesian Inference for Grouped Heterogeneity," *Journal of Applied Econometrics*, 34, 1016–1028.

KOOP, G. (2003): *Bayesian Econometrics*, John Wiley & Sons.

KULIS, B. AND M. I. JORDAN (2011): "Revisiting K-Means: New Algorithms via Bayesian Nonparametrics," *arXiv preprint arXiv:1111.0352*.

LAIO, F. AND S. TAMEA (2007): "Verification Tools for Probabilistic Forecasts of Continuous Hydrological Variables," *Hydrology and Earth System Sciences*, 11, 1267–1277.

LAW, M. H., A. TOPCHY, AND A. K. JAIN (2004): "Clustering with Soft and Group Constraints," in *Joint IAPR International Workshops on Statistical Techniques in Pattern Recognition (SPR) and Structural and Syntactic Pattern Recognition (SSPR)*, Springer, 662–670.

LEE, C. AND D. J. WILKINSON (2019): "A Review of Stochastic Block Models and Extensions for Graph Clustering," *Applied Network Science*, 4, 1–50.

LIN, C.-C. AND S. NG (2012): "Estimation of Panel Data Models with Parameter Heterogeneity When Group Membership is Unknown," *Journal of Econometric Methods*, 1, 42–55.

LIPSET, S. M. (1959): "Some Social Requisites of Democracy: Economic Development and Political Legitimacy," *American Political Science Review*, 53, 69–105.

LIU, L. (2022): "Density Forecasts in Panel Data Models: A Semiparametric Bayesian Perspective," *Journal of Business & Economic Statistics*, 0, 1–15.

LIU, L., H. R. MOON, AND F. SCHORFHEIDE (2020): "Forecasting with Dynamic Panel Data Models," *Econometrica*, 88, 171–201.

LU, Z. (2007): "Semi-Supervised Clustering with Pairwise Constraints: A Discriminative Approach," in *Artificial Intelligence and Statistics*, PMLR, 299–306.

LU, Z. AND T. K. LEEN (2004): "Semi-Supervised Learning with Penalized Probabilistic Clustering," in *NIPS'04 Proceedings of the 17th International Conference on Neural Information Processing Systems*, 849–856.

——— (2007): "Penalized Probabilistic Clustering," *Neural Computation*, 19, 1528–1567.

LUMSDAINE, R. L., R. OKUI, AND W. WANG (2022): "Estimation of Panel Group Structure Models with Structural Breaks in Group Memberships and Coefficients," *Journal of Econometrics*, Forthcoming.

MACQUEEN, J. ET AL. (1967): "Some Methods for Classification and Analysis of Multivariate Observations," in *Proceedings of the Fifth Berkeley Symposium on Mathematical Statistics and Probability*, Oakland, CA, USA, vol. 1, 281–297.

MATHESON, J. E. AND R. L. WINKLER (1976): "Scoring Rules for Continuous Probability Distributions," *Management Science*, 22, 1087–1096.

MEILĂ, M. (2007): "Comparing Clusterings—An Information Based Distance," *Journal of Multivariate Analysis*, 98, 873–895.

MILLER, J. W. (2019): "An Elementary Derivation of the Chinese Restaurant Process from Sethuraman's Stick-Breaking Process," *Statistics & Probability Letters*, 146, 112–117.

MÜELLER, P., F. A. QUINTANA, AND G. PAGE (2018): "Nonparametric Bayesian Inference in Applications," *Statistical Methods & Applications*, 27, 175–206.

NEAL, R. M. (1992): "Bayesian Mixture Modeling," in *Maximum Entropy and Bayesian Methods*, Springer, 197–211.

——— (2000): "Markov Chain Sampling Methods for Dirichlet Process Mixture Models," *Journal of Computational and Graphical Statistics*, 9, 249–265.

NELSON, B. AND I. COHEN (2007): "Revisiting Probabilistic Models for Clustering with Pairwise Constraints," in *Proceedings of the 24th International Conference on Machine Learning*, 673–680.

NEWTON, M. A. AND A. E. RAFTERY (1994): "Approximate Bayesian Inference with the Weighted Likelihood Bootstrap," *Journal of the Royal Statistical Society: Series B (Methodological)*, 56, 3–26.

NOWICKI, K. AND T. A. B. SNIJDERS (2001): "Estimation and Prediction for Stochastic Blockstructures," *Journal of the American Statistical Association*, 96, 1077–1087.

OKUI, R. AND W. WANG (2021): "Heterogeneous Structural Breaks in Panel Data Models," *Journal of Econometrics*, 220, 447–473.

ORBANZ, P. AND J. M. BUHMANN (2008): "Nonparametric Bayesian Image Segmentation," *International Journal of Computer Vision*, 77, 25–45.

PAGANIN, S., A. H. HERRING, A. F. OLSHAN, AND D. B. DUNSON (2021): "Centered Partition Processes: Informative Priors for Clustering," *Bayesian Analysis*, 16, 301–370.

PELLEG, D. AND D. BARAS (2007): "K-Means with Large and Noisy Constraint Sets," in *European Conference on Machine Learning*, Springer, 674–682.

PESARAN, M. H., A. PICK, AND A. TIMMERMANN (2022): "Forecasting with Panel Data: Estimation Uncertainty versus Parameter Heterogeneity," *CEPR Discussion Paper No. DP17123*.

PITMAN, J. (1995): "Exchangeable and Partially Exchangeable Random Partitions," *Probability Theory and Related Fields*, 102, 145–158.

——— (1996): "Some Developments of the Blackwell-MacQueen Urn Scheme," *Lecture Notes-Monograph Series*, 245–267.

PITMAN, J. AND M. YOR (1997): "The Two-Parameter Poisson-Dirichlet Distribution Derived from a Stable Subordinator," *The Annals of Probability*, 25, 855–900.

PRZEWORSKI, A., F. LIMONGI, AND S. GINER (1995): "Political Regimes and Economic Growth," in *Democracy and Development*, Springer, 3–27.

QUINTANA, F. A., P. MÜLLER, A. JARA, AND S. N. MACEACHERN (2022): "The Dependent Dirichlet Process and Related Models," *Statistical Science*, 37, 24–41.

RASMUSSEN, C. (1999): "The Infinite Gaussian Mixture Model," in *Advances in Neural Information Processing Systems*, ed. by S. Solla, T. Leen, and K. Müller, MIT Press, vol. 12, 554–560.

REN, L., D. B. DUNSON, AND L. CARIN (2008): "The Dynamic Hierarchical Dirichlet Process," in *Proceedings of the 25th International Conference on Machine Learning*, 824–831.

ROCKOFF, J. E. (2004): "The Impact of Individual Teachers on Student Achievement: Evidence from Panel Data," *American Economic Review*, 94, 247–252.

RODRIGUEZ, A. AND D. B. DUNSON (2011): "Nonparametric Bayesian Models through Probit Stick-Breaking Processes," *Bayesian Analysis*, 6.

ROSS, J. AND J. DY (2013): "Nonparametric Mixture of Gaussian Processes with Constraints," in *International Conference on Machine Learning*, PMLR, 1346–1354.

RUBIN, D. B. (1974): "Estimating Causal Effects of Treatments in Randomized and Nonrandomized Studies," *Journal of Educational Psychology*, 66, 688–701.

SARAFIDIS, V. AND N. WEBER (2015): "A Partially Heterogeneous Framework for Analyzing Panel Data," *Oxford Bulletin of Economics and Statistics*, 77, 274–296.

SETHURAMAN, J. (1994): "A Constructive Definition of Dirichlet Priors," *Statistica Sinica*, 4, 639–650.

SHENTAL, N., A. BAR-HILLEL, T. HERTZ, AND D. WEINSHALL (2003): "Computing Gaussian Mixture Models with EM using Equivalence Constraints," *Advances in Neural Information Processing Systems*, 16, 465–472.

SHIRAITO, Y. (2016): "Uncovering Heterogeneous Treatment Effects," *Visited on. https://shiraito. github. io/research/files/jmp. pdf*.

SIROWY, L. AND A. INKELES (1990): "The Effects of Democracy on Economic Growth and Inequality: A Review," *Studies In Comparative International Development*, 25, 126–157.

SMITH, A. F. (1973): "A General Bayesian Linear Model," *Journal of the Royal Statistical Society: Series B (Methodological)*, 35, 67–75.

SU, L. AND G. JU (2018): "Identifying Latent Grouped Patterns in Panel Data Models with Interactive Fixed Effects," *Journal of Econometrics*, 206, 554–573.

SU, L., Z. SHI, AND P. C. PHILLIPS (2016): "Identifying Latent Structures in Panel Data," *Econometrica*, 84, 2215–2264.

SU, L., X. WANG, AND S. JIN (2019): "Sieve Estimation of Time-Varying Panel Data Models with Latent Structures," *Journal of Business & Economic Statistics*, 37, 334–349.

SUN, Y. (2005): "Estimation and Inference in Panel Structure Models," *Available at SSRN 794884*.

TEH, Y. W., M. I. JORDAN, M. J. BEAL, AND D. M. BLEI (2006): "Hierarchical Dirichlet Processes," *Journal of the American Statistical Association*, 101, 1566–1581.

VLACHOS, A., Z. GHAHRAMANI, AND T. BRISCOE (2010): "Active Learning for Constrained Dirichlet Process Mixture Models," in *Proceedings of the 2010 Workshop on Geometrical Models of Natural Language Semantics*, 57–61.

VLACHOS, A., Z. GHAHRAMANI, AND A. KORHONEN (2008): "Dirichlet Process Mixture Models for Verb Clustering," in *Proceedings of the ICML Workshop on Prior Knowledge for Text and Language*.

VLACHOS, A., A. KORHONEN, AND Z. GHAHRAMANI (2009): "Unsupervised and Constrained Dirichlet Process Mixture Models for Verb Clustering," in *Proceedings of the Workshop on Geometrical Models of Natural Language Semantics*, 74–82.

WADE, S. AND Z. GHAHRAMANI (2018): "Bayesian Cluster Analysis: Point Estimation and Credible Balls (with Discussion)," *Bayesian Analysis*, 13, 559–626.

WAGER, S. AND S. ATHEY (2018): "Estimation and Inference of Heterogeneous Treatment Effects using Random Forests," *Journal of the American Statistical Association*, 113, 1228–1242.

WAGSTAFF, K. AND C. CARDIE (2000): "Clustering with Instance-Level Constraints," *AAAI/IAAI Proceedings*, 1097, 577–584.

WAGSTAFF, K., C. CARDIE, S. ROGERS, S. SCHROEDL, ET AL. (2001): "Constrained K-Means Clustering with Background Knowledge," in *Proceedings of the 18th International Conference on Machine Learning*, vol. 1, 577–584.

WALKER, S. G. (2007): "Sampling the Dirichlet Mixture Model with Slices," *Communications in Statistics—Simulation and Computation®*, 36, 45–54.

WANG, L. AND D. B. DUNSON (2011): "Fast Bayesian Inference in Dirichlet Process Mixture Models," *Journal of Computational and Graphical Statistics*, 20, 196–216.

WANG, W., P. C. PHILLIPS, AND L. SU (2018): "Homogeneity Pursuit in Panel Data Models: Theory and Application," *Journal of Applied Econometrics*, 33, 797–815.

WANG, W. AND L. SU (2021): "Identifying Latent Group Structures in Nonlinear Panels," *Journal of Econometrics*, 220, 272–295.

YODER, J. AND C. E. PRIEBE (2017): "Semi-Supervised K-Means++," *Journal of Statistical Computation and Simulation*, 87, 2597–2608.

ZHANG, B. (2020): "Forecasting with Bayesian Grouped Random Effects in Panel Data," *arXiv preprint arXiv:2007.02435*.

Supplemental Appendix to "Unobserved Grouped Patterns in Panel Data and Prior Wisdom"

Boyuan Zhang

A Definitions and Terminology

A.1 Dirichlet Process and Related Stochastic Processes

All unknown quantities in a model must be assigned prior distributions in Bayesian inference. A nonparametric prior can be used to reflect uncertainty about the parametric form of the prior distribution. Because of its richness, computational ease, and interpretability, the Dirichlet process (DP) is one of the most often used random probability measures. It can be used to model the uncertainty about the functional form of the prior distribution for parameters in a model.

The DP, which was first established using Kolmogorov consistency conditions (Ferguson, 1973), can be defined from a number of views. Ferguson (1973) shows that the DP can be obtained by normalizing a gamma process. By using exchangeability, the Pólya urn method leads to the GP (Blackwell and MacQueen, 1973). The Chinese restaurant process (CRP) (Aldous, 1985; Pitman, 1996), a distribution over partitions, is a similarly related sequential process that produces the DP when each partition is assigned an independent parameter with a common distribution. Sethuraman (1994) provided a constructive definition of the DP, which led to the characterization as a stick-breaking prior (Ishwaran and James, 2001).

Construction of the DP using a stick-breaking process or a gamma process represents the DP as a countably infinite sum of atomic measures. These approaches suggest that a DPM model can be seen as a mixture model with infinitely many components. The distribution of parameters imposed by a DP can also be obtained as a limiting case of a parametric mixture model (Neal, 1992; Rasmussen, 1999; Neal, 2000). This approach shows that a DPM can easily be defined as an extension of a parametric mixture model without the need to do model selection for determining the number of components to be used.

A.1.1 Dirichlet Process

Ferguson (1973) defines a DP with two parameters, a positive scalar a and a probability measure B_0, referred to as the concentration parameter and the base measure, respectively. The base distribution B_0 is the parameter on which the nonparametric distribution is centered, which can be thought of as the prior guess (Antoniak, 1974). The concentration parameter a expresses the strength of belief in B_0. For small values of a, samples from a DP is likely to be

composed of a small number of atomic measures with large weights. For large values, most samples are likely to be distinct, thus concentrated on B_0.

Technically, a nonparametric prior is a probability distribution on $\mathcal{P}$, the space of all probability measures (say on the real line). Measurable sets in $\mathcal{P}$ are of the form $\{A\colon P(A) < 1\}$. We could specify a prior distribution over $(P(A_1), P(A_2), \ldots, P(A_K))$ where A_1, A_2,..., A_K are measurable finite partition of the measurable set A. Denote

$$P \sim DP(a, B_0)$$

for all partition $(A_1, \cdots, A_K)$, then,

$$(P(A_1), \cdots, P(A_K)) \sim \text{Dir}(aB_0(A_1), \cdots, aB_0(A_K))$$

Dir $(\cdot)$ stands for the Dirichlet distribution with probability distribution function being

$$f(x_1, \cdots, x_K; \eta_1, \cdots, \eta_K) = \frac{\Gamma\left(\sum_{k=1}^{K} \eta_k\right)}{\prod_{k=1}^{K} \Gamma(\eta_k)} \prod_{k=1}^{K} x_k^{\eta_k - 1}$$

where $x_i \in (0,1)$ and $\sum_{i=1}^{K} x_i = 1$. This is a multivariate generalization of the Beta distribution and the infinite-dimensional generalization of the Dirichlet distribution is the Dirichlet process.

The form of the base distribution and the value of the concentration parameter are critical aspects of model selection that influence modeling performance. Given a murky prior distribution, the concentration parameter's value can be derived from the data. It is more difficult to choose the base distribution because the model's performance is largely dependent on its parametric form, even if it is constructed hierarchically for robustness. The choice of the base distribution is determined largely by mathematical and practical convenience. For computational ease, conjugate distributions are recommended.

A draw from DP is, by definition, a discrete distribution. In this sense, given the baseline model, imposing a DP prior on the distribution of α_{g_i} entails limiting the intercepts to some discrete values and assuming that intercepts within a group are identical, which may not be appealing for some empirical applications. A natural extension is to suppose that α_i has a continuous parametric distribution $f(\alpha_i; \theta)$, with θ as parameters, and to use a DP prior for the distribution of θ. The parameters θ are then discrete and has group structure, whereas group heterogeneity α_{g_i} has a continuous distribution, i.e., α_i within a group can be different, but they are all derived from the same distribution. This additional layer of mixing is the general idea of the Dirichlet Process Mixture (DPM) model.

A.1.2 Stick Breaking Process

A nonparametric prior can also be defined as the distribution of a random variable P taking values in $\mathcal{P}$. A construction of DP follows the stick-breaking process (Sethuraman, 1994),

$$
\begin{aligned}
P(A) &= \sum_{k=1}^{\infty} \pi_k \mathbf{1}_{\alpha_k}(A), \\
\alpha_k &\sim B_0, \quad k = 1, 2, \cdots, \\
\pi_k &= \begin{cases} \zeta_1, & k = 1 \\ \prod_{j<k}(1-\zeta_j)\,\zeta_k, & k = 2, 3, \cdots \end{cases} \\
&\text{where } \zeta_k \sim \text{Beta}(1, a), \quad k = 1, 2, \cdots
\end{aligned}
$$

The stick breaking process distinguishes the roles of B_0 and a in that the former governs component value α_k while the latter guides the choice of component probability π_k. Roughly speaking, the DP concentration parameter a is linked to the number of unique components in the mixture density and thus determines and reflects the flexibility of the mixture density. Let K denote the number of unique components. As derived in Antoniak (1974), we have

$$
\begin{aligned}
E[K|a] &\approx a \log\left(\frac{a+N}{a}\right) \\
\text{Var}[K|a] &\approx a\left[\log\left(\frac{a+N}{a}\right) - 1\right]
\end{aligned}
$$

which indicates that a larger a induce more unique components and expected K is increasing in the number of unit N. It is straightforward that using stick-breaking process implicitly allows K increasing with N.

A.1.3 Chinese Restaurant Process / Pólya Urn Process

Another widely used representation of the DP prior is the Chinese restaurant process (CRP). To set the stage, imagine that we have a Chinese restaurant that has infinitely many tables that can each seat infinitely many customers. When a new customer, say the n-th, enters the restaurant, the probability of them sitting at the table k with n_k other customers proportional to n_k, and the probability of this customer sitting alone at a new table is related to a (the concentration parameter in DP),

$$
p(\theta_n \in A_k | \theta_{1:n-1}, a) \propto \begin{cases} n_k & \text{if } k \text{ is an existing table} \\ a & \text{if } k \text{ is a new table.} \end{cases}
$$

which can also be represented as

$$\theta_n|\theta_{1:n-1} \sim \frac{a}{a+n-1}B_0(\cdot) + \frac{1}{a+n-1}\sum_{i=1}^{n-1}\mathbf{1}_{\theta_i}(\cdot). \tag{A.1}$$

Chinese restaurant process shares the same characteristics as the Pólya urn process which can be extend to the two-parameter Pitman–Yor process (Pitman and Yor, 1997). Here is the basic idea of Pólya urn process. Imagine that we have an urn with possibly infinitely many colors. Let a (again, the concentration parameter in DP) be the initial number of balls with each color. The urn evolves in discrete time steps - at each step, one ball is sampled uniformly at random and put it back to the urn; The color of the withdrawn ball is observed, and one additional ball with the same color is returned to the urn. This process is then repeated.

Equation (A.1) is also called the Blackwell-MacQueen prediction rule - the conditional distribution of θ_n given previous sampled $\theta_{1:n-1}$ from the Dirichlet process prior. It characterizes the Chinese restaurant process/Pólya urn process and serves as the key component in the Pólya urn Gibbs sampler (Ishwaran and James, 2001).

Prior literature shows the equivalence between Chinese restaurant process/Pólya urn process and aforementioned processes. Blackwell and MacQueen (1973) present the equivalence between Pólya urn process and Dirichlet process. Miller (2019) formally prove that the Chinese restaurant process is equivalent to the stick breaking process.

The Chinese restaurant process (Pólya urn process) reveals that the Dirichlet process prior has an important clustering property in terms of the group-dependent model parameters: The probability that θ_n takes the same value of θ_i for $i = 1, 2, \ldots, n-1$ is proportional to $\sum_{i=1}^{n-1}\mathbf{1}_{\theta_i}(.)$. This self-reinforcing property is sometimes expressed as *the rich get richer*.

A.2 Hierarchical Dirichlet Process

The hierarchical Dirichlet process (HDP) was developed by Teh et al. (2006). The HDP is a nonparametric Bayesian approach to clustering grouped data, with the known group membership. It equips a Dirichlet process for each group of data, with the Dirichlet processes for all groups sharing a base distribution which is itself drawn from a Dirichlet process. This method allows groups to share statistical strength via sharing of clusters across groups. The base distribution being drawn from a Dirichlet process is important, because draws from a Dirichlet process are atomic probability measures, and the atoms will appear in all group-level Dirichlet processes. Since each atom corresponds to a cluster, clusters are shared across all groups.

The HDP is parameterized by a base distribution H that governs the prior distribution over data items, and a number of concentration parameters that govern the prior number of

clusters and amount of sharing across groups. Assume that we have J groups of data, each consisting of N_j data points, $y_{j1}, \ldots y_{jN_j}$. The process defines a set of random probability measures $(B_j)_{j=1}^{J}$, one for each group. The random probability measure B_j for the j-th group is distributed as a Dirichlet process:

$$B_j | B_0 \sim \mathrm{DP}\left(\gamma, B_0\right), \tag{A.2}$$

where γ is the concentration parameter and B_0 is the base distribution shared across all groups. The distribution of the global random probability measure B_0 is given by,

$$B_0 \sim \mathrm{DP}\left(\alpha_0, H\right), \tag{A.3}$$

with concentration parameter α_0 and base distribution H.

A hierarchical Dirichlet process can be used as the prior distribution over the parameters for grouped data. For each j, let $\left(\phi_{ji}\right)_{i=1}^{n_j}$ be i.i.d. random variables distributed as B_j. Each ϕ_{ji} is a parameter corresponding to a single observation y_{ji}. The likelihood is given by,

$$\begin{aligned} \phi_{ji} | B_j &\sim B_j, \\ y_{ji} | \phi_{ji} &\sim f\left(\phi_{ji}\right). \end{aligned} \tag{A.4}$$

The resulting model above is called a HDP mixture model, with the HDP referring to the hierarchically linked set of Dirichlet processes, and the mixture model referring to the way the Dirichlet processes are related to the data items.

To understand how the HDP implements a clustering model, and how clusters become shared across groups, recall that draws from a Dirichlet process are atomic probability measures with probability one. The base distribution B_0 can be expressed using a stick-breaking representation,

$$B_0 = \sum_{k=1}^{\infty} \beta_k \delta_{\theta_k}, \tag{A.5}$$

where there are an infinite number of atoms, $\theta_k \sim H$, $k = 1, 2, \ldots$. Each atom is associated with a mass β_k and $\beta = (\beta_i)_{i=1}^{\infty} \sim \mathrm{Stick}(\gamma)$ are mutually independent. Since B_0 is the base distribution for the group specific Dirichlet processes, each B_j has the same atoms as B_0 and can be written in the form,

$$B_j = \sum_{k=1}^{\infty} \pi_{jk} \delta_{\theta_k}. \tag{A.6}$$

Let $\pi_j = \left(\pi_{jk}\right)_{k=1}^{\infty}$. Note that the weights π_j are independent given β (since the B_j are independent given B_0). It can be shown that the connection between the weights π_j and the

global weights β is

$$\pi_j \mid \alpha_0, \beta \sim \mathrm{DP}(\alpha_0, \beta). \tag{A.7}$$

Thus the set of atoms is shared across all groups, with each group having its own group-specific atom masses. Relating this representation back to the observed data, we see that each data item is described by a mixture model,

$$y_{ji}|B_j \sim \sum_{k=1}^{\infty} \pi_{jk} f(\theta_k), \tag{A.8}$$

where the atoms θ_k play the role of the mixture component parameters, while the masses π_{jk} play the role of the mixing proportions. As a result, each group of data is modeled using a mixture model, with mixture components shared across all groups and group-specific mixing weights.

Chinese Restaurant Franchise

Teh et al. (2006) have also described the marginal probabilities obtained from integrating over the random measures B_0 and $(B_j)_{j=1}^J$. They show that these marginals can be described in terms of a Chinese restaurant franchise (CRF) that is an analog of the Chinese restaurant process.

Recall that ϕ_{ji} are random variables with distribution B_j. In the following discussion, we will let $\theta_1, \ldots, \theta_K$ denote K i.i.d. random variables distributed according to H, and, for each j, we let $\psi_{j1}, \ldots, \psi_{jT_j}$ denote T_j i.i.d. variables distributed according to B_0.

Each ϕ_{ji} is associated with one ψ_{jt}, while each ψ_{jt} (table id) is associated with one θ_k. Let t_{ji} be the index of the ψ_{jt} associated with ϕ_{ji}, and let k_{jt} (dish id) be the index of θ_k associated with ψ_{jt}. Let n_{jt} be the number of ϕ_{ji}'s associated with ψ_{jt}, while m_{jk} is the number of ψ_{jt}'s associated with θ_k. Define $m_k = \sum_j m_{jk}$ as the number of ψ_{jt}'s associated with θ_k over all j. Notice that while the values taken on by the ψ_{jt}'s need not be distinct, they are distributed according to a discrete random probability measure $B_0 \sim \mathrm{DP}(\gamma, H)$, we are denoting them as distinct random variables.

First consider the conditional distribution for ϕ_{ji} given $\phi_{j1}, \ldots, \phi_{ji-1}$ and B_0, where B_j is integrated out, we have,

$$\phi_{ji}|\phi_{j1}, \ldots, \phi_{ji-1}, \alpha_0, G_0 \sim \sum_{t=1}^{T_j} \frac{n_{jt}}{i-1+\alpha_0} \delta_{\psi_{jt}} + \frac{\alpha_0}{i-1+\alpha_0} G_0, \tag{A.9}$$

This is a mixture, and a draw from this mixture can be obtained by drawing from the terms on the right-hand side with probabilities given by the corresponding mixing proportions. If a term in the first summation is chosen, then we set $\phi_{ji} = \psi_{jt}$ and let $t_{ji} = t$ for the chosen t.

If the second term is chosen, then we increment T_j by one, draw $\psi_{jT_j} \sim B_0$ and set $\phi_{ji} = \psi_{jT_j}$ and $t_{ji} = T_j$.

Now we proceed to integrate out B_0. Notice that B_0 appears only in its role as the distribution of the variables ψ_{jt}. Since B_0 is distributed according to a Dirichlet process, we can integrate it out and writing the conditional distribution of ψ_{jt} directly:

$$\psi_{jt}|\psi_{11}, \psi_{12}, \ldots, \psi_{21}, \ldots, \psi_{jt-1}, \gamma, H \sim \sum_{k=1}^{K} \frac{m_k}{\sum_k m_k + \gamma} \delta_{\theta_k} + \frac{\gamma}{\sum_k m_k + \gamma} H. \tag{A.10}$$

If we draw ψ_{jt} via choosing a term in the summation on the right-hand side of this equation, we set $\psi_{jt} = \theta_k$ and let $k_{jt} = k$ for the chosen k. If the second term is chosen, we increment K by one, draw $\theta_K \sim H$ and set $\psi_{jt} = \theta_K, k_{jt} = K$.

In short, the CRF is comprised of J restaurants with a shared menu across the restaurants. Each restaurant corresponds to an HDP group, and an infinite buffet line of dishes common to all restaurants. The process of seating customers at tables, however, is restaurant specific. Each customer is preassigned to a given restaurant determined by that customer's group j. Upon entering the j th restaurant in the CRF, customer y_{ji} sits at currently occupied tables t_{ji} with probability proportional to the number of currently seated customers, or starts a new table $T_j + 1$ with probability proportional to α. The first customer to sit at a table goes to the buffet line and picks a dish k_{jt} for their table, choosing the dish with probability proportional to the number of times that dish has been picked previously, or ordering a new dish θ_{K+1} with probability proportional to γ. The intuition behind this predictive distribution is that integrating over the global dish probabilities β results in customers making decisions based on the observed popularity of the dishes throughout the entire franchise.

A.3 Random Effects vs. Fixed-Effects

Regarding the connection between Bayesian and frequentists' panel data model, according to Koop (2003), if we impose a

(i) non-hierarchical prior (such as Normal-Inverse-Gamma prior without hyperpriors) on the intercept α_{0i}, the resulting panel data model is equivalent to the frequentist fixed-effects model. This is basically a Bayesian linear regression with standard priors on parameters.

(ii) hierarchical prior on the intercept α_{0i}, the resulting panel data model is equivalent to the frequentists' random effects model. A convenient hierarchical prior assumes that, for $i = 1, \ldots, N$,

$$\alpha_{0i} \sim N\left(\mu_\alpha, V_\alpha\right).$$

The hierarchical structure of the prior arises if we treat μ_α and V_α as unknown parameters which require their own prior. We assume μ_α and V_α to be independent of one another with

$$\mu_\alpha \sim N\left(\underline{\mu}_\alpha, \underline{\sigma}_\alpha^2\right),$$

and

$$V_\alpha^{-1} \sim G\left(\underline{V}_\alpha^{-1}, \underline{v}_\alpha\right).$$

This is analogous to the random effects model as α_i are essentially assumed to draw from the underlying distribution, and data are used to update our prior on the hyperparameters of the underlying distribution.

The discussion in Koop (2003) is in line with the hierarchical models discussed in Smith (1973). The panel data model equipped with a non-hierarchical prior is a two-stage hierarchical model which results in a fixed effects model, while incorporating a hierarchical prior forms a three-stage hierarchical model that corresponds to a random effects model.

Back to our settings, if the baseline prior for α_{0i} is a DP (DPM) prior, then our proposed nonparametric Bayesian prior is a type of non-hierarchical (hierarchical) prior with latent group structure in intercepts and hence we call our proposed estimator as the constrained grouped fixed (random) effects estimator.

B Priors

B.1 Dirichlet Process Priors

B.1.1 Prior on Parameters

Prior on Group-Specific Parameters

$$\left(\alpha_i, \sigma_i^2\right) \sim \sum_{k=1}^{\infty} \pi_k \delta_{\left(\alpha_k, \sigma_k^2\right)} \text{ with } \left(\alpha_k, \sigma_k^2\right) \sim B_0(\phi), \tag{B.1}$$

B_0 is an Independent Normal Inverse-Gamma (INIG) distribution:

$$B_0 := INIG\left(\mu_\alpha, \Sigma_\alpha, \frac{\nu_\sigma}{2}, \frac{\delta_\sigma}{2}\right), \tag{B.2}$$

with a set of hyperparameters $\phi = \left(\mu_\alpha, \Sigma_\alpha, \frac{\nu_\sigma}{2}, \frac{\delta_\sigma}{2}\right) = (0, 1, 6, 5)$.

Prior on Stick Lengths

$$\xi_k \sim Beta\left(1, a\right), \tag{B.3}$$

where a is the concentration parameter.

Hyper-prior on Concentration Parameter

$$a \sim Gamma\,(m, n)\,, \tag{B.4}$$

with $(m, n) = (0.4, 10)$.

Prior on Common and Individual Slope Coefficients (if any) Finally, the prior distribution for the common parameter ρ is chosen to be a normal distribution to stay close to the linear regression framework,

$$\rho \sim N(0, \sigma_\rho^2) \text{ with } \sigma_\rho^2 = 1. \tag{B.5}$$

The prior of heterogeneous parameter β_i follows,

$$\beta_i \sim N(0, \Sigma_\beta) \text{ with } \Sigma_\beta = 1 \times \mathbf{I}_p. \tag{B.6}$$

B.1.2 Determining the Scaling Constant c

Given that the dimension of the space of group partitions increases exponentially with the number of units N, attention must be given while selecting c across analyses with different N. As suggested by Paganin et al. (2021), calibrating the modified prior is computationally intensive. We are facing a trade-off between investing time to get the prior "exactly right" and letting the constant c be an estimated model parameter. As such, we propose to find the optimal c that maximizes marginal data density using grid search.

In the Monte Carlo simulation, the value of c is fixed for simplicity, but in the empirical applications, c is determined by marginal data density (MDD). We calculate MDD using the harmonic mean estimator (Newton and Raftery, 1994), which defined as

$$\hat{m}^{HM}(y) = \left[\frac{1}{S} \sum_{j=1}^{S} \frac{1}{p\left(y|\theta^{(j)}\right)} \right]^{-1}, \tag{B.7}$$

given a sample $\theta^{(j)}$ from the posterior $p(\theta|y)$. The simplicity of the harmonic mean estimator is its main advantage over other more specialized techniques. It uses only within-model posterior samples and likelihood evaluations, which are often available anyway as part of posterior sampling. We finally choose the optimal value for c that maximizes MDD.

B.2 Dirichlet Process Mixture Priors

We also consider the Dirichlet Process Mixture (DPM) prior for α_i as a natural extension to the DP prior. Notice that a draw from DP is, by definition, a discrete distribution. In this sense, given the baseline model, imposing a DP prior on the distribution of α_i entails limiting the intercepts to some discrete values and assuming that intercepts within a group are identical, which may not be appealing for some empirical applications. DPM prior, on the other hand, assumes α_i has a continuous parametric distribution $f(\alpha_i; \mu_\alpha)$, with μ_α as parameters, and uses a DP prior for the distribution of μ_α. The parameters μ_α are then discrete and has group structure, whereas group heterogeneity α_i has a continuous distribution, i.e., α_i within a group can be different, but they are all sampled from the same distribution.

DPM prior adds additional layer of mixture by allowing for *infinite Gaussian mixture*,

$$\alpha_i \sim \sum_{j=1}^{\infty} \pi_j N\left(\alpha_j, \sigma_j^2\right) \text{ where } (\alpha_j, \sigma_j^2) \sim INIG\left(\mu_\alpha, \Sigma_\alpha, \frac{\nu_\sigma}{2}, \frac{\delta_\sigma}{2}\right),$$

where the base distribution is chosen to be a conjugate multivariate-normal-inverse-Wishart distribution, or a normal-inverse-gamma distribution for scalar. It is worth noting that $\sigma_{g_i}^2$ defining in the same manner doesn't have a close-form posterior, we will resort to the random-walk Metropolis-Hastings approach. See the detailed implementation in Liu (2022).

C Posterior Distributions and Algorithms

C.1 Blocked Gibbs Sampler and Algorithm

Initialization:

(i) Preset the initial number of active groups as $K_0^a = N$.

(ii) Set concentration parameter a to its prior mean.

(iii) In ignorance of group heterogeneity ($K = 1$) and heteroskedasticity, use Anderson and Hsiao (1982) IV approach to get $\hat{\alpha}_{IV}$ and $\hat{\Sigma}_{\alpha,IV}$. These IV estimators serve as the mean and covariance matrix in the related priors.

(iv) Generate K_0^a random sample from the distribution $N(\hat{\alpha}_{IV}, \hat{\Sigma}_{\alpha,IV})$.

(v) Initialize group membership G by using assuming no group structure: $G^{(0)} = [1, 2, ..., N]$.

For each iteration $s = 1, 2, .., N_{sim}$

(i) Number of active groups:

$$K^a = \max_{1 \leqslant i \leqslant N} g_i^{(s-1)}.$$

(ii) Group "stick length": for $k = 1, 2, ..., K^a$, draw ξ_k from a Beta distribution in (C.14):

$$\xi_k | a^{(s-1)}, G^{(s-1)} \sim Beta\left(|B_k| + 1, a + \sum_{j=1}^{N} \mathbf{1}(g_j > k) \right),$$

and calculate group probability in accordance to (C.15).

(iii) Group heterogeneity: for $k = 1, 2, ..., K^a$, draw $\alpha_k^{(s)}$ from a normal distribution in (C.12):

$$\alpha_k | \rho^{(s-1)}, \beta^{(s-1)}, \Sigma^{(s-1)}, G^{(s-1)}, Y, X \sim N\left(\bar{\mu}_{\alpha_k}, \bar{\Sigma}_{\alpha_k}\right).$$

(iv) Group heteroscedasticity: for $k = 1, 2, ..., K^a$ and $t = 1, 2, ..., T$, draw $\sigma_k^{2(s)}$ from an inverse Gamma distribution in (C.13):

$$\sigma_k^2 | \rho^{(s-1)}, \beta^{(s-1)}, \alpha^{(s)}, G^{(s-1)}, Y, X \sim IG\left(\frac{\bar{v}_{\sigma,k}}{2}, \frac{\bar{\delta}_{\sigma,k}}{2} \right).$$

(v) Auxiliary variables: for $i = 1, 2, ..., N$, draw u_i from an uniform distribution in (C.18):

$$u_i | \Xi^{(s)}, G^{(s-1)} \sim Unif(0, p_{g_i}^{(s)}).$$

Then calculate u^* according to (C.9).

(vi) DP concentration parameter:

(a) Draw latent variable η from a Beta distribution in (C.16):

$$\eta \sim Beta(a + 1, N)$$

(b) Draw concentration parameter a from a mixture of Gamma distribution in (C.17):

$$a | \eta, K^a \sim \begin{cases} Gamma\left(m + K^a, n - \log(\eta)\right) & \text{with prob. } \pi_a \\ Gamma\left(m + K^a - 1, n - \log(\eta)\right) & \text{with prob. } 1 - \pi_a \end{cases},$$

and π_a is defined as

$$\frac{\pi_a}{1 - \pi_a} = \frac{m + K^a - 1}{N(n - \log(\eta))}.$$

(vii) Potential groups: start with $\tilde{K} = K^a$,

(a) Group probabilities:

(1) if $\sum_{j=1}^{\tilde{K}} \pi_j^{(s)} > 1 - u^*$, set $K^* = \tilde{K}$ and stop.

(2) otherwise, let $\tilde{K} = \tilde{K} + 1$, draw $\xi_{\tilde{K}} \sim Beta\left(1, \alpha^{(s)}\right)$, update $\pi_{\tilde{K}} = \xi_{\tilde{K}} \prod_{j<\tilde{K}} (1 - \xi_j)$ and go to step (1).

(b) Group parameters: for $k = K + 1, \cdots, K^*$, draw $\alpha_k^{(s)}$ and $\sigma_k^{2(s)}$ from their prior distributions.

(xi) Group membership: for $j = 1, 2, ..., J$ and $k = 1, 2, ..., K^a$, draw g_j from a multinomial distribution in (C.19).

C.2 Random Coefficients Model with Soft Constraints

We present the conditional posterior distributions of parameters in the time-invariant random effects model with heteroscedasticity, must-link constraints and cannot-link constraints, which is the most complicated scenarios. For other models, such as its homoscedastic counterparts, adjustment can be easily made by assuming common error variances.

C.2.1 Derivation

Model:

$$y_{it} = \alpha_{g_i}' x_{it} + \varepsilon_{it}, \quad \varepsilon_{it} \sim N\left(0, \sigma_{g_i}^2\right). \tag{C.1}$$

To facilitate derivation, we stack observations and parameters,

$$\begin{aligned}
\text{Dependent variable: } Y &= [y_1, y_2, \ldots, y_N], y_i = [y_{i1}, y_{i2}, \ldots, y_{iT}]', \\
\text{Covariates: } X &= [x_1, x_2, \ldots, x_N], x_i = [x_{i1}, x_{i2}, \ldots, x_{iT}]', \\
\text{Grouped-specific parameters: } \alpha &= [\alpha_1, \alpha_2, \ldots, \alpha_N], \\
\text{Error variance: } \Sigma &= \left[\sigma_1^2, \sigma_2^2, \ldots, \sigma_N^2\right], \\
\text{Stick length: } \Xi &= [\xi_1, \xi_2, \ldots], \\
\text{Group indices: } G &= [g_1, \ldots, g_N], \\
\text{Auxiliary variable: } u &= [u_1, u_2, ..., u_N], \\
\text{Hyper parameters: } \phi &= [\mu_\alpha, \Sigma_\alpha, \nu_\sigma, \delta_\sigma].
\end{aligned}$$

In order to write down the posterior of unknown parameters given a set of pairwise constraints, a probabilistic model of how weights of constraints are obtained must be specified. Inspired by Shental et al. (2003), we have the following assumptions:

Assumption 3. *(Data)*

(i) Data points are first sampled i.i.d from the full probability distribution conditional on G.

(ii) From this sample, pairs of points are randomly chosen according to a uniform distribution. In case both points in a pair belong to the same source a must-link constraint is formed and a cannot-link if formed when they belong to different sources.

The posterior of unknown objects in the random coefficients model is,

$$\begin{aligned} & p(\alpha, \sigma^2, \Xi, a, G|Y, X, W, \phi) \\ \propto\ & p(Y|X, \alpha, \sigma^2, G) p(\alpha, \sigma^2|\phi) p(G|\Xi, W) p(\Xi|a) p(a). \end{aligned} \tag{C.2}$$

All priors have been well-defined except for $p(G|\Xi, W)$ - the prior for group indices G conditional on stick lengths Ξ and the weights of constraints W.

Using the Bayes rule, the modified prior for the group indices is

$$p(G|\Xi, W) = \frac{p(W|G)p(G|\Xi)}{\sum_{G'} p(W|G')p(G'|\Xi)} \propto p(W|G)p(G|\Xi), \tag{C.3}$$

where the sum in the denominator is taken over all possible group partitioning, $p(W|G)$ is the weighting function of the form:

$$p(W|G) = \prod_{i,j} \exp\left(cW_{ij}\delta_{ij}\right),$$

and $p(G|\Xi)$ is the density of a categorical distribution with probabilities generated by the stick-breaking process.

From (C.3), the prior of g_i conditional on the group indices of the other $G^{(-i)}$ is

$$p(g_i|\Xi, W_i, G^{(-i)}) \propto p\left(W_i|G\right) p(g_i|\Xi), \tag{C.4}$$

where $W_i = \{W_{ij}|j = 1, ..., N\}$ and

$$p(W_i|G) = \prod_{j=1}^{N} \exp\left(2cW_{ij}\delta_{ij}\right). \tag{C.5}$$

Given the expression of $p(g_i|\Xi, W_i, G^{(-i)})$ and the DP prior specified in Appendix B.1,

the posterior of unknown objects in the random coefficients model can be written as,

$$
\begin{aligned}
& p(\alpha, \sigma^2, \Xi, a, G|Y, X, W, \phi) \\
\propto\ & p(Y|X, \alpha, \sigma^2, G) p(\alpha, \sigma^2|\phi) p(G|\Xi, W) p(\Xi|a) p(a) \\
\propto\ & \prod_{i=1}^{N} p\left(y_i|x_i, \alpha_{g_i}, \sigma^2_{g_i}\right) \prod_{j=1}^{\infty} p(\alpha_j, \sigma_j^2|\phi) \prod_{j=1}^{\infty} p(\xi_j|a) \prod_{i=1}^{N} p\left(g_i|\Xi, W_i, G^{(-i)}\right) p(a) \\
=\ & \left[\prod_{i=1}^{N} p\left(y_i|x_i, \alpha_{g_i}, \sigma^2_{g_i}\right) p\left(g_i|\Xi, W_i, G^{(-i)}\right)\right] \left[\prod_{j=1}^{\infty} p(\alpha_j, \sigma_j^2|\phi) p(\xi_j|a)\right] p(a) \\
=\ & \left[\prod_{i=1}^{N} p\left(y_i|x_i, \alpha_{g_i}, \sigma^2_{g_i}\right) p\left(W_i|G\right) p(g_i|\Xi)\right] \left[\prod_{j=1}^{\infty} p(\alpha_j, \sigma_j^2|\phi) p(\xi_j|a)\right] p(a). \qquad \text{(C.6)}
\end{aligned}
$$

In the following derivation and algorithm, we adopt the slice sampler (Walker, 2007) that avoids approximation in Ishwaran and James (2001). Walker (2007) augments the posterior distribution with a set of auxiliary variables $u = [u_1, u_2, ..., u_N]$, which are i.i.d. standard uniform random variables, i.e, $u_i \overset{iid}{\sim} U(0,1)$. Then the augmented posterior is written as,

$$
\begin{aligned}
& p(\alpha, \sigma^2, \Xi, a, G, u|Y, X, W, \phi) \\
\propto\ & \left[\prod_{i=1}^{N} p\left(y_i|x_i, \alpha_{g_i}, \sigma^2_{g_i}\right) \mathbf{1}(u_i < \pi_{g_i}) p\left(W_i|G\right)\right] \left[\prod_{j=1}^{\infty} p(\alpha_j, \sigma_j^2|\phi) p(\xi_j|a)\right] p(a) \\
=\ & \left[\prod_{i=1}^{N} p\left(y_i|x_i, \alpha_{g_i}, \sigma^2_{g_i}\right) p(u_i|\pi_{g_i}) \pi_{g_i} p\left(W_i|G\right)\right] \left[\prod_{j=1}^{\infty} p(\alpha_j, \sigma_j^2|\phi) p(\xi_j|a)\right] p(a), \qquad \text{(C.7)}
\end{aligned}
$$

where $\pi_{g_i} = p(g_i|\Xi)$, $p(u_i|\pi_{g_i})$ is a uniform distribution defined on $[0, \pi_{g_i}]$, and $\mathbf{1}(\cdot)$ is the indicator function, which is equal to zero unless the specific condition is met. The original posterior can be recovered by integrating out u_i for $i = 1, 2, ..., N$. As we don't limit the upper bound of the number of groups, it is impossible to sample from an infinite-dimensional posterior density. The merit of slice-sampling is that it reduces the dimensions and allows us to solve a manageable problem with finite dimensions, which we will see below.

With a set of auxiliary variables $u = [u_1, u_2, ..., u_N]$, we define the largest possible number of potential components as

$$
K^* = \min_k \left\{ u^* > 1 - \sum_{j=1}^{k} \pi_j \right\}, \qquad \text{(C.8)}
$$

where

$$u^* = \min_{1 \leqslant i \leqslant N} u_i. \tag{C.9}$$

Such a specification ensures that for any group $k > K^*$ and any unit $i \in \{1, 2, ..., N\}$, we have $u_i > \pi_k$.[12] This crucial property limits the dimension of (α_k, σ_k^2) to K^* as the densities of (α_k, σ_k^2) and equal 0 for $k > K^*$ due to $\mathbf{1}(u_i < \pi_k) = 0$, which will be clear in the subsequent posterior derivation. Intuitively, the latent variable u_i has an effect of "dynamically truncating" the number of groups needed to be sampled.

Next, we define the number of active groups

$$K^a = \max_{1 \leqslant i \leqslant N} g_i. \tag{C.10}$$

It can be shown that $K^a \leqslant K^*$.[13]

As the base distribution B_0 is the Independent-Normal-Inverse-Gamma distribution, the prior density of α_i and σ_i^2 are independent.

Conditional posterior of α (grouped coefficients).

$$p(\alpha|\sigma^2, G, Y, X, \phi) \propto \left[\prod_{i=1}^{N} p\left(y_i|x_i, \alpha_{g_i}, \sigma_{g_i}^2\right)\right] \left[\prod_{j=1}^{\infty} p(\alpha_j, \sigma_j^2|\phi)\right].$$

For $k = 1, 2, ..., K^a$, define a set of units that belong to the group k,

$$B_k = \{i|g_i = k, i \in \{1, 2, ..., N\}\}, \tag{C.11}$$

then the posterior density for α_k read as

$$\begin{aligned}
& p(\alpha_k|\sigma_k^2, G, Y, X, \phi) \\
\propto & \left[\prod_{i \in B_k} p(y_i|x_i, \alpha_{g_i}, \sigma_{g_i}^2)\right] p(\alpha_k|\phi) \\
\propto & \exp\left[-\frac{1}{2\sigma_k^2} \sum_{i \in B_k} (y_i - x_i\alpha_k)' (y_i - x_i\alpha_k)\right] \exp\left[-\frac{1}{2} (\alpha_k - \mu_\alpha)' \Sigma_\alpha^{-1} (\alpha_k - \mu_\alpha)\right] \\
\propto & \exp\left[-\frac{1}{2} (\alpha_k - \bar{\mu}_{\alpha_k})' \bar{\Sigma}_{\alpha_k}^{-1} (\alpha_k - \bar{\mu}_{\alpha_k})\right].
\end{aligned}$$

[12] See proof in theorem 4.
[13] See proof in theorem 4.

Assuming an independent normal conjugate prior for α_k, the posterior for α_k is given by

$$\alpha_k|\sigma_k^2, G, Y, X, \phi \sim N\left(\bar{\mu}_{\alpha_k}, \bar{\Sigma}_{\alpha_k}\right). \tag{C.12}$$

where

$$\begin{aligned}
\bar{\Sigma}_{\alpha_k} &= \left(\Sigma_\alpha^{-1} + \sigma_k^{-2} \sum_{i \in B_k} x_i' x_i\right)^{-1}, \\
\bar{\mu}_{\alpha_k} &= \bar{\Sigma}_{\alpha_k} \left(\Sigma_\alpha^{-1} \mu_\alpha + \sigma_k^{-2} \sum_{i \in B_k} x_i' y_i^\alpha\right), \\
y_i^\alpha &= y_i - x_i \alpha_{g_i}.
\end{aligned}$$

Conditional posterior of σ^2 (grouped variance). Under the cross-sectional independence, for $k = 1, 2, ..., K^a$,

$$p(\sigma_k^2|\alpha_k, G, Y, X, \phi) \propto \left[\prod_{i \in B_k} p\left(y_i|x_i, \alpha_{g_i}, \sigma_{g_i}^2\right)\right] p(\sigma_k^2|\phi).$$

With a inverse-gamma prior $\sigma_k^2 \sim IG\left(\frac{v_\sigma}{2}, \frac{\delta_\sigma}{2}\right)$, the posterior distribution of σ_k^2 is

$$\begin{aligned}
& p(\sigma_k^2|\alpha_k, G, Y, X, \phi) \\
\propto & \prod_{i \in B_k} \left[\left(\sigma_k^2\right)^{-\frac{T}{2}} \exp\left(-\frac{1}{2\sigma_k^2}\left(y_i - x_i\alpha_k\right)'\left(y_i - x_i\alpha_k\right)\right)\right] \left(\frac{1}{\sigma_k^2}\right)^{\frac{v_\sigma}{2}+1} \exp\left(-\frac{\delta_\sigma}{2\sigma_k^2}\right) \\
= & \left(\frac{1}{\sigma_k^2}\right)^{\frac{v_\sigma + T|B_k|}{2}+1} \exp\left[-\frac{\delta_\sigma + \sum_{i \in B_k}\left(y_i - x_i\alpha_k\right)'\left(y_i - x_i\alpha_k\right)}{2\sigma_k^2}\right].
\end{aligned}$$

This implies

$$\sigma_k^2|\alpha_k, G, Y, X, \phi \sim IG\left(\frac{\bar{v}_{\sigma,k}}{2}, \frac{\bar{\delta}_{\sigma,k}}{2}\right), \tag{C.13}$$

where

$$\begin{aligned}
\bar{v}_{\sigma,k} &= v_\sigma + T|B_k|, \\
\bar{\delta}_{\sigma,kt} &= \delta_\sigma + \sum_{i \in B_k}\left(y_i - x_i\alpha_k\right)'\left(y_i - x_i\alpha_k\right), \\
|B_k| &= \#\text{ of units in group } k.
\end{aligned}$$

Conditional posterior of Ξ (stick length).

$$\begin{aligned} & p(\Xi|a,G) \\ \propto & \left[\prod_{i=1}^{N} p(u_i|\pi_{g_i})\pi_{g_i}\right]\left[\prod_{j=1}^{\infty} p(\xi_j|a)\right] \\ \propto & \left[\prod_{i=1}^{N} p(u_i|\pi_{g_i})\xi_{g_i}\prod_{l<g_i}(1-\xi_l)\right]\left[\prod_{j=1}^{\infty} p(\xi_j|a)\right]. \end{aligned}$$

For $k = 1, 2, ..., K^a$,

$$\begin{aligned} p(\Xi|a,G) \propto & \left(\prod_{i\in B_k}\xi_k\right)(1-\xi_k)^{\sum_{j=1}^{N}\mathbf{1}(g_j>k)}(1-\xi_k)^{a-1}, \\ \propto & \xi_k^{|B_k|}(1-\xi_k)^{a+\sum_{j=1}^{N}\mathbf{1}(g_j>k)-1}. \end{aligned}$$

where B_K is the set of units that currently belong to group k, see equation (C.11).

Therefore, posterior distribution of ξ_k is

$$\xi_k|a,G \sim Beta\left(|B_k|+1, a+\sum_{j=1}^{N}\mathbf{1}(g_j>k)\right). \tag{C.14}$$

Give $\Xi = [\xi_1, \xi_2, ..., \xi_{K^a}]$, update group probabilities $\pi_1, \pi_2, ..., \pi_{K^a}$:

$$\pi_k|G,\Xi = \begin{cases} \xi_1, & k=1 \\ \xi_k\prod_{j<k}(1-\xi_j), & k=2,\ldots,K^a \end{cases}. \tag{C.15}$$

Conditional posterior of a (concentration parameter). Regarding the DP concentration parameter, the standard posterior derivation doesn't work due to the unrestricted number of components in the current sampler. Instead, we implement the 2-step procedure proposed by Escobar and West (1995) (p.8-9). Following their approach, we first draw a latent variable η,

$$\eta \sim Beta\,(a+1, J). \tag{C.16}$$

Then, conditional on η and K^a, we draw a from a mixture of two Gamma distribution:

$$p(a|\eta, K^a) = \pi_a Gamma\left(m + K^a, n - \log(\eta)\right) + (1 - \pi_a) Gamma\left(m + K^a - 1, n - \log(\eta)\right), \tag{C.17}$$

with the weights π_a defined by

$$\frac{\pi_a}{1 - \pi_a} = \frac{m + K^a - 1}{N[n - \log(\eta)]}.$$

Conditional posterior of u (auxiliary variable). Conditional on the group "stick lengths" ξ_k and group indices G, it is straightforward to show that the posterior density of u_i is a uniform distribution defined on $(0, \pi_{g_i})$, that is

$$u_i|\Xi, G \sim Unif\left(0, \pi_{g_i}\right), \tag{C.18}$$

where $\pi_{g_i} = \xi_{g_i} \prod_{j<g_j}(1 - \xi_j)$. Moreover, it is worth noting that the values for K^* and u^* need to be updated according to equation (C.8) and (C.9) after this step.

Conditional posterior of G (group indices). We derive the posterior distribution of g_i consider on $G^{(-i)}$, where $G^{(-i)}$ is a set including all member indices except for g_i, i.e., $G^{(-i)} = G \backslash g_i$. As a result, for $k = 1, 2, ..., K^*$,

$$\begin{aligned} & p\left(g_i = k|y_i, x_i, \alpha_k, \sigma_k^2, G^{(-i)}, u_i\right) \\ \propto\ & p\left(y_i|x_i, \alpha_k, \sigma_k^2\right) \mathbf{1}(u_i < \pi_k) p\left(W_i|G\right) \\ =\ & p\left(y_i|x_i, \alpha_k, \sigma_k^2\right) \mathbf{1}(u_i < \pi_k) \prod_{j=1}^{N} \exp\left(2cW_{ij}\delta_{ij}\right). \end{aligned} \tag{C.19}$$

Finally, we normalize the point mass to get a valid distribution.

D Technical Proofs

D.1 Slice Sampling

Theorem 4. *Suppose that we have a model with posterior as given in Appendix C.2. Given the definition of the number of potential component K^* in (C.8), the minimum of auxiliary variables u^* in (C.9) and the number of active group K in (C.10), we have*

(i) $u_i > \pi_k$ for $\forall i = 1, 2, ..., n$ and $\forall k > K^*$;

(ii) $K < K^*$.

Proof. (i) By definition, $u^* = \min_{1 \leqslant i \leqslant N} u_i$ for $i = 1, 2, ..., n$, then,

$$u_i \geqslant u^* > 1 - \sum_{j=1}^{K^*} \pi_j = \sum_{j=K^*}^{\infty} \pi_j \geqslant \pi_k, \forall k > K^*.$$

(ii) Let i' be an unit i such that $g_{i'} = K$. According to the posterior of G, the group K exists if $u_{i'} < \pi_K$, otherwise $p(g_i = K|\cdot) = 0$. Then by definition,

$$u^* \leqslant u_{i'} < \pi_K \Rightarrow 1 - u^* > 1 - \pi_K = \sum_{j=1}^{K-1} \pi_j.$$

Since K^* is the smallest number $s.t.\ 1 - u^* < \sum_{j=1}^{K^*} \pi_j$, then $K \leqslant K^*$.

□

D.2 Connection to Lu and Leen (2004) and Lu and Leen (2007)

In this section, we will first show the close connection between the modified prior in the presence of soft constraints defined in (2.13) and the framework of penalized probabilistic clustering proposed by Lu and Leen (2004) and Lu and Leen (2007). Then we will discuss the properties of the weights W_{ij}.

We start with joint prior odds in (2.13):

$$\prod_{i,j} \left(\frac{\psi_{ij}}{1 - \psi_{ij}} \right)^{cT_{ij}\delta_{ij}} = \prod_{i,j} \exp \left[c\delta_{ij} \log \left(\frac{\psi_{ij}}{1 - \psi_{ij}} \right)^{T_{ij}} \right]. \tag{D.1}$$

Define the weight as $W_{ij} = \log \left(\frac{\psi_{ij}}{1 - \psi_{ij}} \right)^{T_{ij}}$. Then when $T_{ij} = 1$, we have

$$W_{ij} = \log \left(\frac{\psi_{ij}}{1 - \psi_{ij}} \right) \Leftrightarrow \psi_{ij} = \frac{\exp\left(W_{ij}\right)}{1 + \exp\left(W_{ij}\right)}. \tag{D.2}$$

When $T_{ij} = -1$, we get

$$W_{ij} = \log \left(\frac{1 - \psi_{ij}}{\psi_{ij}} \right) \Leftrightarrow 1 - \psi_{ij} = \frac{\exp\left(W_{ij}\right)}{1 + \exp\left(W_{ij}\right)}. \tag{D.3}$$

Combining (D.2) and (D.3) yields that

$$\frac{\exp\left(W_{ij}\right)}{1+\exp\left(W_{ij}\right)} = \psi_{ij}^{\frac{1}{2}(1+T_{ij})}(1-\psi_{ij})^{\frac{1}{2}(1-T_{ij})}. \tag{D.4}$$

This is exactly the equation (7) in Lu and Leen (2007) with $\gamma_{ij} = \psi_{ij}$ and $L_{ij} = \frac{1}{2}\left(T_{ij}+1\right)$, which uniquely defines the expression for the weights associated with each pairwise constraint given γ_{ij} and L_{ij}. Since both L_{ij} and T_{ij} are indicators for the type of constraints, they don't affect the formula for W_{ij}, thus the following formula weights coincides with the one used in Lu and Leen (2007) and the both frameworks converge,

$$W_{ij} = \begin{cases} \log\left(\frac{\psi_{ij}}{1-\psi_{ij}}\right) & \text{if } T_{ij} = 1 \\ \log\left(\frac{1-\psi_{ij}}{\psi_{ij}}\right) & \text{if } T_{ij} = -1 \\ 0 & \text{if } T_{ij} = 0. \end{cases} \tag{D.5}$$

Accordingly, the prior defined in (D.1) can be rewritten in term of W_{ij} as

$$\prod_{i,j}\left(\frac{\psi_{ij}}{1-\psi_{ij}}\right)^{cT_{ij}\delta_{ij}} = \prod_{i,j}\exp\left(cW_{ij}\delta_{ij}\right). \tag{D.6}$$

The weight W_{ij} associated with the constraint between unit i and j as in (D.5) has the following properties:

(a) Unboundedness: $W_{ij} \in [-\infty, \infty]$;

(b) Symmetry: $W_{ij} = W_{ji}$;

(c) Sign reflects constraint's type: If $(i,j) \in \mathcal{M}$ or $L_{ij} = 1$, then $W_{ij} = \log\left(\frac{\psi_{ij}}{1-\psi_{ij}}\right) > 0$; If $(i,j) \in \mathcal{C}$ or $L_{ij} = -1$, then $W_{ij} = \log\left(\frac{1-\psi_{ij}}{\psi_{ij}}\right) < 0$; If (i,j) doesn't involve in any constraint or $L_{ij} = 0$, then $W_{ij} = 0$.

(d) Absolute value reflects constraint's accuracy:

$$\frac{e^{|W_{ij}|}}{1+e^{|W_{ij}|}} = \psi_{ij}.$$

It is straightforward to show that $|W_{ij}|$ is monotonically increasing in ψ_{ij}.

D.3 *Prior Similarity Matrix*

Proof of Theorem 1. Given equation (2.9) and (2.16), the prior probability of unit i and j being in the same group is

$$\begin{aligned}
&\Pr(g_i = g_j|W) \\
&= \sum_{G\in\mathcal{G}_{ij}} \frac{1}{M} p(G) \exp\left(c\sum_{m,n} W_{mn}\delta_{mn}\right) \\
&= \sum_{G\in\mathcal{G}_{ij}} \frac{1}{M}\frac{\Gamma(a)}{\Gamma(a+N)}\left[\prod_{k=1}^{K} a\Gamma\left(|B_k|\right)\right] \exp\left(c\sum_{m,n} W_{mn}\delta_{mn}\right) \\
&= \sum_{G\in\mathcal{G}_{ij}} A(G) \exp\left(c\sum_{m,n} W_{mn}\delta_{mn}\right) \qquad \text{(D.7)}
\end{aligned}$$

where $\mathcal{G}_{ij}$ is the set of all possible group indices that satisfies $g_i = g_j$ and M is the normalization constant in (2.16).

$\mathcal{G}_{ij}$ and $\mathcal{G}_{ik}$ are closed related. It is straightforward to see that the numbers of element in $\mathcal{G}_{ij}$ and $\mathcal{G}_{ik}$ are equal since they are all equal to the number of permutation of other $N-2$ units. Moreover, as unit j and k are exchangeable, $\mathcal{G}_{ik}$ can be constructed from $\mathcal{G}_{ij}$ by swapping the group index of unit j and k.

As a result, we can find an one-on-one mapping between $\mathcal{G}_{ij}$ and $\mathcal{G}_{ik}$. That is, for any $G \in \mathcal{G}_{ij}$, if we swap the group index of unit j and k, the resulting partition $s_{jk}(G)$ belongs to $\mathcal{G}_{ik}$, and vice versa. As the constant $A(G)$ depends only on the size of partitions, we have $A(G) = A(s_{jk}(G))$.

The properties between $\mathcal{G}_{ij}$ and $\mathcal{G}_{ik}$ enable we to compare each summand in $\Pr(g_i = g_j|W)$ and $\Pr(g_i = g_k|W)$. The difference between these two probabilities is

$$\begin{aligned}
&\Pr(g_i = g_j|W) - \Pr(g_i = g_k|W) \\
&= \sum_{G\in\mathcal{G}_{ij}} A(G)\exp\left(c\sum_{m,n} W_{mn}\delta_{mn}\right) - \sum_{G\in\mathcal{G}_{ik}} A(G)\exp\left(c\sum_{m,n} W_{mn}\delta_{mn}\right) \\
&= \sum_{G\in\mathcal{G}_{ij}} A(G)\exp\left(c\sum_{m,n} W_{mn}\delta_{mn}\right) - A(s_{jk}(G))\exp\left(c\sum_{m,n} W_{mn}\delta'_{mn}\right) \\
&= \sum_{G\in\mathcal{G}_{ij}} A(G)\left[\exp\left(c\sum_{m,n} W_{mn}\delta_{mn}\right) - \exp\left(c\sum_{m,n} W_{mn}\delta'_{mn}\right)\right]. \qquad \text{(D.8)}
\end{aligned}$$

where δ'_{mn} is evaluated at $s_{jk}(G)$.

We can classify a group partitioning G into two cases:

(i) $G = s_{jk}(G)$. This happens when units j and k are assigned to the same group. Swapping them doesn't affect the group partitioning, which indicates that $\sum_{m,n} W_{mn}\delta_{mn} = \sum_{m,n} W_{mn}\delta'_{mn}$ and hence $\Pr(g_i = g_j|W) = \Pr(g_i = g_k|W)$.

(ii) $G \neq s_{jk}(G)$. These are the more common cases. We again compare $\sum_{m,n} W_{mn}\delta_{mn}$ with $\sum_{m,n} W_{mn}\delta'_{mn}$. $W_{mn}\delta_{mn}$ and $W_{mn}\delta'_{mn}$ are equal when $m \neq j,k$ and $n \neq j,k$ as these terms remain unchanged regardless of the group indices of units j and k. For $m = j,k$, note that $\delta_{jn} = \delta'_{kn}$ and $\delta_{kn} = \delta'_{jn}$ for all $n = 1,2,..,N$. Therefore, under the assumption that $W_{jn} = W_{kn}$ for $\forall n$, we have,

$$\sum_{n=1}^{N} W_{jn}\delta_{jn} + \sum_{n=1}^{N} W_{kn}\delta_{kn} = \sum_{n=1}^{N} W_{jn}\delta'_{kn} + \sum_{n=1}^{N} W_{kn}\delta'_{jn} = \sum_{n=1}^{N} W_{kn}\delta'_{kn} + \sum_{n=1}^{N} W_{jn}\delta'_{jn}, \quad \text{(D.9)}$$

and hence

$$\begin{aligned}
&\sum_{m,n} W_{mn}\delta_{mn} \\
&= \sum_{m,n\notin(j,k)} W_{mn}\delta_{mn} + 2\left(\sum_{n=1}^{N} W_{jn}\delta_{jn} + \sum_{n=1}^{N} W_{kn}\delta_{kn}\right) \\
&= \sum_{m,n\notin(j,k)} W_{mn}\delta'_{mn} + 2\left(\sum_{n=1}^{N} W_{jn}\delta'_{jn} + \sum_{n=1}^{N} W_{kn}\delta'_{kn}\right) \\
&= \sum_{m,n} W_{mn}\delta'_{mn},
\end{aligned}$$

where the first and third equalities use facts that $W_{mn} = W_{nm}$, $\delta_{mn} = \delta_{nm}$ and $W_{nn} = 0$ for $\forall n, m$. The second equality follows the result in (D.9).

In both cases, we have $\sum_{m,n} W_{mn}\delta_{mn} = \sum_{m,n} W_{mn}\delta'_{mn}$ for all $G \in \mathcal{G}_{ij}$ and therefore

$$\Pr(g_i = g_j|W) - \Pr(g_i = g_k|W) = 0. \quad \text{(D.10)}$$

□

D.4 *PC-KMeans*

Proof of Theorem 2. We start with a brief discussion of *PC-KMeans* algorithm (Basu et al., 2004a). Given a set of observations $(y_1, y_2, \ldots, y_N)$, a set of must-link constraints $\mathcal{M}$, a set of cannot-link constraints $\mathcal{C}$, the cost of violating constraints $w = \{w^m_{ij}, w^c_{ij}\}$ and the number of groups K, the *PC-KMeans* algorithm aims to partition the N units into K groups so as to

minimize the following objective function,

$$L(G) = \underbrace{\frac{1}{2}\sum_{k=1}^{K}\sum_{i\in B_k}\|z_i-\mu_k\|^2}_{\text{within-cluster sum of squares}} + \underbrace{\sum_{(i,j)\in\mathcal{M}}\omega_{ij}^{m}\mathbf{1}\left(g_i\neq g_j\right)+\sum_{(i,j)\in\mathcal{C}}\omega_{ij}^{c}\mathbf{1}\left(g_i=g_j\right)}_{\text{cost of violation}}, \tag{D.11}$$

where μ_k is the centroid of group k, i.e., $\mu_k = \frac{1}{|B_k|}\sum_{i\in B_k} y_i$, B_k is the set of units that are assigned to group k, and $|B_k|$ is the size of group k. Equation (D.11) can be rewritten as

$$L(G) = \frac{1}{2}\sum_{i=1}^{N}\|y_i-\mu_{g_i}\|^2 - \sum_{i,j} cW_{ij}\delta_{ij} + Const, \tag{D.12}$$

where $Const = c\left(\sum_{(i,j)\in\mathcal{M}} W_{ij} - \sum_{(i,j)\in\mathcal{C}} W_{ij}\right)$ is a constant, c is the scaling constant introduced in (2.13), and

$$W_{ij} = \begin{cases} \frac{\omega_{ij}^{m}}{2c} & \text{if } (i,j)\in\mathcal{M} \\ -\frac{\omega_{ij}^{c}}{2c} & \text{if } (i,j)\in\mathcal{C} \\ 0 & \text{otherwise.} \end{cases} \tag{D.13}$$

The clustering process includes minimizing the objective function over both group partition G (assignment step) and the model parameters $\mu = \{\mu_1, \mu_2, \ldots, \mu_K\}$ (update step). Next, we will show that the *PC-KMeans* algorithm is embodied in our proposed Gibbs sampler with soft constraints.

Under assumption (i), we can rewrite the baseline model with a set of variables z_{it} that don't have grouped heterogeneous effects on y_{it},

$$y_{it} = \alpha'_{g_i}x_{it} + \beta_i' z_{it} + \varepsilon_{it} = \alpha_{g_i} + \beta_i' z_{it} + \varepsilon_{it},$$

where the second equality holds due to the assumption of $x_{it} = 1$. β_i can be equal across units, i.e., $\beta_i = \beta$.

Under assumption (ii), we fix the number of groups upfront and thus we don't rely on slice sampling in which K is unknown and determined dynamically. Hereinafter, we focus on posterior distribution without the auxiliary variable u_i. Notice that the indicator function $\mathbf{1}(u_i < \pi_{g_i})$ in the posterior density reduces to π_{g_i}.

Part 1: Assignment Step

Assume we have soft pairwise constraints and weights are specified in (D.13). Under the

assumptions (iii) and (iv), the posterior density of the group membership indicators G is,

$$\begin{aligned}
&p(G|\alpha,\beta,\sigma^2,Y,X,Z,W) \\
&= \frac{1}{Z_S}\prod_{i=1}^{N}\left[p(y_i|\beta_i,\alpha_{g_i},\sigma^2_{g_i},x_i,z_i)\pi_{g_i}\right]p(W|G) \\
&= \frac{1}{Z_S}\prod_{i=1}^{N}p(y_i|\beta_i,\alpha_{g_i},\sigma^2_{g_i},x_i,z_i)\pi_{g_i}\prod_{i,j=1}^{N}\exp\left(\frac{cW_{ij}}{\sigma^2}\delta_{ij}\right) \\
&= \frac{1}{Z_S}\prod_{i=1}^{N}(2\pi\sigma^2)^{-\frac{T}{2}}\pi_{g_i}\exp\left[-\frac{1}{2\sigma^2}\left\|\tilde{y}_i-\alpha_{g_i}\right\|^2\right]\prod_{i,j=1}^{N}\exp\left(\frac{cW_{ij}}{\sigma^2}\delta_{ij}\right), \qquad \text{(D.14)}
\end{aligned}$$

where $\tilde{y}_i = y_i - \beta_i' z_i$, $z_i = [z_{i1}\ z_{i2}\ldots\ z_{iT}]'$ and Z_S is the normalization constant.

Next, we define the optimal group partition G^* that minimizes the objective function of *PC-KMeans* defined in (D.12) with $x_i = \tilde{y}_i$ and $\mu_k = \alpha_k$, that is,

$$\begin{aligned}
G^* &\equiv \arg\min_G L(G) \\
&= \arg\min_G \frac{1}{2}\sum_{i=1}^{N}\left\|\tilde{y}_i-\alpha_{g_i}\right\|^2 - \sum_{i,j}cW_{ij}\delta_{ij}. \qquad \text{(D.15)}
\end{aligned}$$

Now we consider the asymptotic behavior of the posterior probability in (D.14). We will show that as σ^2 goes to 0, the posterior probability of G approaches 0 for all group partitions except for G^*:

$$\lim_{\sigma^2\to 0} p(G|\rho,\beta,\alpha,\Sigma,Y,X,W) \to \begin{cases} 1 & \text{if } G = G^*; \\ 0 & \textit{otherwise.} \end{cases}$$

We start with the log posterior density of G in (D.14),

$$\begin{aligned}
l(G) \equiv\ & \log p(G|\rho,\beta,\alpha,\Sigma,Y,X,W) \\
=\ & -\frac{1}{2\sigma^2}\sum_{i=1}^{N}\left\|\tilde{y}_i-\alpha_{g_i}\right\|^2 + \sum_{i,j=1}^{N}\left(\frac{cW_{ij}}{\sigma^2}\delta_{ij}\right) \\
& -\frac{NT}{2}\log(2\pi\sigma^2) + \sum_{i=1}^{N}\log(\pi_{g_i}) - \log Z_S. \qquad \text{(D.16)}
\end{aligned}$$

The difference between two log posterior probabilities evaluated at G^* and any other G

is

$$
\begin{aligned}
& l(G^*) - l(G) \\
= & \frac{1}{\sigma^2}\left[\left(\frac{1}{2}\sum_{i=1}^{N}\left\|\tilde{y}_i - \alpha_{g_i}\right\|^2 - \sum_{i,j=1}^{N} cW_{ij}\delta_{ij}\right) - \left(\frac{1}{2}\sum_{i=1}^{N}\left\|\tilde{y}_i - \alpha_{g_i^*}\right\|^2 - \sum_{i,j=1}^{N} cW_{ij}\delta^*_{ij}\right)\right] \\
& + \sum_{i=1}^{N}\left[\log(\pi_{g_i^*}) - \log(\pi_{g_i})\right]. \qquad \text{(D.17)}
\end{aligned}
$$

The first term is strictly positive according the definition of G^* in (D.15). For simplicity, we denote the expression within the first square brace as V and $V > 0$. The second term is finite since

$$
\left|\sum_{i=1}^{N}\left[\log(\pi_{g_i^*}) - \log(\pi_{g_i})\right]\right| \leqslant N\left|\max(\pi_j) - \min(\pi_j)\right| < +\infty
$$

Thus, for any $G \neq G^*$, in the limit as $\sigma^2 \to 0$, we have

$$
\lim_{\sigma^2\to 0} l(G^*) - l(G) = \lim_{\sigma^2\to 0}\frac{V}{\sigma^2} + \sum_{i=1}^{N}\left[\log(\pi_{g_i^*}) - \log(\pi_{g_i})\right] = +\infty. \qquad \text{(D.18)}
$$

This indicates that

$$
\lim_{\sigma^2\to 0}\frac{p(G|\alpha,\sigma^2,Y,X,Z,W)}{p(G^*|\alpha,\sigma^2,Y,X,Z,W)} = \lim_{\sigma^2\to 0}\exp\left[l(G) - l(G^*)\right] = \exp(-\infty) = 0.
$$

We take the sum over all possible group partitions and get,

$$
\begin{aligned}
& \lim_{\sigma^2\to 0}\frac{\sum_{G'} p(G'|\alpha,\sigma^2,Y,X,Z,W)}{p(G^*|\alpha,\sigma^2,Y,X,Z,W)} \\
= & \lim_{\sigma^2\to 0}\frac{\sum_{G'\neq G} p(G'|\alpha,\sigma^2,Y,X,Z,W) + p(G^*|\alpha,\sigma^2,Y,X,Z,W)}{p(G^*|\alpha,\sigma^2,Y,X,Z,W)} \\
= & 1.
\end{aligned}
$$

Since $\sum_{G'} p(G'|\alpha,\sigma^2,Y,X,Z,W) = 1$, we have

$$
\lim_{\sigma^2\to 0} p(G^*|\alpha,\sigma^2,Y,X,Z,W) = 1. \qquad \text{(D.19)}
$$

Therefore, when $\sigma^2 \to 0$, every posterior draw of G from the proposed Gibbs sampler is the solution to the assignment step of the *PC-KMeans* algorithm, conditional on the posterior draws of other parameters.

Part 2: Update Step

During Gibbs sampling, once we have performed one complete set of Gibbs moves on the group assignments and non-group-specific parameters including β_i and σ^2, we need to sample the α_k conditioned on all assignments and observations.

Let $|B_k|$ be the number of units assigned to group k, then the posterior density for α_k read as

$$p(\alpha_k|\beta,\sigma^2,Y,X,Z) \propto \exp\left[-\frac{1}{2}\left(\alpha_k-\bar{\mu}_{\alpha_k}\right)'\bar{\Sigma}_{\alpha_k}^{-1}\left(\alpha_k-\bar{\mu}_{\alpha_k}\right)\right], \tag{D.20}$$

where

$$\begin{aligned}
\bar{\Sigma}_{\alpha_k} &= \left(\Sigma_\alpha^{-1}+|B_k|\sigma^{-2}I_T\right)^{-1},\\
\bar{\mu}_{\alpha_k} &= \bar{\Sigma}_{\alpha_k}\left(\Sigma_\alpha^{-1}\mu_\alpha+\sigma^{-2}\sum_{i\in B_k}\tilde{y}_i\right),\\
\tilde{y}_i &= y_i-\rho y_{-1,i}-x_i\beta_i.
\end{aligned}$$

We can see that the mass of the posterior distribution becomes concentrated around the posterior group mean $\bar{\mu}_{\alpha_k}$ as $\sigma^2 \to 0$. Meanwhile, the posterior group mean $\bar{\mu}_{\alpha_k}$ equals the group "sample" mean in the limit:

$$\begin{aligned}
\lim_{\sigma^2\to 0}\bar{\mu}_{\alpha_k} &= \lim_{\sigma^2\to 0}\left(\Sigma_\alpha^{-1}+|B_k|\sigma^{-2}I_T\right)^{-1}\left(\Sigma_\alpha^{-1}\mu_\alpha+\sigma^{-2}\sum_{i\in B_k}\tilde{y}_i\right)\\
&= \lim_{\sigma^2\to 0}\left(\sigma^2\Sigma_\alpha^{-1}+|B_k|I_T\right)^{-1}\left(\sigma^2\Sigma_\alpha^{-1}\mu_\alpha+\sum_{i\in B_k}\tilde{y}_i\right)\\
&= |B_k|^{-1}\sum_{i\in B_k}\tilde{y}_i.
\end{aligned}$$

In other words, after we determine the assignments of units to groups, we update the means as the "sample" mean of the units in each group. This is equivalent to the standard *KMeans* cluster update step in general. Of course, we need additional steps to draw β_i and σ^2 before updating group means. □

E Monte Carlo Simulation

In this section, we conducted Monte Carlo simulations to examine the performance of various constrained BGFE estimators under different data generating processes (DGPs) and

prior belief on G. Two sets of DGPs are considered. For the simple DGPs, we introduce various group pattern in the fixed-effects only. The general DGPs, on the other hand, include more covariates with group-specific slope coefficients. Such designs enable us to investigate not only how our proposed estimators perform under various DGPs with specific features, but also the accuracy of estimating the number of groups.

We consider a short-panel environment in which the sample size is $N = 200$ and the time span is $T = 11$. As we focus on one-step ahead forecasts, the last observation of each unit serves as the hold-out sample for evaluation. A similar framework can be applied to H-step ahead forecasts by generating additional H observations. The true number of groups is set to $K_0 = 4$. Given N and K^0, we divide the entire sample into K^0 balanced blocks with N/K_0 units in each block.[14] For each DGP, 1,000 datasets are generated, and we run the block Gibbs samplers for each data set with $M = 5,000$ iterations after a burn-in of 5,000 draws.

E.1 Data Generating Processes

E.1.1 Simple DGPs

We begin with a simple dynamic panel data model with group pattern in the fixed-effects and no covariates or heteroskedasticity.

DGP 1 & 2:

$$y_{it} = \alpha_{g_i} + \rho y_{it-1} + \varepsilon_{it}, \tag{E.1}$$

where $\rho = 0.7$ and $\varepsilon_{it} \sim N(0, 1)$. The distributions of initial values are selected to ensure the simulation paths are stationary. Idiosyncratic error ε_{it} are independent across i and t, and mutually independent. ε_{it} is also independent of all regressors.

We assume α_k has zero mean and takes the form $\alpha_k = m(k - 2.5)$, where m controls the cross-sectional variance of α_i. Two sets of α_k are specified: $m = 1.79$ such that var $(\alpha_k) = 1/4$ in DGP 1 and $m = 0.51$ such that var $(\alpha_k) = 1/50$ in DGP 2, see details in Appendix E.1.2. The difference in α_k between these two DGPs distinguishes their properties. As depicted in Figure E.1, the group pattern is readily apparent in DGP 1. Different groups of units are perfectly divided, and the simulated paths are pretty flat. DGP 2 has a less visible group structure than DGP 1 because the difference between group means of α_k is smaller. The simulated pathways are considerably noisier and fluctuate around the unconditional mean.

[14] If N/K_0 is not an integer, we assign $\lfloor N/K_0 \rfloor$ units for group 1,2,..,$K_0 - 1$ and the last group contains the remainder.

Figure E.1: Simulated Paths for Units in Different DGPs

(a) DGP 1: Sharp Group (b) DGP 2: Noisy Group

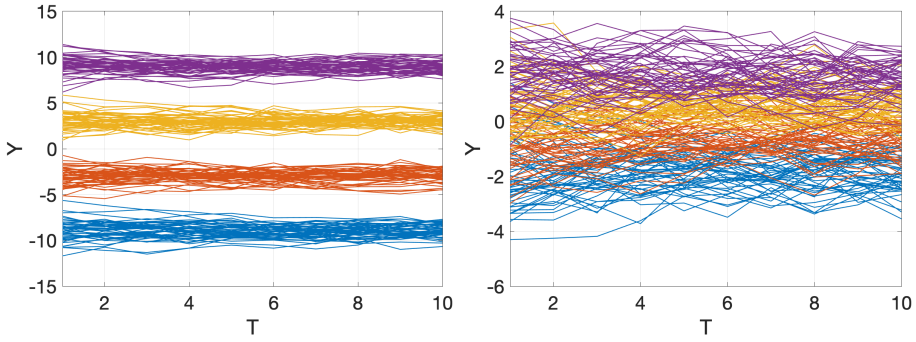

E.1.2 Details of the Simple DGPs

We start with the mean of α_k. Assume the values of α_k for group k take the form of $\alpha_k = m(k-c)$, where c is a shifting constant and m is a scaling constant. With loss of generality, we fix the mean of α_k to 0,

$$\sum_{k=1}^{K_0} \alpha_k = m \sum_{k=1}^{K_0} (k-c) = 0 \tag{E.2}$$

It immediately follows that $c = \frac{K_0+1}{2}$ and

$$\alpha_k = m\left(k - \frac{K_0+1}{2}\right), \quad \text{for } k = 1, 2, .., K_0. \tag{E.3}$$

Next, m is the only unknown coefficient in the DGP. To find a reasonable value for m, we connect it to the variance of α_i. As α_i are assume to be identical within a group, the sample variance of α_i is given by

$$V(\alpha_i) = \frac{1}{N}\sum_{i=1}^{N} \alpha_i^2 = \frac{1}{N}\frac{N}{K_0}\sum_{k=1}^{K_0} \alpha_k^2 = \frac{1}{K_0}\sum_{k=1}^{K_0} \alpha_k^2$$

Plugging in the expression of α_k in (E.3), we have

$$V(\alpha_i; m, K_0) = \frac{m^2}{K_0}\sum_{k=1}^{K_0}\left(k - \frac{K_0+1}{2}\right)^2. \tag{E.4}$$

To make the DGPs more comparable as more groups are considered, we assume $V(\alpha_i; m, K_0)$ is monotonically increasing in K_0^2, e.g., $V(\alpha_i; m, K_0) = V_0 K_0^2$ for some constant V_0. As a result,

we can deduct the value of m from (E.4),

$$m(K_0, V_0) = \left[\frac{V_0 K_0}{\sum_{k=1}^{K_0} \left(k - \frac{K_0+1}{2}\right)^2} \right]^{\frac{1}{2}}. \tag{E.5}$$

It is straightforward to find V_0 controls the dispersion of the underlying DGP. A larger V_0 indicate α_k are more separated and hence the group pattern become sharper, and vice versa.

E.1.3 General DGPs

The general DGP is based on the dynamic panel data model specified in (2.1) with an exogenous predictor z_{it} that has common effect for all units. This DGP incorporates group heterogeneity in the fixed-effects, the lagged term $x_{it}^{(1)} = y_{it-1}$ and an exogenous predictor $x_{it}^{(2)}$, as well as error variance $\sigma_{g_i}^2$.

DGP 3:

$$y_{it} = \alpha_{g_i}' x_{it} + \gamma z_{it} + \sigma_{g_i} \varepsilon_{it}, \tag{E.6}$$

where $x_{it} = [1, x_{it}^{(1)}, x_{it}^{(2)}]'$, $\gamma = 1.5$, $y_{i0} \sim N(0,1)$ and $\varepsilon_{it} \sim N(0,1)$. For each i, the initial value is specified to guarantee that the time series $(y_{i0}, y_{i1}, ..., y_{iT})$ is strictly stationary. We assume there are $K^0 = 4$ balanced groups, with the true grouped coefficients summarized in Table (E.1). The AR(1) coefficients represent different degree of persistence persistence. The exogenous variable $x_{it}^{(2)}$ is drawn from $N(0,1)$ and z_{it} is drawn from $Gamma(1,1)$, capped by 10.

Table E.1: True Grouped Coefficients in the General DGP

	$\alpha_{0,k}$	$\alpha_{1,k}$	$\alpha_{2,k}$	σ_k^2
	(FE)	(lagged)	(exo var.)	(variance)
Group 1	-0.15	0.4	0.16	0.500
Group 2	-0.05	0.8	0.14	0.375
Group 3	0.05	0.5	0.12	0.250
Group 4	0.15	0.7	0.10	0.125

E.2 Construction of Soft Pairwise Constraints

Number of constraints: We set the number of constraints N_{ML} and N_{CL} as a function of N and K_0 to facilitate performance comparisons across different settings and to ensure that the

information of constraints does not vanish as N increases. Specifically, N_{ML} and N_{CL} are a predetermined proportion of the total number of correct constraints for each type which are given by,

$$N^*_{ML}(N,K) = KC^2_{N/K} = K\frac{N/K(N/K-1)}{2} = \frac{N(N-K)}{2K}, \tag{E.7}$$

$$N^*_{CL}(N,K) = \left(\frac{N}{K}\right)^2 C^2_K = \left(\frac{N}{K}\right)^2 \frac{K(K-1)}{2} = \frac{N^2(K-1)}{2K}. \tag{E.8}$$

In the setting with $(N, K_0) = (200, 4)$, we have $N^*_{ML}(200, 4) = 4,900$ and $N^*_{CL}(200, 4) = 15,000$. We choose randomly select 5% of these constraints, leading to $N_{ML} = 245$ and $N_{CL} = 750$.

Type of pairwise constraints: The pairwise constraints are generated randomly. Given the number of ML constraints N_{ML}, each ML constraint is generated by randomly selecting a group and uniformly selecting two units within that group to be must-linked. Similarly, for each of N_{CL} CL constraints, two unique groups are chosen at random and one unit is randomly selected from each. Regarding the remaining unselected units, we assume they are not restricted and have no prior belief on them.

Accuracy of pairwise constraints: Each constraint is annotated with a level of accuracy ψ generating from a transformed Beta distribution defined on $[0.5, 1]$. We begin by drawing ν from a Beta distribution: if the constraint is correct, $\nu \sim \text{Beta}(3, 2)$ for some $\alpha > 1$; otherwise, $\nu \sim \text{Beta}(2, 3)$. Then the level of confidence is $\psi = \frac{\nu}{2} + 0.5$ so that its domain is $[0.5, 1]$. We derive ψ in this manner to reflect the assumption that an expert should have less certainty in erroneous constraints than in correct ones.

Perturbation in pairwise constraints: To examine the performance with soft constraints under inaccurate prior belief, we artificially add errors to the randomly generated constraints. A fraction e of the constraints are mislabeled – a must-link would be mislabeled as a cannot-link and vice versa. We turn eN_{ML} true ML into CL and eN_{CL} true CL into ML with $e = 20\%$.

All DGPs are equipped with the same set of pairwise constraints, e.g., we only draw pairwise constraints and weights once.

E.3 Alternative Estimators

We explore various types of estimators that differ in the prior belief on G.

(i) *BGFE*: The baseline Bayesian grouped fixed-effects (BGFE) estimator are correctly-specified, i.e. assuming that the true model exhibits time-invariant grouped heterogeneity and that variance of error term is constant (varying) across units in the simple (general) DGPs. No prior belief on G is available for this estimator.

(ii) *BGFE-cstr*: The baseline BGFE estimator that takes pairwise constraints into consideration.

(iii) *BGFE-oracle*: This estimator is a variant of the BGFE estimator equipped with *known* true G.

We also evaluate the other Bayesian estimators with different prior assumptions on α_i that don't model group structure.

(iv) *Pooled*: Bayesian pooled estimator views α_i as a common parameter and, consequently, all units have the same prior level of α_i.

(v) *Flat*: flat-prior estimator assumes $p(\alpha_i) \propto 1$. There is no pooling across units in this case and α_i's are individually estimated using their own history. This also amounts to sampling from a posterior whose mode is the MLE estimate.

E.4 Posterior Predictive Densities and Performance Evaluation

E.4.1 Posterior Predictive Densities

Given S posterior draws, the posterior predictive distribution estimated from the MCMC draws is

$$\hat{p}(y_{iT+1}|Y,X) = \frac{1}{S}\sum_{j=1}^{S}\left[\sum_{k=1}^{K^{(j)}(G)} \mathbf{1}(g_i = k) p\left(y_{iT+1}|Y,X,\Theta^{(j)}\right)\right]. \tag{E.9}$$

We can therefore draw samples from $\hat{p}(y_{iT+1}|Y,X)$ by simulating (2.1) forward conditional on the posterior draws of Θ and observations.

E.4.2 Point Forecasts

The optimal posterior forecast under quadratic loss function is obtain by minimizing the posterior risk, with is the posterior mean. Conditional on posterior draws of parameters, the mean forecast can be approximated by the Monte Carlo averaging,

$$\hat{y}_{i,T+1|T} \approx \frac{1}{S}\sum_{j=1}^{S}\hat{y}_{iT+1|T}^{(j)} = \frac{1}{S}\sum_{j=1}^{S}\hat{\alpha}_{g_i}^{(j)'}x_{iT+1}, \tag{E.10}$$

and the RMSFE across units is given by

$$RMSFE_{T+1} = \sqrt{\frac{1}{N}\sum_{i=1}^{N}\left(y_{i,T+1} - \hat{y}_{i,T+1}\right)^2}. \tag{E.11}$$

E.4.3 Set Forecasts

We construct set forecasts CS_{iT+1} from the posterior predictive distribution of each unit. In particular, we adopt a Bayesian approach and report the highest posterior density interval (HPDI), which is the narrowest connected interval with coverage probability of $1-\alpha$. In other words, it requires that the probability of $y_{iT+1} \in CS_{iT+1}$ conditional on having observed the history Y be at least $1-\alpha$, i.e.,

$$P(y_{iT+1} \in CS_{iT+1}) \geqslant 1-\alpha, \quad \text{for all } i, \tag{E.12}$$

and this interval is the shortest among all possible single connected candidate sets. Let δ^l be the lower bound and δ_u be the upper bound, then $CS_{iT+1} = \left[\delta_i^l, \delta_i^u\right]$.

The assessment of set forecasts in simulation studies and empirical applications is based on two metrics: (1) the cross-sectional coverage frequency,

$$Cov_{T+1} = \frac{1}{N}\sum_{i=1}^{N} \mathbf{1}\left(y_{iT+1} \in CS_{iT+1}\right), \tag{E.13}$$

and (2) the average length of the sets C_{iT+1},

$$AvgL_{T+1} = \frac{1}{N}\sum_{i=1}^{N}\left(\delta_i^u - \delta_i^l\right). \tag{E.14}$$

E.4.4 Density Forecasts

To compare the performance of density forecasts for various estimators, we examine the continuous ranked probability score (Matheson and Winkler, 1976; Hersbach, 2000) across units. The continuous ranked probability score (CRPS) is frequently used to assess the respective accuracy of two probabilistic forecasting models. It is a quadratic measure of the difference between the predictive cumulative distribution function, $F_i^{T+1|T}(y)$, and the empirical CDF of the observation with the formula as follows,

$$\begin{aligned} CRPS_{T+1} &= \frac{1}{N}\sum_{i=1}^{N} CRPS(F_i^{T+1|T}, y_{iT+1}) \\ &= \frac{1}{N}\sum_{i=1}^{N}\int_0^{\infty}\left[F_i^{T+1|T}(y) - \mathbf{1}\left(y_{iT+1} \leqslant y\right)\right]^2 dy, \end{aligned} \tag{E.15}$$

where y_{iT+1} is the realization at $T+1$.

In practice, the true predictive cumulative distribution function $F_i^{T+1|T}(y)$ or the PIT of y_{iT+1} is not available. We approximate it via the empirical distribution function for each unit

based on the posterior draws from the predictive density,

$$\hat{F}_i^{T+1|T}(y) = \frac{1}{S}\sum_{j=1}^{S} \mathbf{1}\left(y_{iT+1|T}^{(j)} \leqslant y\right), \tag{E.16}$$

Based on sorted posterior draws $\widetilde{y}_{iT+1}^{(j)}$, we can calculate CRPS using the below representation by Laio and Tamea (2007),

$$CRPS\left(\hat{F}_i^{T+1|T}, y_{iT+1}\right) = \frac{2}{S^2}\sum_{j=1}^{S}\left(\widetilde{y}_{iT+1|T}^{(j)} - y_{iT+1}\right)\left(1\left\{y_{iT+1} < \widetilde{y}_{iT+1|T}^{(j)}\right\} s - i + \frac{1}{2}\right). \tag{E.17}$$

Moreover, we report the average log predictive scores (LPS) to assess the performance of the density forecast from the view of the probability distribution function. As suggested in Geweke and Amisano (2010), the LPS for a panel reads as,

$$LPS_{T+1} = -\frac{1}{N}\sum_{i=1}^{N} \ln \int p\left(y_{iT+1}|Y, X, \Theta\right) p(\Theta|Y, X) d\Theta, \tag{E.18}$$

where the expectation can be approximated using posterior draws,

$$\ln p\left(y_{iT+1}|Y, X, \Theta\right) \approx \ln\left[\frac{1}{S}\sum_{j=1}^{S} p\left(y_{iT+1}|Y, X, \Theta^{(j)}\right)\right]. \tag{E.19}$$

E.5 Simulation Results

E.5.1 Simple Dynamics Panel Data

To evaluate the advantage of pooling units into groups, we report the RMSE, bias, standard deviation, average length of 95% credible set, and frequentist coverage of the posterior estimate of ρ across Monte Carlo repetitions. For the fixed effects α, we only present the average bias as it may not be of importance for most empirical study.

The comparison across alternative estimators is shown in Table E.2. In DGP 1,the BGFE-cstr and BGFE estimators are equally accurate as the oracle estimator. This is not surprising because the units are well-separated by design, and the data provide sufficient information for the BGFE estimator to determine the group pattern. In this situation, prior knowledge of G or the true group indices has quite marginal influence. The pooled estimator, on the other hand, erroneously pools all groups together, resulting in inaccurate estimates of α_i and ρ. Despite the fact that the flat estimator treats units separately, it is still inferior to the BGFE-type estimators. This is because it cannot utilize cross-sectional information to estimates parameters in this short panel and hence bears much larger bias.

In DGP 2, where the group pattern is less apparent, the BGFE-cstr estimator is arguably the most accurate. In contrast to the standard BGFE estimator, it uses cross-sectional data and pairwise constraints to determine the group pattern. These properties substantially reduce the biases of $\hat{\beta}$ and $\hat{\alpha}_i$, enabling the BGFE-cstr estimator to outperform the unconstrained estimator by a significant margin and to perform comparable to the oracle estimator. Remember that we manually add 20% incorrect constraints into the prior knowledge. Despite the presence of these misspecified constraints, the BGFE-cstr estimator is still able to extract relevant information from constraints in order to enhance the overall performance. The BGFE estimator, however, is unable to correctly reconstruct the group structure due to the noisy data, which results in the algorithm improperly grouping the units and hence generating inaccurate estimates.

Table E.2: Monte Carlo: Estimates, Soft Constraint

		$\hat{\rho}$					$\hat{\alpha}_i$	Group
		RMSE	Bias	Std	AvgL	Cov	Bias	Avg K
DGP 1	BGFE-oracle	0.0104	0.0037	0.0072	0.0276	0.92	0.0371	4
	BGFE-cstr	0.0102	0.0030	0.0072	0.0282	0.94	0.0369	4.92
	BGFE	0.0103	0.0037	0.0071	0.0274	0.92	0.0377	4.4
	Pooled	0.3543	0.3543	0.0032	0.0125	0	1.7889	-
	Flat	0.1713	0.1711	0.0073	0.0283	0	0.8668	-
DGP 2	BGFE-oracle	0.0186	0.0030	0.0137	0.0527	0.95	0.0235	4
	BGFE-cstr	0.0202	0.0058	0.0143	0.0557	0.93	0.0373	5.06
	BGFE	0.0546	0.0443	0.0212	0.0809	0.66	0.1357	4.78
	Pooled	0.2920	0.2919	0.0077	0.0298	0	0.5060	-
	Flat	0.1170	0.0834	0.0131	0.0509	0.14	0.2344	-

Table E.3 provides a summary of the prediction performance of each estimator. In general, the conclusions of the one-step-ahead forecast agree with those of the estimation. In DGP 1, the performance of the three BGFE estimators are quite similar, followed by the flat and pooled estimators. In DGP 2, the BGFE-cstr estimator, which utilizes prior belief on G, beats the other feasible estimators in point, set, and density forecast and is comparable to the oracle estimator.

E.5.2 General Panel Data

As the number of parameters increases for DGP 3, we present the RMSE and absolute bias of $\alpha_{g_i} = [\alpha_{1,g_i}\ \alpha_{2,g_i}\ \alpha_{3,g_i}]'$ and γ, as well as metrics for point and density prediction. In addition, all BGFE estimators now account for heteroskedasticity because the cross-sectional variance in DGP 3 is informative to group structure. As a result, we have the *BGFE-he-oracle*, *BGFE-he-cstr* and *BGFE-he* estimators in this exercise, where "*he*" denotes heteroskedasticity. For comparison, we also offer the *BGFE-ho-cstr* estimator, which assumes homoskedasticity, and *Flat-he* estimator, which is the heteroskedastic flat estimator.

Table E.3: Monte Carlo: Forecast, Soft Constraint

		Point Forecast			Set Forecast		Density Forecast	
		RMSFE	Error	Std	AvgL	Cov	LPS	CRPS
DGP 1	BGFE-oracle	0.4989	0.0001	0.4989	1.9627	0.95	0.7254	0.2818
	BGFE-cstr	0.4991	0.0004	0.4990	1.9666	0.95	0.7256	0.2819
	BGFE	0.4990	0.0001	0.4990	1.9616	0.95	0.7255	0.2818
	Pooled	0.6401	0.0006	0.6404	3.0114	0.98	1.0064	0.3657
	Flat	0.5620	0.0003	0.5622	2.4265	0.97	0.8544	0.3184
DGP 2	BGFE-oracle	0.4990	0.0001	0.4989	1.9629	0.95	0.7254	0.2819
	BGFE-cstr	0.5021	0.0001	0.5021	1.9790	0.95	0.7314	0.2836
	BGFE	0.5186	0.0002	0.5187	2.0546	0.95	0.7633	0.2930
	Pooled	0.5396	0.0005	0.5395	2.2444	0.96	0.8079	0.3052
	Flat	0.5286	0.0002	0.5287	2.1165	0.95	0.7841	0.2987

Table E.4: Results for Estimation, Point Forecast and Estimated K

	Estimates								Forecast		Group	
	$R(\hat{\alpha}_0)$	$B(\hat{\alpha}_0)$	$R(\hat{\alpha}_1)$	$B(\hat{\alpha}_1)$	$R(\hat{\alpha}_2)$	$B(\hat{\alpha}_2)$	$R(\hat{\gamma})$	$B(\hat{\gamma})$	RMSFE	LPS	AvgK	PctK
Flat-he	0.258	0.199	0.131	0.098	0.200	0.149	0.026	0.014	0.667	1.108	-	-
BGFE-he-oracle	0.126	0.137	0.092	0.101	0.119	0.132	0.569	0.602	0.840	0.706	4	1
BGFE-he-cstr	0.171	0.164	0.290	0.179	0.125	0.135	0.566	0.608	0.847	0.716	4.087	0.914
BGFE-ho-cstr	0.218	0.198	0.328	0.220	0.140	0.144	0.625	0.671	0.850	0.769	4.342	0.682
BGFE-he	0.303	0.317	0.560	0.482	0.137	0.147	0.601	0.640	0.871	0.756	3.575	0.534
Pooled	0.444	0.503	1.262	1.527	0.131	0.148	0.734	0.805	0.993	0.910	-	-

Notes: The first line gives the levels of the each metrics based on the Flat-he estimator, which is the benchmark model, and the following lines in the columns head "Estimates" and "Forecast" present ratios of the respective method relative those based on the flat-he estimator. In the columns head "Group", we show the average of number of groups (AvgK) and the percentage of iterations that the posterior sampler selects K_0 (PctK) averaged over 1,000 runs of algorithm. $R(\cdot)$ is RMSE of the posterior mean estimator. $B(\cdot)$ is the absolute bias of the posterior mean estimator.

Table E.4 presents the relative performance of estimation and forecasting for DGP 3. The benchmark model is *Flat-he*. Several findings arise. First, the gain from incorporating pairwise constraints is evident. It reduces the RMSE and bias for all parameters and improve both point and density forecast, when comparing BGFE-he-cstr to BGFE-he. The percentage of the Gibbs sampler that visits the true number of groups K_0 grows considerably from 53.4% to 91.4%. Even when pairwise constraints are taken into account, this percentage is just 68.2% if heteroskedasticity is ignored. Second, when we include prior belief on G, the improvement in α_{1,g_i}, the AR coefficient, is the greatest among all three grouped coefficients with a bias reduction of more than 60%. This also suggests that the AR coefficient may be more sensitive to the estimated group structure. Thirdly, BGFE-he-cstr and BGFE-ho-cstr have comparable RMSFE values, but BGFE-he-cstr has a significantly lower LPS, showing that modeling heteroskedasticity in the current setting is favorable for the density forecast. The empirical results below also confirm this finding. Lastly, all BGFE-type estimators generate similar estimates for the exogenous variables that don't have group effects on y_{it} as the

improvement in α_{2,g_i} and γ are marginal when prior belief on group is included or when true group is imposed.

F Data Description

F.1 Inflation of the U.S. CPI Sub-Indices

The seasonally adjusted series of CPI for All Urban Consumers (CPI-U) for subcategories at all display level are obtained from the BLS Online Databases.[15] The raw data contains 318 series, which are recorded on a monthly basis and spanned the period from January 1947 to August 2022. Notice that the raw dataset doesn't include an indicator for the expenditure categories. We manually merge the raw dataset with the table of content of CPI entry level items[16] by entry level item (ELI) code, the series description and universal classification (UCC) codes, if necessary.[17]

Series can enter and exit the sample. The BLS discontinued and launched series on a regular basis owing to changes in source data and methodology, for example, see the Post for the updates on series since 2017. The measure of certain subcategories was impacted by the Pandemic and hence missing. Since the Pandemic, the related activities and venues (sports events, bars, schools) were canceled and close temporarily, such as admission to sporting events (SS62032), distilled spirits away from home (SS20053), food at elementary and secondary schools (SSFV031A), etc. We chose to not impute the missing values since there was no clear benchmark to compare with, especially given the depressed economic conditions.

The CPI-U consists of eight major expenditure categories (1) Apparel; (2) Education and Communication; (3) Food and beverages; (4) Housing; (5) Medical Care; (6) Recreation; (7) Transportation; (8) Other goods and services. Each major category contains multiple sub-categories, resulting in a hierarchy of categories with increasing specificity. BLS provides a detailed table[18] that records the series code, series name, and display level. We resort to the display level to build the tree structure of the CPI sub-indices and eliminate those parent nodes, as illustrated in Figure F.1.

[15] https://data.bls.gov/PDQWeb/cu

[16] https://www.bls.gov/cpi/additional-resources/entry-level-item-descriptions.xlsx

[17] Some series are labeled by UCC rather than ELI. The concordance provided by the BLS can be found here: https://www.bls.gov/cpi/additional-resources/ce-cpi-concordance.htm.

[18] https://download.bls.gov/pub/time.series/cu/cu.item.

Figure F.1: Hierarchical Structure of CPI: Eliminating Parent Nodes

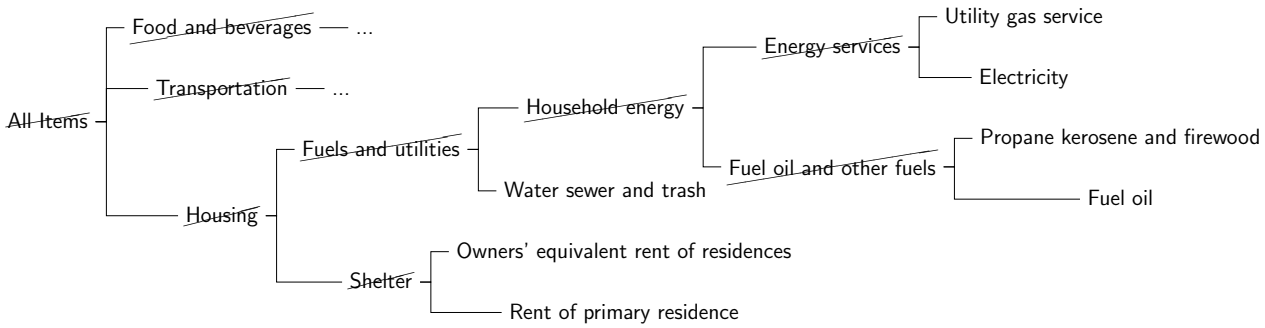

Because all CPI data is available on a monthly basis, we use the unemployment gap as labor market slack measures in the Phillips curve model. We use the seasonally adjusted unemployment rate[19] from FRED and construct the "gap" measures using the Hamilton filter (Hamilton, 2018). The Hamilton filter has two parameters: number of lags p and number of lookahead periods h. We follow Hamilton's suggestion and set $h = 24$ and $p = 12$, or an AR(12) process, additionally lagged by 24 lookahead periods for the monthly time series.

F.2 Income and Democracy

All data in this section are taken from the replication files of BM.[20] The data set contains a balanced panel of 89 countries and 7 periods at a five-year interval over 1970-2000. The main measure of democracy is the Freedom House Political Rights Index. A country receives the highest score if political rights come closest to the ideals suggested by a checklist of questions, beginning with whether there are free and fair elections, whether those who are elected rule, whether there are competitive parties or other political groupings, whether the opposition plays an important role and has actual power, and whether minority groups have reasonable self-government or can participate in the government through informal consensus. See more details in Acemoglu et al. (2008), Section 1.

Table F.1: Summary Statistics for the Democracy Data Set

	Mean	Median	S.E.	Min	Max
Democracy index	0.5760	0.6667	0.3712	0	1.0000
GDP per capita (in logarithm)	8.2981	8.3039	1.0685	6.0937	10.4450

[19] https://fred.stlouisfed.org/series/UNRATE
[20] https://www.dropbox.com/s/ssjabvc2hxa5791/Bonhomme_Manresa_codes.zip?dl=0

G Additional Empirical Results

G.1 Inflation of the U.S. CPI Sub-Indices

Figure G.1 shows the posterior mean of the number of active groups (red) along with total number of available CPI sub-indices (dark blue). Note that we choose not to show the credible set or the distribution of K because the distributions are concentrated around a single number in most samples.

Figure G.1: Number of Active Groups, BGFE-he-cstr

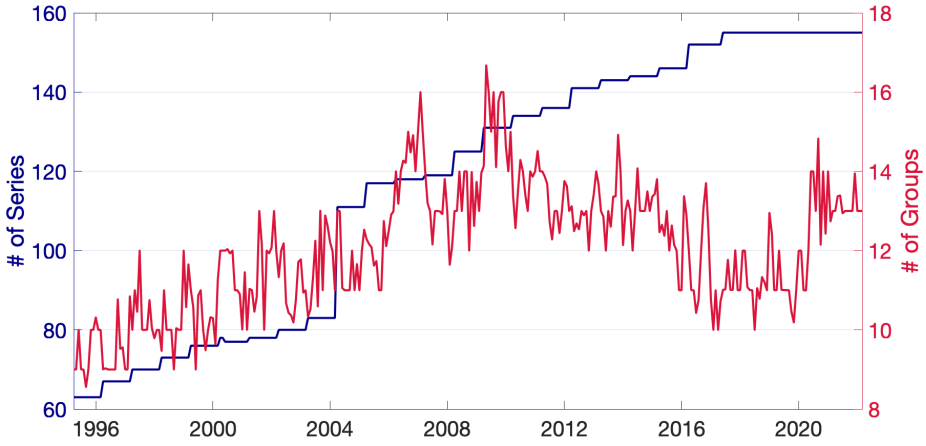

Figure G.2 shows the selected scaling constant c over time.

Figure G.2: Scaling Constant, BGFE-he-cstr

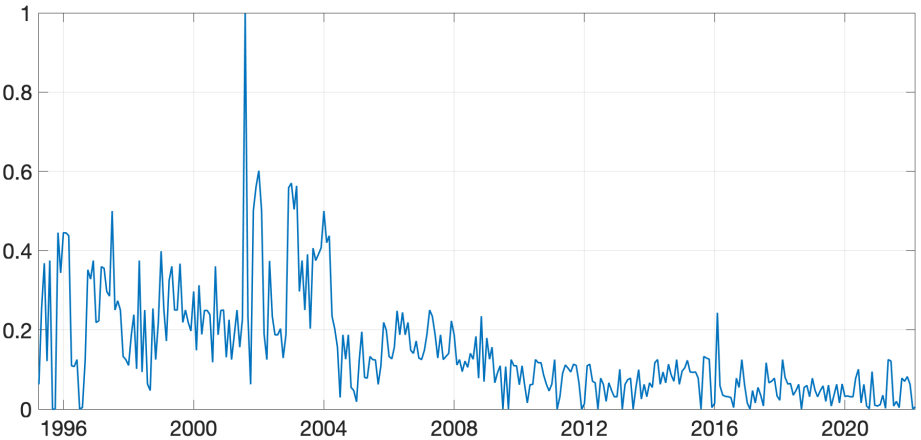

Figure G.3 shows the ratio of RMSE between BGFE-he-cstr and the benchmark AR-he.

Pink, blue and green shaded areas denote the period during which BGFE-he-cstr, BGFE-he and all other estimators reach the lowest RMSE, respectively.

Figure G.3: Relative RMSE, BGFE-he-cstr

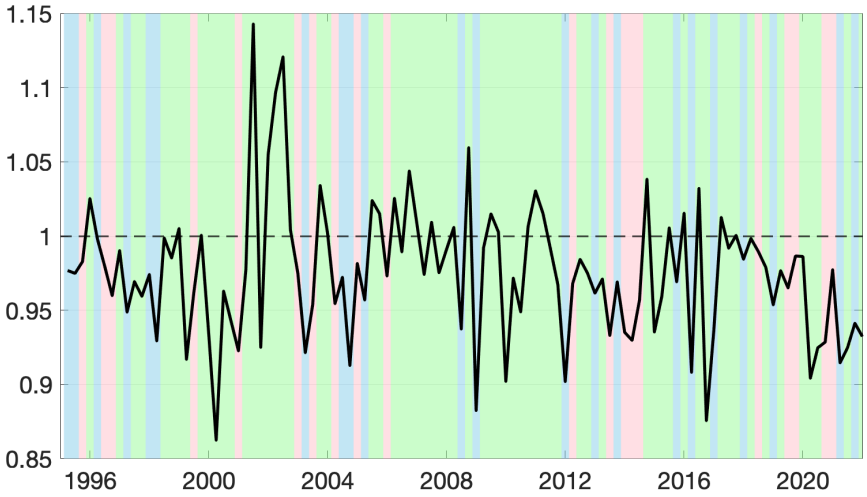

Figure G.4 shows the difference of LPS between BGFE-he-cstr and the benchmark AR-he. Pink, blue and green shaded areas denote the period during which BGFE-he-cstr, BGFE-he and all other estimators reach the lowest LPS, respectively.

Figure G.4: Relative LPS, BGFE-he-cstr

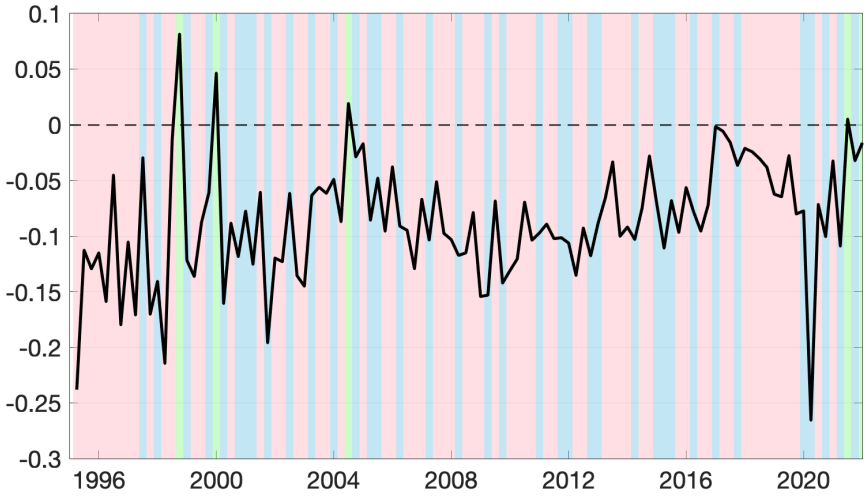

Table G.1 and G.2 present the ratio of RMSE between each estimator and AR-he for each expenditure category in five periods: 1995-1999, 2000-2004, 2005-2009, 2010-2014, 2015-2019, 2020-2022. Similar results for the difference of LPS are shown in Table G.3 and G.4.

Table G.1: Relative RMSE by Expenditure Category and Period

	Full	95 - 99	00 - 04	05 - 09	10 - 14	15 - 19	20 - 22
	Average of All Series						
BGFE-he-cstr	0.97	0.97	0.97	0.99	0.96	0.97	0.94
BGFE-he	0.98	0.98	0.98	1.00	0.97	0.98	0.95
BGFE-ho	1.00	1.04	0.98	1.00	0.98	0.99	1.00
AR-he-PC	1.01	1.02	1.03	0.99	1.00	1.01	1.04
Pooled	1.00	1.04	0.98	1.03	1.01	0.99	0.94
	Category 1: Apparel						
BGFE-he-cstr	0.97	0.98	0.99	0.97	0.96	0.98	0.91
BGFE-he	0.97	0.98	0.99	0.98	0.97	0.98	0.92
BGFE-ho	0.98	0.99	1.00	0.98	0.98	0.99	0.93
AR-he-PC	1.02	1.02	1.00	1.03	1.01	1.01	1.08
Pooled	0.99	1.00	0.97	0.99	1.03	1.03	0.90
	Category 2: Education and Communication						
BGFE-he-cstr	0.96	0.93	0.99	0.95	0.94	0.97	0.93
BGFE-he	0.95	0.95	1.00	0.94	0.95	0.97	0.92
BGFE-ho	1.08	2.18	1.02	1.00	1.00	0.97	0.91
AR-he-PC	1.01	1.03	0.99	1.00	0.95	1.01	1.08
Pooled	1.16	2.24	1.21	1.05	1.12	1.03	0.97
	Category 3: Food and Beverages						
BGFE-he-cstr	0.98	0.99	0.99	1.00	0.97	0.98	0.95
BGFE-he	0.98	0.99	1.00	1.00	0.97	0.98	0.95
BGFE-ho	0.99	1.03	0.99	0.97	0.97	0.98	0.95
AR-he-PC	1.00	1.01	1.02	0.99	1.00	1.01	0.98
Pooled	1.01	1.03	1.01	1.05	1.01	0.99	0.93
	Category 4: Housing						
BGFE-he-cstr	0.97	0.96	0.95	1.03	0.94	0.96	0.96
BGFE-he	0.96	0.97	0.93	1.03	0.94	0.96	0.96
BGFE-ho	0.98	1.14	0.93	1.02	0.96	0.97	0.95
AR-he-PC	1.03	1.03	1.04	1.04	0.99	1.01	1.07
Pooled	0.99	1.14	0.92	1.06	0.97	0.97	0.94

Notes: Benchmark model = AR-he.

Table G.2: Relative RMSE by Expenditure Category and Period, *cont.*

	Full	95 - 99	00 - 04	05 - 09	10 - 14	15 - 19	20 - 22
	Category 5: Medical Care						
BGFE-he-cstr	0.95	0.93	0.98	0.95	1.01	0.96	0.87
BGFE-he	0.95	0.93	0.98	0.95	1.01	0.96	0.85
BGFE-ho	1.06	1.32	1.15	1.07	1.09	0.99	0.86
AR-he-PC	1.03	1.04	0.99	1.02	1.03	1.02	1.07
Pooled	1.15	1.30	1.38	1.23	1.15	1.04	0.92
	Category 6: Recreation						
BGFE-he-cstr	0.97	0.97	0.99	0.99	0.98	0.96	0.94
BGFE-he	0.97	0.97	1.00	0.99	0.99	0.96	0.92
BGFE-ho	1.02	1.18	1.09	1.05	1.00	0.97	0.94
AR-he-PC	1.03	1.03	1.03	1.02	1.01	1.01	1.08
Pooled	1.12	1.17	1.24	1.31	1.17	0.99	0.96
	Category 7: Transportation						
BGFE-he-cstr	0.99	0.97	1.01	0.99	0.99	1.00	0.96
BGFE-he	0.99	0.97	1.01	0.98	0.99	1.00	0.96
BGFE-ho	1.03	1.07	1.02	1.00	1.01	1.02	1.07
AR-he-PC	1.02	1.04	1.05	0.97	1.01	0.99	1.07
Pooled	0.99	1.07	1.02	0.99	0.97	0.96	0.97
	Category 8: Other Goods and Services						
BGFE-he-cstr	0.97	0.98	0.99	1.02	0.89	0.96	0.93
BGFE-he	0.95	0.94	0.95	1.05	0.89	0.97	0.91
BGFE-ho	0.96	0.99	0.97	0.99	0.89	0.97	0.91
AR-he-PC	1.02	1.01	1.02	1.02	0.97	1.00	1.11
Pooled	0.98	0.99	1.04	0.99	0.89	0.99	0.94

Notes: Benchmark model = AR-he.

Table G.3: Relative LPS, by Expenditure Category and Period

	Full	95 - 99	00 - 04	05 - 09	10 - 14	15 - 19	20 - 22
	Average of All Series						
BGFE-he-cstr	−0.08	−0.08	−0.07	−0.08	−0.09	−0.07	−0.08
BGFE-he	−0.06	−0.06	−0.05	−0.06	−0.07	−0.05	−0.08
BGFE-ho	0.64	0.77	0.72	0.77	0.48	0.53	0.45
AR-he-PC	0.01	0.02	0.02	0.01	0.01	0.01	0.01
Pooled OLS	0.66	0.84	0.73	0.79	0.53	0.52	0.44
	Category 1: Apparel						
BGFE-he-cstr	−0.05	−0.03	−0.02	−0.05	−0.05	−0.02	−0.14
BGFE-he	−0.04	−0.02	−0.02	−0.04	−0.05	−0.01	−0.14
BGFE-ho	0.1	0.25	0.07	0.07	0.11	0.06	0.03
AR-he-PC	0.03	0.03	0.01	0.03	0.02	0.01	0.09
Pooled	0.12	0.25	0.07	0.10	0.18	0.11	−0.05
	Category 2: Education and Communication						
BGFE-he-cstr	−0.12	−0.06	−0.07	−0.19	−0.17	−0.10	−0.11
BGFE-he	−0.13	−0.08	−0.11	−0.20	−0.16	−0.09	−0.12
BGFE-ho	0.92	1.44	1.04	0.87	0.91	0.56	0.56
AR-he-PC	0.01	0.00	0.01	0.02	0.00	0.01	0.07
Pooled	0.98	1.45	1.09	0.95	0.99	0.62	0.62
	Category 3: Food and Beverages						
BGFE-he-cstr	−0.04	−0.03	−0.02	−0.06	−0.05	−0.05	−0.07
BGFE-he	−0.04	−0.04	−0.02	−0.05	−0.05	−0.05	−0.08
BGFE-ho	0.37	0.66	0.36	0.34	0.27	0.39	0.03
AR-he-PC	0.00	0.01	0.03	−0.01	0.01	0.00	−0.08
Pooled	0.44	0.84	0.41	0.44	0.33	0.41	0.03
	Category 4: Housing						
BGFE-he-cstr	−0.12	−0.13	−0.14	−0.10	−0.11	−0.12	−0.07
BGFE-he	−0.11	−0.12	−0.13	−0.10	−0.11	−0.12	−0.07
BGFE-ho	0.81	0.96	1.13	0.83	0.60	0.60	0.70
AR-he-PC	0.02	0.00	0.03	0.04	0.01	0.01	0.06
Pooled	0.82	0.97	1.13	0.88	0.63	0.60	0.68

Notes: Benchmark model = AR-he.

Table G.4: Relative LPS by Expenditure Category and Period, *cont.*

	Full	95 - 99	00 - 04	05 - 09	10 - 14	15 - 19	20 - 22
	Category 5: Medical Care						
BGFE-he-cstr	−0.15	−0.29	−0.14	−0.14	−0.16	−0.05	−0.09
BGFE-he	−0.15	−0.29	−0.13	−0.14	−0.16	−0.05	−0.09
BGFE-ho	1.16	1.64	1.34	1.11	1.14	0.78	0.78
AR-he-PC	0.02	0.02	0.01	0.03	0.02	0.01	0.04
Pooled	1.21	1.64	1.39	1.20	1.20	0.84	0.84
	Category 6: Recreation						
BGFE-he-cstr	−0.04	−0.04	−0.05	−0.02	−0.02	−0.05	−0.05
BGFE-he	−0.03	−0.03	−0.05	−0.01	−0.01	−0.04	−0.07
BGFE-ho	0.55	0.91	0.79	0.58	0.49	0.25	0.12
AR-he-PC	0.02	0.03	0.03	0.02	0.01	0.01	0.06
Pooled	0.61	0.91	0.84	0.70	0.58	0.29	0.13
	Category 7: Transportation						
BGFE-he-cstr	−0.04	−0.10	−0.03	−0.05	−0.07	0.00	0.00
BGFE-he	−0.03	−0.10	0.00	−0.04	−0.06	0.00	0.00
BGFE-ho	1.59	0.98	1.56	2.83	0.79	1.51	2.11
AR-he-PC	0.01	0.03	0.03	−0.02	−0.01	0.00	0.07
Pooled	1.42	0.98	1.41	2.38	0.75	1.24	1.98
	Category 8: Other Goods and Services						
BGFE-he-cstr	−0.03	0.22	−0.09	−0.07	−0.14	−0.06	−0.05
BGFE-he	−0.03	0.25	−0.09	−0.06	−0.13	−0.06	−0.06
BGFE-ho	0.64	0.59	0.66	0.69	0.83	0.53	0.49
AR-he-PC	0.01	0.02	0.00	0.03	0.00	0.01	0.04
Pooled	0.69	0.61	0.71	0.77	0.89	0.57	0.53

Notes: Benchmark model = AR-he.

G.1.1 Network Visualization of Posterior Similarity Matrix

In our empirical work, we estimate the posterior similarity matrix (PSM) among 154 series for the last sample (August 2022). Presenting and examining $154 \times 154 = 23,716$ estimates pairwise posterior probabilities in PSM would be thoroughly uninformative. Hence we characterize the estimated PSM graphically as network graphs, which contain node names, node color, and link size (one per link since the network is undirected).

- *Node name* shows the item names of CPI sub-indices.
- *Node color* indicates the group structure used in the prior, e.g, expenditure category.
- *Link size* represents the pairwise probabilities in the PSM.

We use the *qgraph* package in R for network visualization. Node locations are determined by a modified version of a force-embedded algorithm proposed by Fruchterman and Reingold (1991). Figure G.5 show the full-sample CPI sub-index network graphs.

Figure G.5: Individual CPI Sub-Index Network Graph based on Posterior Similarity Matrix, August 2022

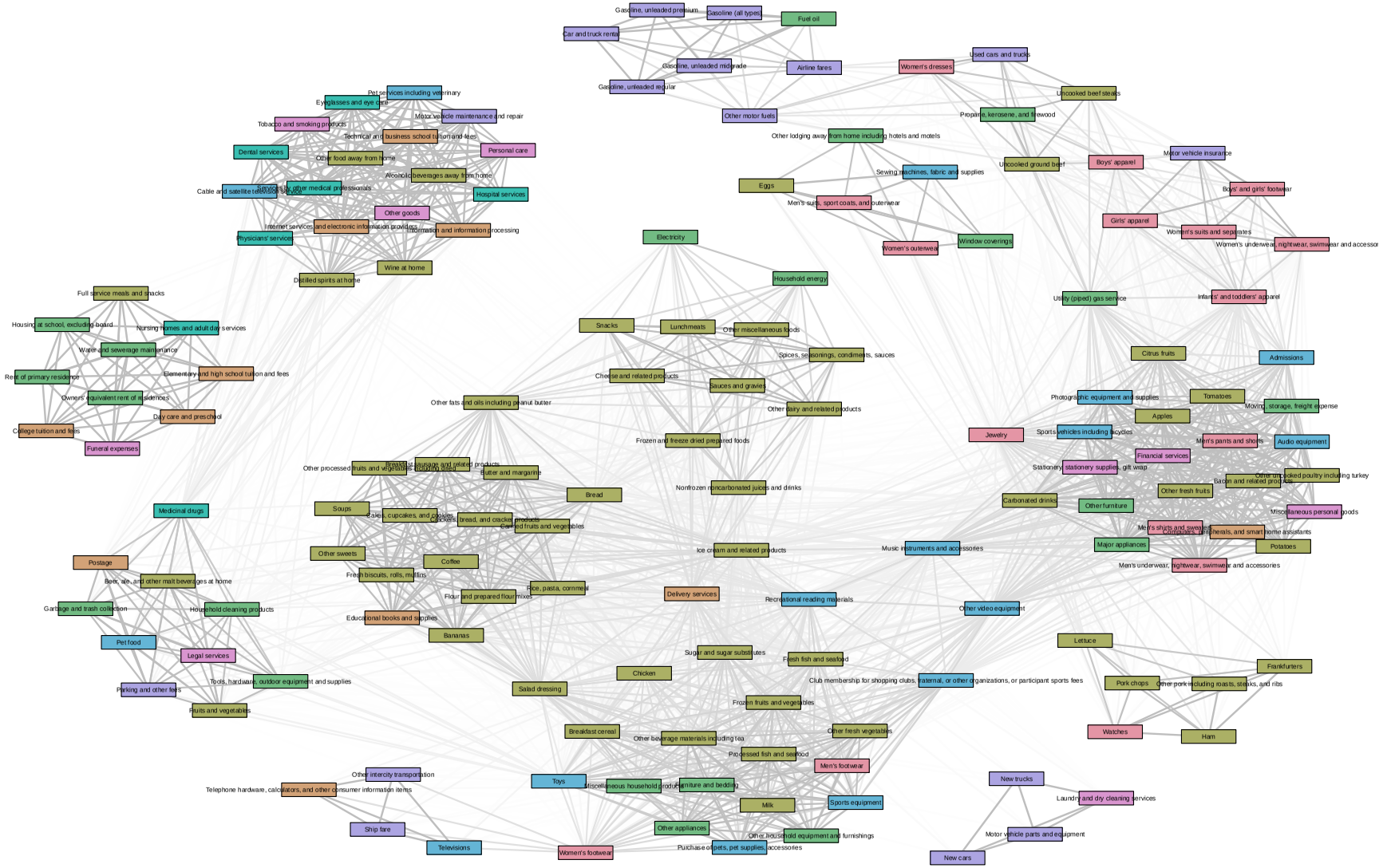

G.2 Income and Democracy

G.2.1 Results of Specification 1

We start our analysis with the specification 1 in (5.12). Table G.5 demonstrates the posterior probability of the number of groups utilizing various estimators. Notably, the BGFE-ho in this specification is identical to the primary model in BM, allowing us to evaluate the optimal number of groups. BGFE-ho creates 8 groups in all posterior draws, which is consistent with BM's conclusion of using BIC: the upper bound of the true number of groups is 10. Despite the fact that BM is unable to validate the ideal number of groups for their study, our BGFE-ho estimator provides an accurate estimate of it. Intriguingly, accounting for heteroskedasticity drastically reduces the number of groups, with BGFE-he identifying three groups in 92.9% of posterior draws. Adding pairwise constraints based on geographic information increase the number groups. Two-third of posterior draws from BGFE-he-cstr generate 5 group.

Table G.5: Probability for the number of groups

	BGFE-he-cstr	BGFE-he	BGFE-ho
$Pr(K < 3)$	0.000	0.000	0.000
$Pr(K = 3)$	0.000	**0.929**	0.000
$Pr(K = 4)$	0.344	0.071	0.000
$Pr(K = 5)$	**0.656**	0.000	0.000
$Pr(K > 5)$	0.000	0.000	**1.000**

The marginal data density (MDD) of each estimators in Table G.6 provides some insight on different models. Even while BGFE-ho produces eight groups and has a tendency to overfit, its MDD is the lowest of the three estimators. BGFE-he with fewer groups is superior to BGFE-ho with higher MDD. BGFE-he-cstr has the highest MDD because the pairwise constraints give direction on grouping and identify the ideal group structure, which BGFE-he cannot uncover without our prior knowledge.

Table G.6: Marginal Data Density

BGFE-he-cstr	BGFE-he	BGFE-ho
425.690	381.218	368.918

We focus on the BGFE-he-cstr estimator and use the approach outlined in Section 3.2 to identify the unique group partitioning $\widehat{G}$. The left panel of Figure G.6 presents the world map colored by $\widehat{G}$, while the right panel present the group-specific averages of democracy index over time. The estimated group structure $\widehat{G}$ features four distinct groups, which is

coincident to the choice of BM. As described in BM, we refer to groups 1-4 as the "high-democracy", "low-democracy", "early transition", and "late transition" group, respectively. With the exception of the "early transition" group that is slight at odd with the counterpart in BM, the group-specific averages of the democracy index for all other groups are relatively similar to those in BM. Notice that BM manually sets the number of groups to four, but we discover that four is the optimal number. Consequently, by employing model specification 1 and accounting for heteroskedasticity, we find the support for BM's main results.

Figure G.6: Point Estimation of Group Partitioning and Average Democracy

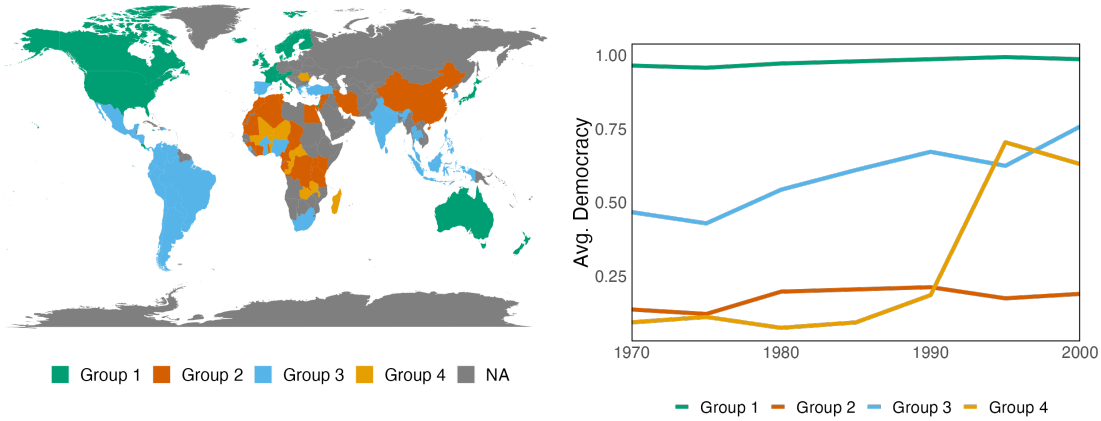

Table G.7 shows the posterior mean and 90% credible set for each coefficient, with G fixing at the point estimate $\widehat{G}$. Comparing to the pooled OLS, $\hat{\rho}$ and $\hat{\beta}$ once we incorporate the group-specific time patterns. The results are essentially consistent with the conclusion in BM: there is modest persistence and a positive effect of income on democracy, but the cumulative income effect $\beta/(1-\rho) = 0.08$ is quantitatively small.

Table G.7: Coefficient estimates across groups

	Lagged democracy (ρ)		Lagged Income (β)	
	Coef.	Cred. Set	Coef.	Cred. Set
BGFE-he-cstr	0.499	[0.438, 0.558]	0.040	[0.027, 0.053]
Pooled OLS	0.665	[0.616, 0.718]	0.082	[0.065, 0.100]

G.2.2 Network Visualization of Posterior Similarity Matrix

Figure G.7 and G.8 show the full-sample country network graphs, for specification 1 and 2 respectively. Node color reflects the geographic information used to construct the group structure in the prior.

Figure G.7: Individual Country Network Graph based on Posterior Similarity Matrix, Specification 1

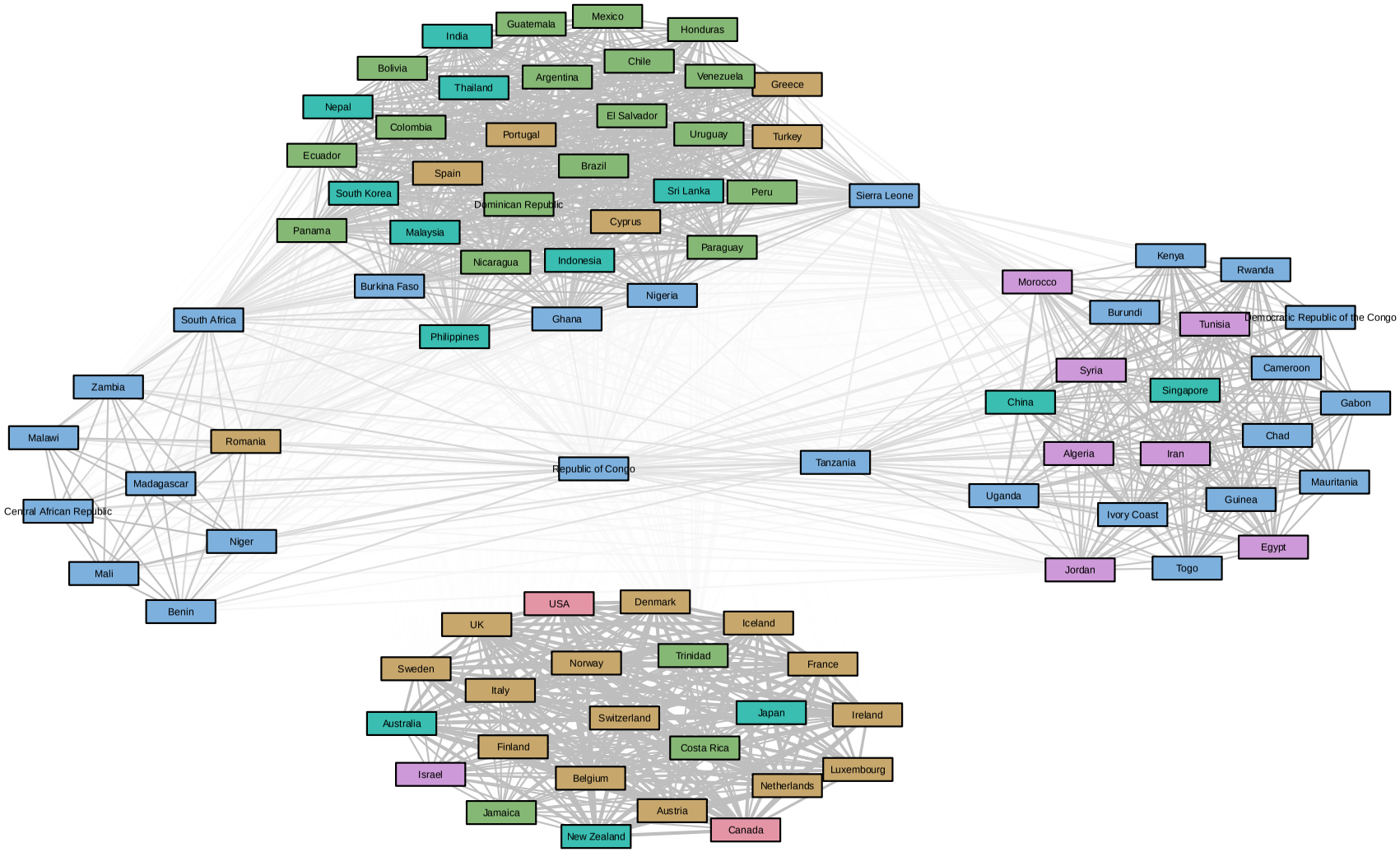

Figure G.8: Individual Country Network Graph based on Posterior Similarity Matrix, Specification 2